Structural Features That Promote Catalysis in Two-Component Systems Involved in Sulfur Metabolism

by

Richard Allen Hagen

A dissertation to the Graduate Faculty of
Auburn University
in partial fulfillment of the
requirements for the Degree of
Doctor of Philosophy

Auburn, Alabama
August 8, 2020

Approved by

Holly R. Ellis, Chair, Professor of Chemistry and Biochemistry
Douglas C. Goodwin, Professor of Chemistry and Biochemistry
Evert C. Duin, Professor of Chemistry and Biochemistry
Steven Mansoorabadi, Associate Professor of Chemistry and Biochemistry

Abstract

Sulfur is an essential element important in the synthesis of biomolecules. Bacteria are able to assimilate inorganic sulfur for the biosynthesis of L-cysteine. Inorganic sulfate is often unavailable, so bacteria have evolved multiple metabolic pathways to obtain sulfur from alternative sources. Interestingly, many of the enzymes involved in sulfur acquisition are flavin-dependent two-component systems. These two-component systems consist of a flavin reductase and monooxygenase that utilize flavin to cleave the carbon-sulfur bonds of organosulfur compounds. The two-component systems differ in their characterized sulfur substrate specificity. Enzymes SsuE/SsuD are involved in the desulfonation of linear alkanesulfonates (C_2-C_{10}), enzymes MsuE/MsuD utilize methanesulfonate (C_1), and enzymes SfnF/SfnG utilize $DMSO_2$ as a sulfur source.

The flavin reductases involved in sulfur assimilation utilize FMN as a substrate but differ in their ability to utilize NADH or NADPH. The alkanesulfonate monooxygenase system was the first two-component flavin-dependent system expressed during sulfur limiting conditions that was characterized. The flavin reductase (SsuE) and monooxygenase (SsuD) have distinct structural and functional properties, but the two enzymes must synchronize their functions for catalysis to occur. Once flavin is reduced, protein-protein interactions between the SsuE and SsuD facilitate reduced flavin to protect reactive intermediates from bulk solvent. The flavin reductase undergoes an oligomeric conversion from a tetramer to a dimer in the presence of flavin or SsuD. These oligomeric changes have been proposed to promote protein-protein interactions and flavin transfer. The π-helix is a conserved structural feature of all the flavin reductases in these two-component systems, that was initially proposed to be generated by a single amino insertion into a conserved α-helical region. The π-helix in proteins often provide a gain of function for the enzyme. The π-

helix in SsuE is formed by the insertion of a Tyr residue (Tyr118) into a conserved α-helix. The π-helix has been proposed to play a role in the observed oligomeric conversion from a tetramer to a dimer needed for protein-protein interactions between SsuE and SsuD. The ability of other FMN reductases (MsuE and SfnE) to undergo this conversion is currently unknown. Interestingly, both MsuE and SfnE contain a similar π-helix with a histidine insertional residue in the π-helix.

A goal of these research studies was to identify common functional features among the π-helices in two-component FMN reductases and determine how they differ from canonical flavin reductases. Variants of Tyr118 were generated and their three-dimensional structures determined to evaluate how these alterations affect the structural integrity of the π-helix. The structure of the Y118A SsuE π-helix was converted to an α-helix, similar to the FMN-bound members of the NADPH:FMN reductase family. Although the π-helix was altered, the FMN binding region remained unchanged. Conversely, deletion of Try118 disrupted the secondary structural properties of the π-helix, generating a random coil region in the middle of helix 4. Both the Y118A and Δ118 SsuE SsuE variants crystallized as a dimer.

Single amino acid substitutions of Y118 to His in SsuE and MsuE (H126) were generated to determine if the variants would maintain the functional attributes of the wild-type enzymes. Exchanging the π-helix insertional residue of each enzyme did not result in the expected, equivalent kinetic properties. The His126 conversion to Tyr in MsuE did not change the kinetic properties of the enzyme and the variant was able to provide reduced flavin to both MsuD and SsuD. Conversely, the Y118H SsuE variant did not possess reductase activity, and was unable to support flavin transfer to MsuD or SsuD. Structure-based sequence analysis further demonstrated the presence of a similar Tyr residue in a FMN-bound reductase in the NADPH:FMN reductase family that is not sufficient to generate a π-helix. Results from structural and functional studies of

the FMN-dependent reductases suggest that the insertional residue alone is not solely responsible for generating the π -helix, and additional structural adaptions occur to provide the altered gain of function. Further analysis identified a structurally similar enzyme, ChrR, in the same family that has a similar residue Tyr126 in similar location as Try118 of SsuE. ChrR has two glutamate residues located in similar position as conserved residues proline and aspartic acid for flavin reductases. These conserved residues may play a role in stabilizing the π-helical region for flavin reductases. Results from the variants generated suggest the residues play a role in stabilizing the overall oligomeric structure due to the low success during purification and unsuccessful transfer of substrates to partner enzymes.

The monooxygenases SsuD, MsuD, and SfnG catalyze the desulfonation of organosulfur substrates. High amino acid sequence identity between SsuD and MsuD suggest they utilize similar structural and functional features for catalysis. The SsuD enzyme has a TIM-barrel fold, but diverges from classic TIM-barrel structures due to insertional regions. This SsuD insertional region contains a long loop region that protrudes over the active site. Once substrates are transferred to the monooxygenase, this mobile loop interacts with substrate to initiate conformational changes that protect reactive intermediates. Arg297 is located on the mobile loop and previous studies suggest the amino acid forms interactions the flavin phosphate. Similar interactions have been observed in TIM-barrel enzymes. These structural features may play a role in substrate specificity and protect reactive intermediates from solvent for FMN-dependent two-component systems. FMN substrate fragments were used to evaluate the role of the phosphate group in assisting in loop closure. There was no activity observed with riboflavin and increasing phosphite concentrations as the substrate, suggesting the loop stabilization may not occur with the FMN phosphate alone.

The monooxygenase enzymes involved in the desulfonation of alkanesulfonates have been proposed to have different substrate specifies. The MsuD enzyme has been proposed to have a substrate preference for methanesulfonate, while SsuD shows a preference for alkanesulfonates between C6-C10 carbons. The SsuD and MsuD enzymes share ~60% amino acid sequence identity. Structural models of MsuD suggested they likely share similar active site architectures. Therefore, it was unclear what structural features contribute to the substrate specificity. In coupled assays, MsuD was able to utilize a wide range of alkanesulfonate substrates including methanesulfonate. SsuD was able to utilize similar substrates as MsuD, but was unable to catalyze the desulfonation of methanesulfonate. The inability of SsuD to utilize methanesulfonate agrees with previous results, but is curious given their nearly identical active sites.

The results from these described studies have provided important information on the structural features conserved in two-component monooxygenase enzymes that determine specific functions. It is clear that flavin transfer in these enzymes creates an added challenge for these two component flavin-dependent systems. While these enzymes share similar structures and functions, they have evolved to maintain their own distinctive features for catalytic function. These differences would provide bacteria with more diverse processes for sulfur acquisition.

Acknowledgements

It was an honor to attend Auburn University for my graduate degree. I have dreamed of attending Auburn University since I was a young child. I would like to first say a very big thank you to my supervisor Dr. Holly R. Ellis for all the support and encouragement she gave me during the time I have spent in her lab. Dr. Ellis believed in me and my abilities when I doubted myself. Without her guidance and constant feedback, this PhD would not be achievable. Her advice on both research as well as on my career have been invaluable. I cannot express enough thanks to my committee for their continued support and encouragement: Dr. Douglas C. Goodwin, Dr. Evert C. Duin, and Dr. Steven Mansoorabadi. I offer my sincere appreciation for their guidance and allowing access to the instrumentation in their respective labs. Also, I would like to thank Dr. Russell Muntifering for his time as my University Reader. Thank you to my former and current lab mates from Dr. Ellis' group for thoughtful discussions and support: Dr. Jonathan Musila, Dr. Dianna Forbes, Dr. Claire Graham, Dr. Katie Tombrello, Chioma Helen Aloh, Shruti Somai, Chidozie Ugochukwu, Chukwuemeka Steve Adindu, and Luke Martz. This experience would not have been possible without a strong support system that I have been blessed to have. This support system begins with one of the most amazing people I know, my wonderful wife Emily Hagen. Thank you for staying up with me on those late nights when I was studying and writing, waiting up for me when I was trying to keep my protein alive, and being understanding with the process. You have constantly pushed me to be a better person and I would not be here at Auburn without you. I would also like to thank my beautiful daughter, Annaliese Hagen. You have always kept my spirits up during this process and motivated me to continue. I am truly grateful to be your dad. With this, I dedicate my dissertation work to the two most amazing women in my life, Emily and Annaliese Hagen. I love you both. WAR EAGLE!

Table of Contents

List of Tables

List of Schemes

List of Figures

CHAPTER ONE

LITERATURE REVIEW

1.1 Sulfur Metabolism

1.1.1 Prevalence of Sulfur in Environment

Sulfur makes up about 0.1% of the earth's crust as sulfide or sulfate minerals.[1] Sulfur is also found near active or dormant volcanoes, in ocean water, and as gas in the atmosphere.[2] The valence state of sulfur is commonly found as -2 (S^{2-}), but is also found as S^{6+} when all the electrons in the outer valence shell are removed.[2] The S^{6+} can form a strong bond with oxygen to form sulfate (SO_4^{2-}).[2] Other valence states of sulfur include intermediates such as oxidation states +5, +4, +3, +2, -2, -1, and native state S^0.[2,3]

In general, sulfur is found in the lithosphere (burning fossil fuels), hydrosphere, atmosphere, and biosphere (oxidation of organic matter from the soil and burning of biomass) (Figure 1.1).[4] In agricultural soils, sulfate is in the form of ammonium sulfate, gypsum, potassium magnesium sulfate, and sulfates of micronutrients.[4,5] Plants are able to utilize sulfur sources to produce sulfide (S^{2-}) from reductive metabolism, and are supplied with usable sulfur from metabolic processing by soil bacteria.[4-6] In the environmental soil, sulfur is found as organic or inorganic forms such as sulfate or elemental sulfur.[4] The sulfate can undergo dissimilatory reduction when it is used as the final acceptor of electrons in anerobic metabolism to produce H_2S.[4] The sulfate also goes through assimilatory reduction by prokaryotes, algae, plants, and fungi for the biosynthesis of organic compounds such as amino acids.[4]

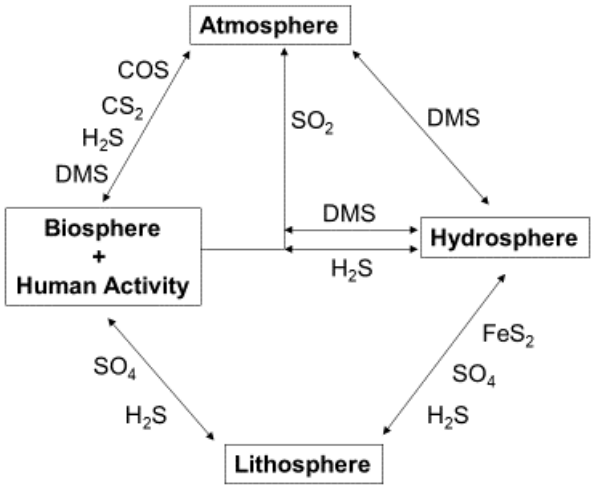

Figure 1.1. Sulfur cycle that involves human activity and soil microorganisms with the transfer of sulfur sources between the lithosphere, atmosphere, and hydrosphere.(Adapted from [3])

Although sulfur is common in the environment, some forms are inaccessible to living organisms.[1] To obtain sulfur, plants and bacteria utilize an inorganic sulfur source for the biosynthesis of the amino acid cysteine.[1] Plants can synthesize both cysteine and methionine, whereas animals can only synthesize cysteine.[7] In plants and microorganisms, methionine is synthesized from cysteine or homocysteine.[8,9,10,11] Methionine is synthesized by three convergent pathways that provide the carbon backbone of aspartate, sulfur atom of cysteine, and the methyl group from the β-carbon of serine.[12] For mammals, cysteine is essential for protein synthesis and is the primary source of reduced sulfur in lipoic acid, thiamin, coenzyme A, L-methionine, molybdopterin, and other organic molecules.[13]

These sulfur-containing cofactors are widely distributed and are essential in many biochemical reactions.[14] As the primary sulfur source for most sulfur-containing cofactors, cysteine is converted to alanine by cysteine desulfurase.[15] Cysteine desulfurase is a pyridoxal 5-phosphate-containing enzyme that produces persulfide (R-S-S-R) from the thiol (-SH) of cysteine

(Figure 1.2).[14] This persulfide is then incorporated into several sulfur-containing cofactors.[15] IscS is a cysteine desulfurase in *E. coli* that mobilizes sulfur for different biosynthetic pathways (Figure 1.2).[16,17,18] Sulfur acceptors of IscS such as ThiI, IscU, and TusA are further involved in the biosynthesis of thio-cofactors (Figure 1.3).[14] ThiI and IscU are both required for the synthesis of 4-thiourine modification of tRNA (s^4U) and thiamin.[19,20,21] Both pathways are initiated with the transfer reaction of a persulfide sulfur from IscS to ThiI.[21,22] TusA interacts with IscS and inserts sulfur into pyranopterin phosphate to generate molybdenum cofactors.[23,24] TusA is also involved in an additional pathway that generates a s^2U intermediate in the biosynthesis of 2-thiouridine.[25] IscU is part of the complex ISC system involved in Fe-S cluster biogenesis.[26] IscU can hold transient [2Fe-2S] and [4Fe-4S] clusters that are directly or indirectly transferred to apo-proteins.[27,28,29] The Fe-S clusters generated from IscU are a source of sulfur for the synthesis of other cofactors.[14] Enzyme BioB catalyzes the insertion of sulfur into the biotin cofactor using the sulfur from the 2Fe-2S cluster.[30] Biotin (vitamin B_1) is an enzymatic cofactor that is required for the transfer of carbon dioxide.[30] Lipoic acid is synthesized by enzyme LipA and is a cofactor utilized by pyruvate dehydrogenase and α-ketoglutarate dehydrogenase.[31] A [4Fe-4S] prosthetic group is also involved in the synthesis of 2-methylthio-N^6-isopentenyl-adenosine 37 of tRNA (ms^2i^6A) by MiaB that enhances base-pairing interactions between mRNA codons and tRNA by decreasing slippage and maintaining the ribosomal reading frame during translation.[32,33,34,35,36] Lastly, tRNA 2-thiocytidine synthetase (TtcA) catalyzes the sulfur insertion step that coordinates a (4Fe-4S) cluster.[37] This generates 2-thiocytidine (s^2C) which aids in tRNA structural stability and is important for translational fidelity and efficiency.[37,38]

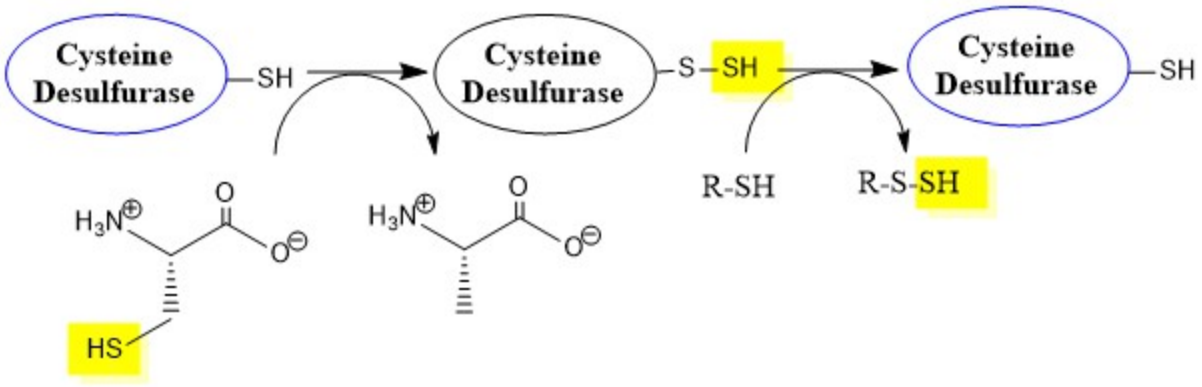

Figure 1.2. Catalyzation of free L-cysteine with cysteine desulfurase enzymes with persulfide formation.[14] Copyright © 2014 Elsevier B.V.

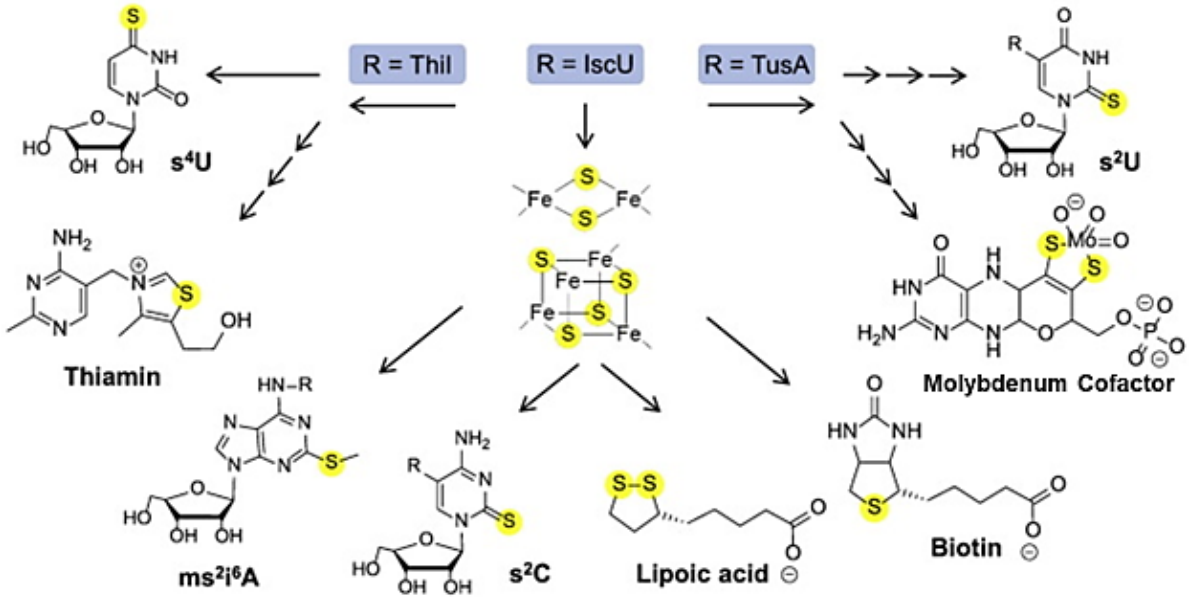

Figure 1.3. The three sulfur acceptors (ThiI, IscU, and TusA) and cofactors produced.[14] Copyright © 2014 Elsevier B.V.

1.1.2 Breakdown and Synthesis of Inorganic Sulfur in Bacteria in *E. coli*

Biosynthesis of cysteine begins with inorganic sulfate in microorganisms and plants.[39] Inorganic sulfur compounds that are utilized by *E. coli* include sulfate, sulfite, thiosulfate, and

sulfide.[39] The sulfur assimilation pathway in bacteria is required for sulfate reduction and synthesis of cysteine (Figure 1.4). The synthesis of cysteine from inorganic sulfur is catalyzed by proteins expressed from the *cys* operon.[39] Cysteine synthesis begins with the uptake of inorganic sulfur by CysU and CysW that form a transport channel, membrane-associated enzyme CysA, and the sulfate-thiosulfate permease binding protein CysP.[39] Once sulfate is transported into the cell, ATP sulfurylase enzymes CysD and CysN synthesize adenosine 5'-phosphosulfate (APS) and PP_i from ATP and sulfate. Following APS formation, APS kinase (CysC) utilizes a second ATP molecule to phosphorylate the 3'OH position of APS.[39] This phosphorylation of APS produces 3-phosphoadenylsulfate (PAPS) and ADP.[39] Once PAPS is generated, the PAPS sulfotransferase (CysH) reduces PAPS to produce sulfite.[39] The sulfite is then reduced to sulfide by enzymes CysI, CysJ, and CysG.[39] Finally, the sulfite is condensed with O-acetyl-L-serine by enzymes CysK and CysM to produce L-cysteine.[39]

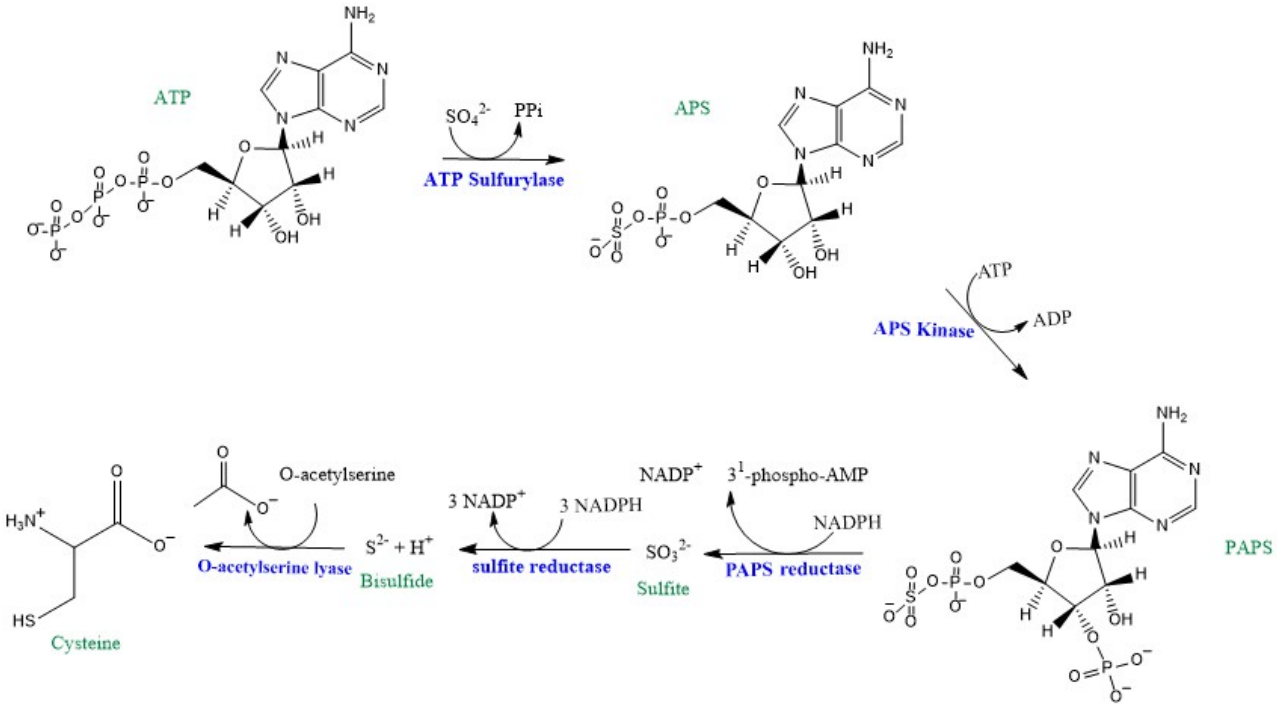

Figure 1.4. Biosynthesis of cysteine. (Adapted from[40,41])

1.1.3 Alternative Pathways for the Assimilation of Inorganic Sulfur

Along with *E. coli*, other organisms such as *Pseudomonas aeruginosa*, and *Pseudomonas putida* all have proposed mechanisms for sulfur assimilation. Both *P. aeruginosa* and *P. putida* synthesize cysteine directly from sulfide and O-acetyl-L-serine by O-acetyl-L-serine sulfhydrylase similar to *E. coli*.[39] In addition, *P. aeruginosa* catalyzes the sulfhydrylation of O-succinyl-L-homoserine to generate homocysteine. The homocysteine can be converted to cystathionine by cystathionine β-synthase, and cystathionine is then converted to cysteine, ammonia, and 2-oxobutyrate.[42,43] *P. aeruginosa* is also able to utilize methionine for the biosynthesis of cysteine through a reverse transsulfuration pathway.[44]

1.1.4 Utilization of Organosulfur when Inorganic Sulfur is Limiting

Sulfur compounds are found in diverse environments. Organically bound sulfur compounds exist as sulfate esters in grassland soils or sulfonates in forest soils.[45, 46] Examples of organically bound sulfur compounds include sulfonates, sulfate esters, methionine, sulfamates, organosulfides, or thioethers.[1] Sulfonates have been found in all soil strata and may be derived from plant sulfonolipid, the oxidation products of low molecular weight thiol compounds, or by the addition of sulfide to carbon-carbon double bonds.[47] Organic and inorganic sulfur compounds are also common in water environments such as streams, water columns, and lake outlets.[48] Sulfonates or ester sulfates comprise between 1-18% of the total sulfur compounds found in water systems.[48] Many bacteria will utilize sulfonates as a primary sulfur source when inorganic sulfate is limiting.

Bacteria are usually grown within the lab with either excess inorganic sulfate provided by mineral salts or complex media that contains sulfate and amino acid sulfur derived from cell

hydrolysates.[1] Bacteria express specific proteins in the absence of these inorganic sulfur compounds.[1] These set of proteins are categorized as sulfate starvation-induced proteins (SSI proteins).[1] The proteins expressed are involved in the transport of organosulfur compounds, sulfur acquisition enzymes, and enzymes that protect the organism from reactive oxygen species.[49,50,51] SSI proteins were first identified in *E. coli* grown in minimal media with alternative sulfur compounds other than sulfate or cysteine as the sole sulfur source.[50] Further studies identified two operons that expressed SSI proteins when *E. coli* was grown in media supplemented with sulfonate compounds, and were classified as the *ssu* and *tau* operon.[52, 53] The operons express enzymes involved in the desulfonation of alkanesulfonate compounds, and transporters specific for the cellular transport of their respective substrates.

The α-ketoglutarate-dependent taurine dioxygenase (TauD) from *E. coli* is expressed from the tau operon and catalyzes the oxidation of taurine to produce sulfite (Figure 1.5).[54] The enzyme TauD produces an intermediate product, hydroxytaurine, which is unstable.[54] The unstable intermediate undergoes desulfonation to form aminoacetaldehyde and sulfite.[54] One of the oxygen atoms is used to hydroxylate the substrate while the second is transferred to α-ketoglutarate.[54] The TauD enzyme not only is involved in the desulfonation of taurine, but also can desulfonate short-chain alkanesulfonates (C_4-C_6).[54]

Another set of enzymes that are expressed when sulfur is limiting is SsuE and SsuD from *E. coli*. The SsuE flavin reductase is responsible for providing reduced flavin to the monooxygenase SsuD that catalyzes the cleavage of C-S bonds in linear alkanesulfonates (Figure 1.6).[53] The SsuD monooxygenase has a broad substrate range and is able to catalyze the desulfonation of C_2-C_{10} alkanesulfonates, sulfonate buffer (HEPES, MOPES, or PIPES), and 1,3-dioxo-2-isoindolineethanesulfonic acid producing sulfite and the corresponding aldehyde.[53]

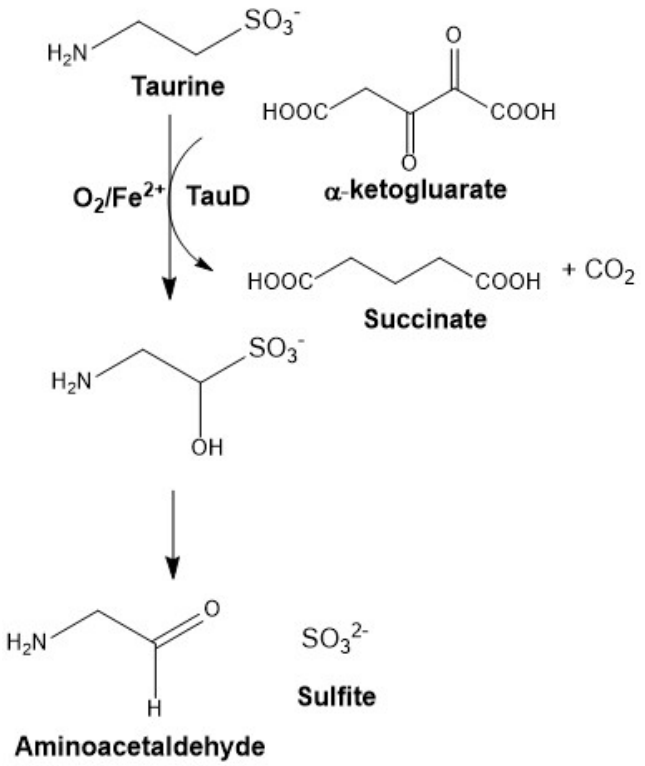

Figure 1.5. Taurine desulfonation with α-ketoglutarate-dependent taurine dioxygenase (TauD) from *Escherichia coli*.(Adapted from [54])

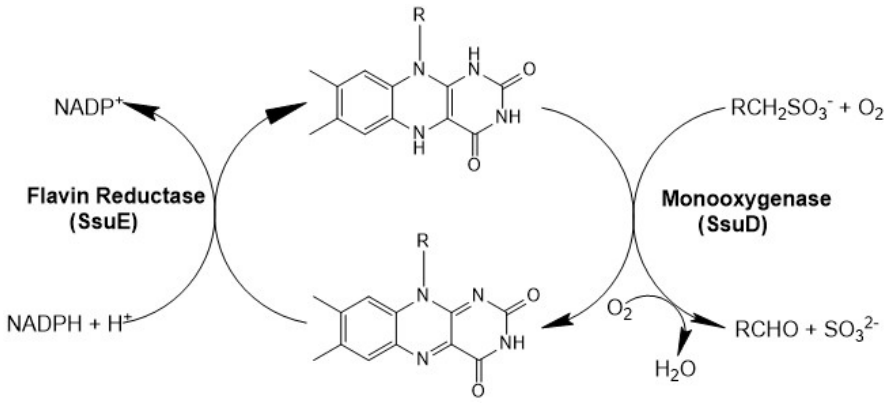

Figure 1.6. Desulfonation of linear alkanesulfonates with FMN-dependent two-component system SsuED.(Adapted from [53])

1.1.5 The *ssu* Operon

The *ssu* operon has been identified in diverse bacterial phyla, demonstrating its physiological importance in maintaining adequate sulfur levels. Genetic organization for several *ssu* operons have been determined in *E. coli*, *P. aeruginosa*, and *P. putida* (Figure 1.7).[55] The operons from these organisms consist of a flavin reductase (SsuE) and a monooxygenase (SsuD) that cleave the carbon-sulfur bond of linear alkanesulfonates. Both *P. aeruginosa* and *P. putida* also encode an *ssuF* gene whose function has not been identified.[55]

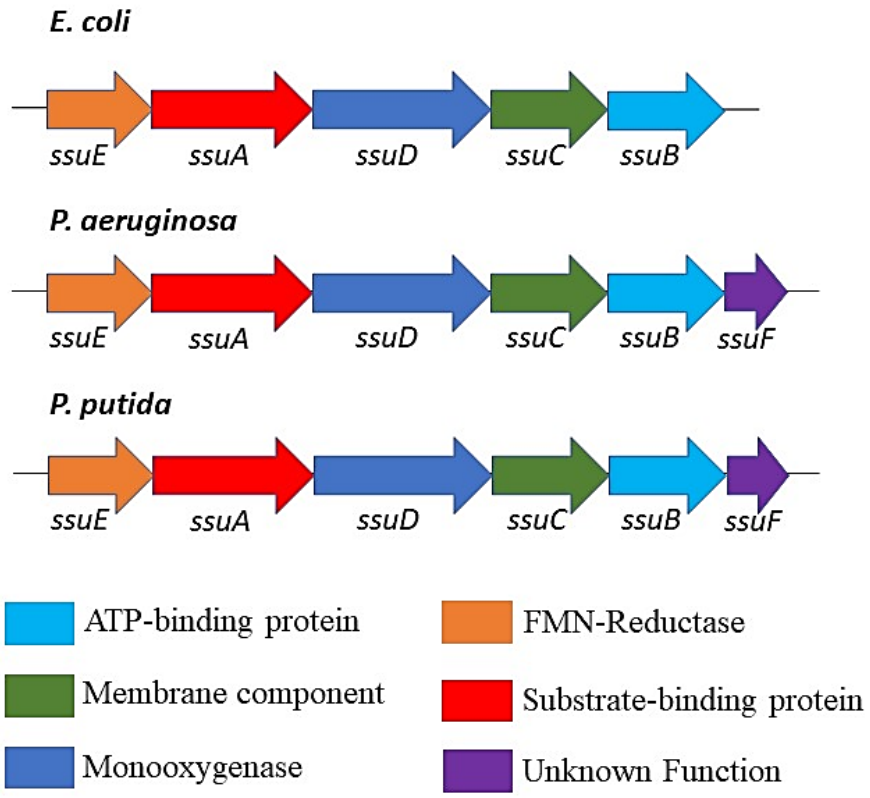

Figure 1.7. *ssu* genes from *E. coli*, *P. aeruginosa*, and *P. putida*.(Adapted from [1])

The *ssu* operons all encode an ABC-type transport system (Figure 1.8).[56] These SsuABC proteins belong to the ATP-binding cassette transporter superfamily. ABC transporters are found

in all organisms and are responsible for substrate uptake.[56] Substrates include amino acids, sugars, vitamins and large organic compounds.[56] ABC transporters pump substrates against a chemical gradient, which requires the hydrolysis of ATP.[56] The SsuABC transport system catalyzes the uptake of alkanesulfonates.[56] SsuA functions as the periplasmic sulfonate binding protein.[56] SsuB is structurally analogous to ATP-binding proteins, and SsuC is similar to integral membrane components.[56]

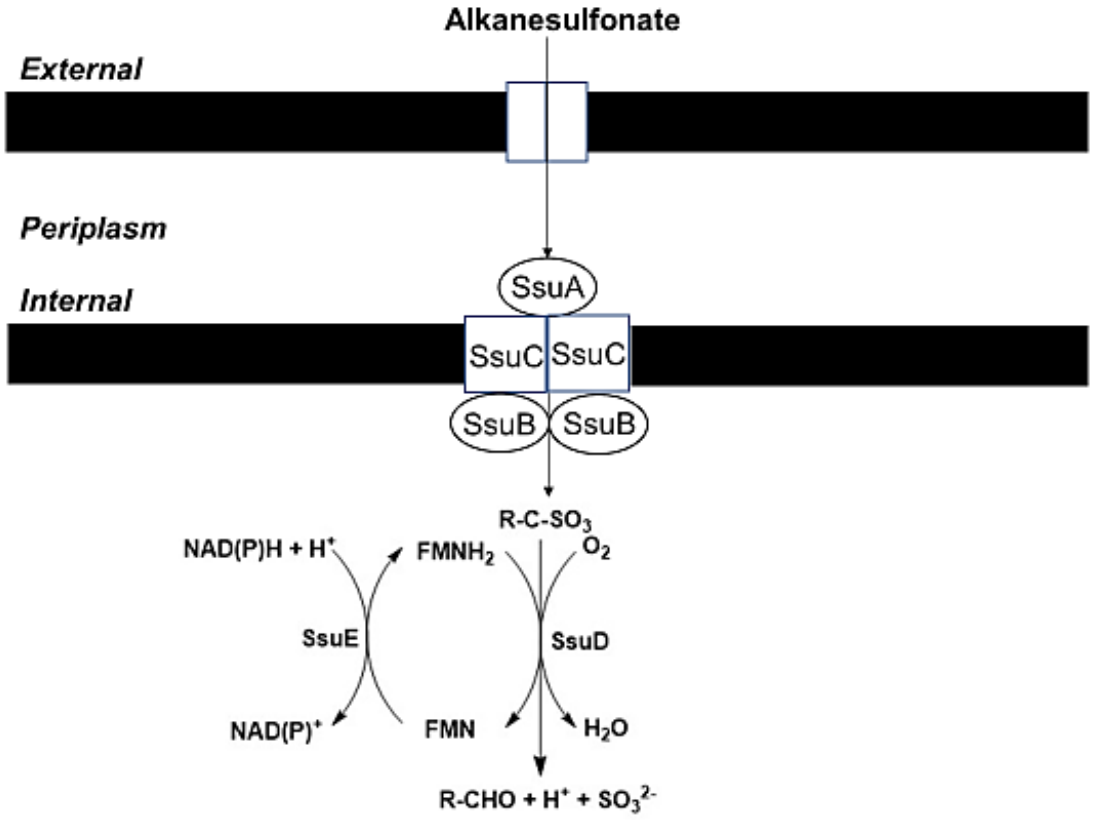

Figure 1.8. The uptake and desulfonation of alkanesulfonates with that involve the ABC-type transport system. (Adapted from [56])

1.1.6 The Regulation of the *ssu* Operon

The genes involved in cysteine biosynthesis and those of organosulfur metabolism require sulfate-limiting conditions for full expression.[1] Regulation of the genes involved in maintaining sulfur homeostasis in *E. coli* involve the LysR-type transcriptional regulator, CysB.[57] As a class 1 transcriptional activator, the CysB protein binds to the promoter region of operons expressing proteins involved in cysteine biosynthesis (*cys* operon) and sulfur assimilation (*tau* operon).[58] CysB is also involved in acid resistance in *E. coli* and alginate biosynthesis in *P. aeruginosa* in addition to regulating cysteine biosynthesis and organosulfur metabolism.[59,60]

There are two different regulation levels of control described for CysB. First, *N*-acetylserine is an inducer of CysB, and the concentrations of *N*-acetylserine in the cell are regulated by cellular cysteine levels.[61] Cysteine, the end product of the cysteine biosynthesis pathway, exerts feedback inhibition of serine transacetylase.[61] The serine transacetylase converts serine to O-acetylserine. *O*-acetylserine is not stable under alkaline conditions and is isomerized to *N*-acetylserine. Therefore, when cysteine levels are elevated, *N*-acetylserine is not produced and CysB is not activated.[61] The second level of control involves sulfide and thiosulfate.[61] Both sulfide and thiosulfate act as anti-inducers for *cys* regulation by competing with *N*-acetylserine for binding to the CysB-DNA complex.[61] Although sulfate does not initiate expression itself, expression of the *cys* genes is initiated when sulfur is limiting since there is a conversion of sulfate to sulfide and cysteine.[57] Sulfide will repress the expression of enzymes that catalyze the activation of sulfate to PAPS.[62]

Expression of the *ssu* operon in *E. coli* requires the Cbl transcriptional regulator (Figure 1.9).[13,63] Expression of Cbl is regulated by CysB with CysB binding to the promoter region of the *cbl* gene.[64] The Cbl protein regulates the expression of sulfate starvation-induced proteins such as

sulfate binding protein Sbp and acetylserine (thiol) lyase CysK.[57] Cbl and the *N*-acetylserine inducer activates transcription of the *ssu* and *tau* operon in *E. coli*.[63,53, 57] Therefore, although CysB is not directly involved in the expression of *ssu*, Cbl is expressed through CysB activation (Figure 1.9).[63]

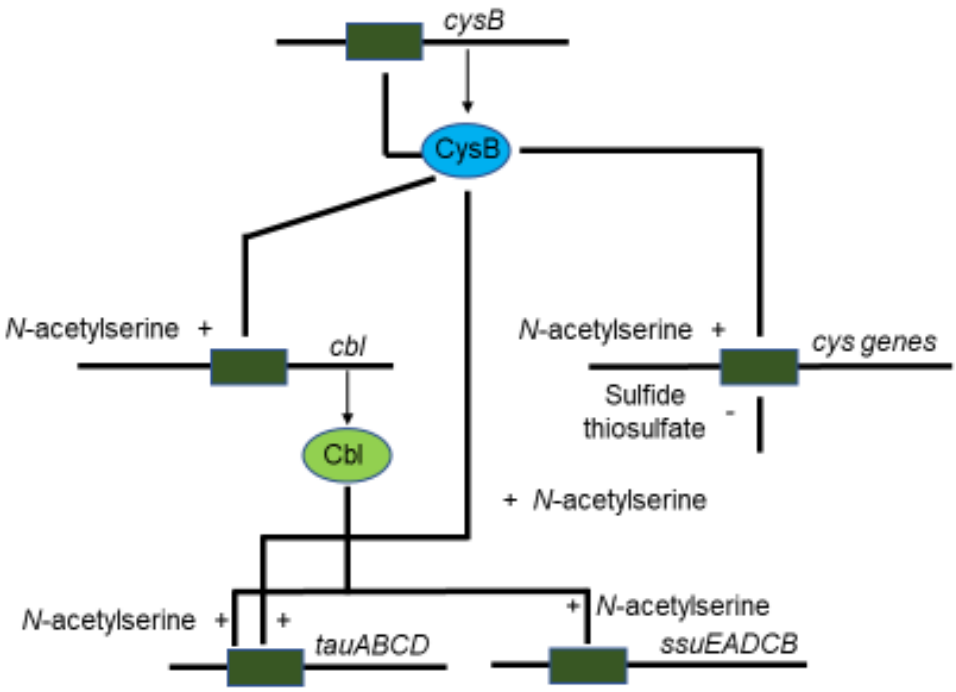

Figure 1.9. Regulation of the organosulfur assimilation pathways in *E. coli*.(Adapted from [1])

1.1.7 Sulfur Utilization in *Pseudomonas Sp.*

Although there are numerous ways of sulfur reaching the atmosphere such as volcanic SO_2 and H_2S, sulfate dust, sea sulfate, native sulfur, and organic sulfur compounds, dimethyl sulfide is the most abundant sulfur compound in the atmosphere.[2] Dimethylsulfoniopropionate (DMSP) is an important organic sulfur produced in marine environments from phytoplankton and bacteria.[65] There are two major pathways in which DMSP can be catabolized. The first in the demethylation pathway that removes the methyl groups, producing acetyldehyde that is further oxidized to acetate

and methanethiol.[66] The second pathway, the cleavage pathway, involves the degradation of DMSP to produce a volatile product dimethylsulfide (DMS).[67] DMS plays an important role in global biogeochemical cycles of the sulfur element between land and sea.[67] Once emitted into the atmosphere, DMS is oxidized to dimethyl sulfoxide (DMSO) and dimethylsulfone ($DMSO_2$).[67]

Compared with *E. coli*, *Pseudomonas sp.* are able to utilize a more diverse range of organosulfur compounds when sulfur is limiting in the environment. The *sfnABFG* genes expressed in *P. putida* (Figure 1.10) have been linked to both $DMSO_2$ and methanethiol utilization. The FMN-dependent two-component system involves a monooxygenase (SfnG) and a flavin reductase (SfnF) that coverts $DMSO_2$ to methanesulfinate (Figure 1.11).The metabolic function of the *sfnAB* genes remains unknown, but *sfnA* transposon mutants were unable to grow with methanethiol as a sulfur source.[68] Methanethiol in *P. putida* is formed from the breakdown of methionine by methionine γ-lyase. Other *sfn* genes expressed during sulfur limitation in *P. putida* are the *sfnECR* operon.[69] SfnE is a possible flavin reductase, and SfnC is classified as a monooxygenase.[69] The *sfnECR* operon encodes a transcription regulator for the expression of *sfnABFG*. *P. aeruginosa* only expresses the *sfnG* gene, and the partner *sfnF* reductase has not been identified.[68, 70, 71]

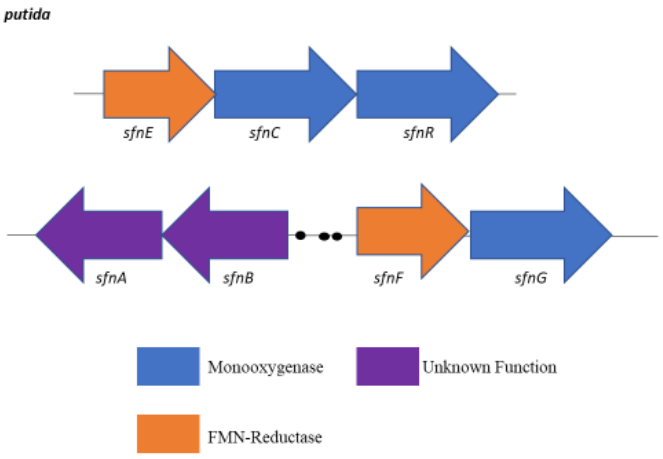

Figure 1.10. *sfn* genes from *Pseudomonas putida* with binding sites for SfnR with three DNA regions (sites 1,2, and 3) that are located between the *sfnAB* and *sfnFG* genes.(Adapted from [68])

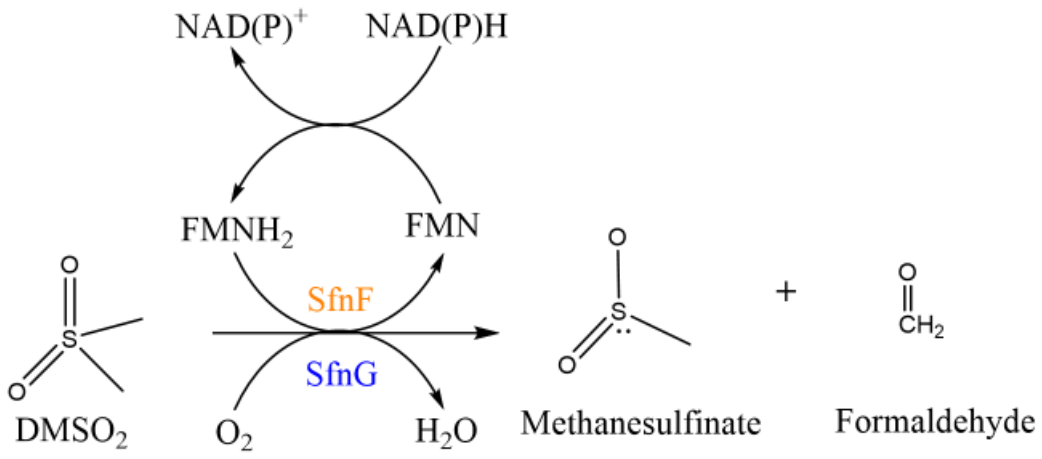

Figure 1.11. The FMN-dependent two-component system that involves a monooxygenase (SfnG) and a flavin reductase (SfnF) which converts $DMSO_2$ to methanesulfinate. (Adapted from [68])

Another two-component system that is synthesized by *P. aeruginosa* and *P. putida* when sulfur is limiting is the *msu* operon which consists of a flavin reductase (MsuE) and two monooxygenase enzymes (MsuC and MsuD) (Figure 1.12). The MsuE enzyme supplies reduced flavin ($FMNH_2$) to MsuC to convert methanesulfinate to methanesulfonate with the insertion of an oxygen atom (Figure 14). The MsuE flavin reductase has ~29% amino acid sequence identity with SsuE from *E coli*.[72] MsuC has 52% amino acid sequence identity with the FMN-dependent DBT (dibenzothiophene) monooxygenase from *Rhodococcus erythropolis* involved in degradation of dibenzothiophene.[72] MsuD catalyzes the desulfonation of methanesulfonate utilizing the reduced flavin provided by MsuE to produce the sulfite product and formaldehyde (Figure 1.13).[72, 73] MsuD shares ~60% amino acid sequence identity with SsuD. It has been hypothesized that the *msu* operon may have evolved from the *ssu* operon to enable soil bacteria to utilize methanesulfonate as a sulfur source.[72] Unlike the *ssu* operon, the *msu* operon does not encode an ABC-transport system.[71]

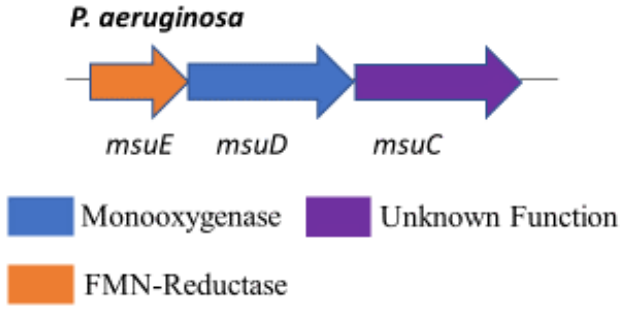

Figure 1.12. *msu* genes from *Pseudomonas aeruginosa*. (Adapted from [72])

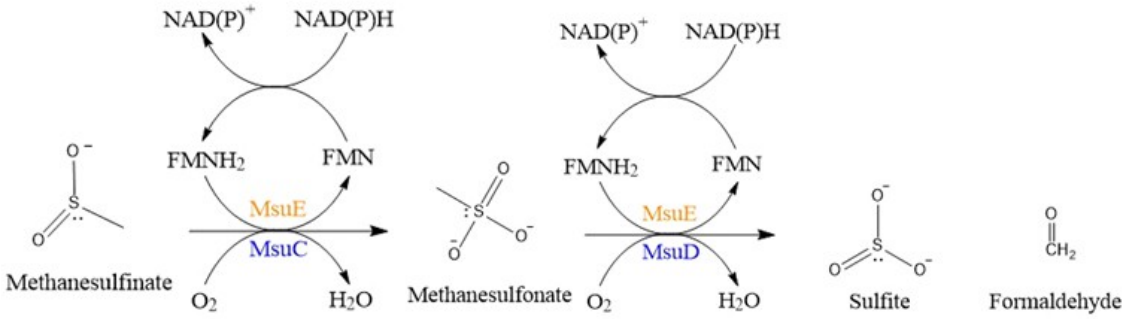

Figure 1.13. The FMN-dependent two-component system MsuEDC consists of an MsuE enzyme that interacts and supplies reduced flavin to both MsuC and MsuD. The two-component systems are responsible for the conversion of methanesulfinate to sulfite.[72, 73]

In *P. putida*, a response for sulfur limitation is initiated by SfnR, which is activated in response to DMS, DMSO, and $DMSO_2$.[71] SfnR is expressed from the *sfnECR* operon by CysB. SfnR interacts with σ^{54}-RNA polymerase to activate the *sfnFG* and *sfnAB* involved in sulfur acquisition.[68,69] The SfnR binds to three promoter regions (sites 1, 2, and 3) located between the *sfnAB* and *sfnFG* genes.[68] Site 1 is involved in the expression of the *sfnFG* genes, whereas the roles of sites 2 and 3 are still unknown, although it is postulated that these sites are involved in the expression of the *sfnAB* genes.[68]

In *P. aeruginosa*, there are two transcriptional regulators (SfnR1 and SfnR2) that promote the expression of the *msu* operon and *sfnG* gene.[71] SfnR1 is expressed from the same operon as *msuEDC*.[71] The gene for *sfnR2* is located near the *msuEDC* operon separated by a single hypothetical protein, and is activated by CysB in response to low sulfur levels. SfnR2 then activates the transcription of the *msuEDC-sfnR1* operon and *sfnG*.[71] Once expressed, SfnR1 contributes to the expression of *msuEDC-sfnR1*, *sfnG*, and additional target genes involved in DMS-related metabolism in *P. aeruginosa* PAO1.

1.2 Two-Component Systems

1.2.1 Reactions of Two-Component Systems

Two-component flavin-dependent systems consist of a flavin reductase and monooxygenase. Both the flavin reductase and monooxygenase in two-component systems are often found within the same operon.[74] All monooxygenases rely on the flavin reductase to supply reduced FMN or FAD for activity (Figure 1.14). Once the flavin reductase successfully transfers reduced flavin to the partner monooxygenase, the monooxygenase utilizes reduced flavin to activate molecular oxygen for the oxygenation of substrates.[74] The two-component flavin-dependent systems catalyze a broad range of reactions from bacterial bioluminescence, desulfonation of organosulfur compounds, antibiotic biosynthesis, and the degradation of synthetic compounds in the environment.[75]

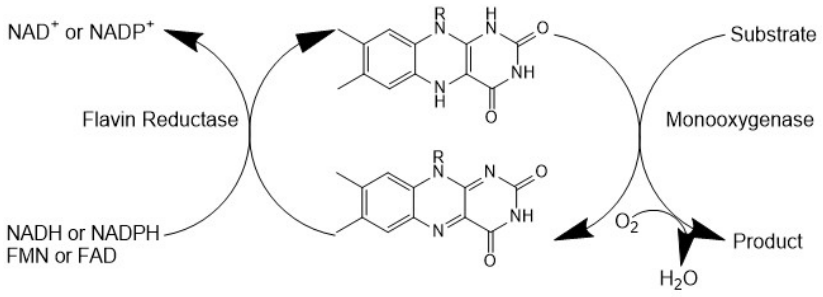

Figure 1.14. General Two-component system mechanism.(Adapted from [75])

Multiple two-component systems have been identified with bacterial luciferase being the first monooxygenase extensively characterized (Figure 1.15). Bacterial luciferase utilizes reduced flavin to produce aliphatic carboxylic acid, and blue-green light from long-chain aliphatic aldehyde substrates (Figure 1.15A).[76,77,78,79] LadA from *Geobacillus thermodentrificans* catalyzes the initial reaction in the terminal oxidation pathway of long-chain alkanes (C15-C36) to produce a primary alcohol (Figure 1.15B).[80,81] Enzymes EmoA and EmoB (*Mesorhizobium spp*, and *Agrobacterium spp*.) catalyze the degradation of EDTA (ehylenediaminetetraacetate) (Figure 1.15C).[82] The flavin reductase EmoB supplies reduced flavin to the monooxygenase EmoA which oxidizes EDTA to ethylenediaminetriacetate (ED3A) and glyoxylate.[83,84] The ED3A substrate is further oxidized to ethylenediaminediacetate.[83] Other monooxygenases found in two-component systems include enzymes involved in dibenzothiophene (DBT) desulfurization.[85] The desulfurization pathway utilizes two different monooxygenases, DszC and DszA with both using a single flavin reductase (Figure 1.15D).[85] Monooxygenase DszC is involved with the conversion of DBT to DBT sulfone while monooxygenase DszA converts DBT sulfone to 2-hydroxybiphenyl-2-sulfinate.[85] The ActVA enzyme (*Streptomyces coelicolor*) catalyzes the hydrolysis of dihydrokalafungen to produce actinorhodin (Figure 1.15E).[86,87,88] Monooxygenase SnaA (PII_A synthase) in *Streptomyces sp*. catalyzes the oxidation of the dehydroproline functional group in PII_B to form PII_A

(polyunsaturated cyclic peptolide pristinamycin II_A) (figure 1.15F).[89,90] Hydrolation with either FAD or FMN from a flavin reductase of p-hydroxyphenylacetate (HPA) to 3,4-dihydroxyphenylacetate (DHPA) is catalyzed by the C_2 of HPA hydroxylase from *Acinetobacter baumannii* (Figure 1.15G).[91] With a Mg^{2+}-NTA complex, monooxgenase NtaA from *Chelatobacter heintzii* ATCC 29600 catalyzes the conversion of nitrilotriacetate (NTA) to iminodiacetate and glyoxylate (Figure 1.15H).[92,93,94]

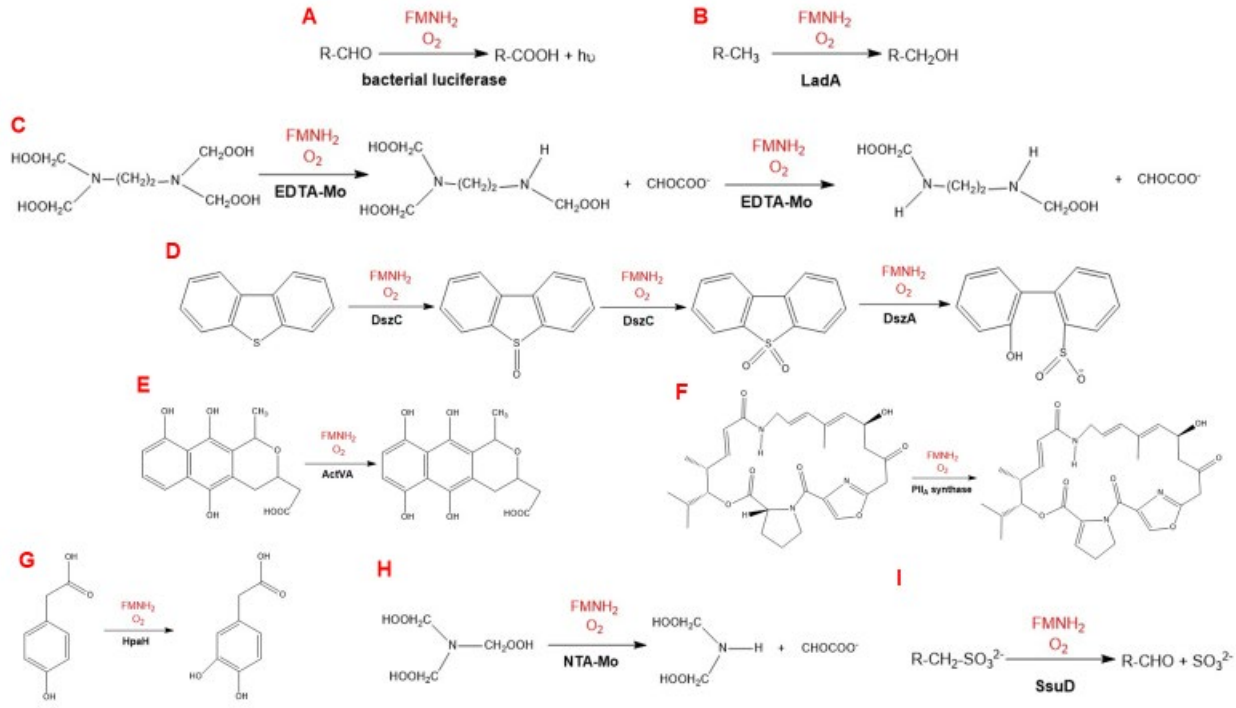

Figure 1.15. Reactions catalyzed by the FMN-dependent monooxygenase systems.(Adapted from [74])

Many of the enzymes important in sulfur acquisition are two-component systems.[52] The two-component FMN-dependent monooxygenases involved in sulfur metabolism depend on the flavin reductase for reduced flavin in order to catalyze the desulfonation of alkanesulfonates (Figure 1.15I). The alkanesulfonate monooxygenase two-component system cleaves the C-S bond of alkanesulfonates to produce sulfite and the corresponding aldehyde.[53] In addition to the

alkanesulfonate monooxygenase system, *Pseudomonas sp.* have additional pathways and reaction mechanisms for sulfur acquisition. These organisms are able to use $DMSO_2$ as a sulfur source by converting $DMSO_2$ to sulfite and formaldehyde (Figure 1.16).[95] The flavin reductase SfnF partners with the SfnG monooxygenase to catalyze the conversion of dimethylsulfone to methanesulfinate (Figure 1.16A).[96] The MsuE enzyme supplies reduced flavin to MsuC to convert methanesulfinate to methanesulfonate with the insertion of an oxygen atom (Figure 1.16B). Desulfonation of methanesulfonate occurs by MsuD utilizing the reduced flavin provided by MsuE to produce the sulfite product and formaldehyde (Figure 1.16C).[72, 73] The high amino acid sequence identify and structural similarities between the flavin reductases (SsuE/MsuE/SfnF) and monooxygenases (SsuD/MsuD/SfnG and MsuC/DszC) involved in sulfur acquisition suggest they may utilize similar mechanistic approaches for sulfur acquisition.

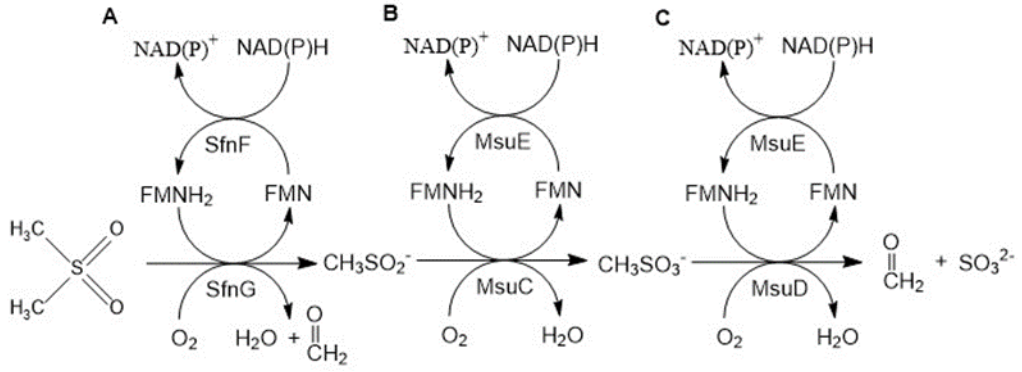

Figure 1.16. Proposed Sulfur Acquisition Pathway for SnfFG and MsuEDC.

1.3 Flavins

1.3.1 Flavin Properties

Two-component systems in sulfur acquisition are FMN-dependent, and all biologically important flavins are derived from riboflavin (7,8-dimethylisoalloxazine) (Figure 1.17).[97] Riboflavin is also known as vitamin B_2 and is a heterocyclic isoalloxazine derivative with a ribityl side chain. Riboflavin is biosynthesized by plants and many microorganisms, but animals must obtain riboflavin in their diet.[98] Riboflavin is the central source for flavin derivatives and was purified from milk in 1879.[99] All flavins contain an isoalloxazine ring but differ in the R-groups at the N10 position (Figure 1.17). Lumiflavin is the smallest flavin derivative with a methyl group located at the N10 position.[100] Riboflavin is characterized with a ribityl sugar side chain while FMN has a similar ribityl sugar side chain but with the addition of a phosphate group at the C5-position of the ribityl chain. FAD contains an adenine dinucleotide group attached to the ribityl chain. Flavins are versatile and are found to be utilized by flavoproteins. Through additional biosynthetic reactions, riboflavin is converted to flavin mononucleotide (FMN) and flavin adenine dinucleotide (FAD).

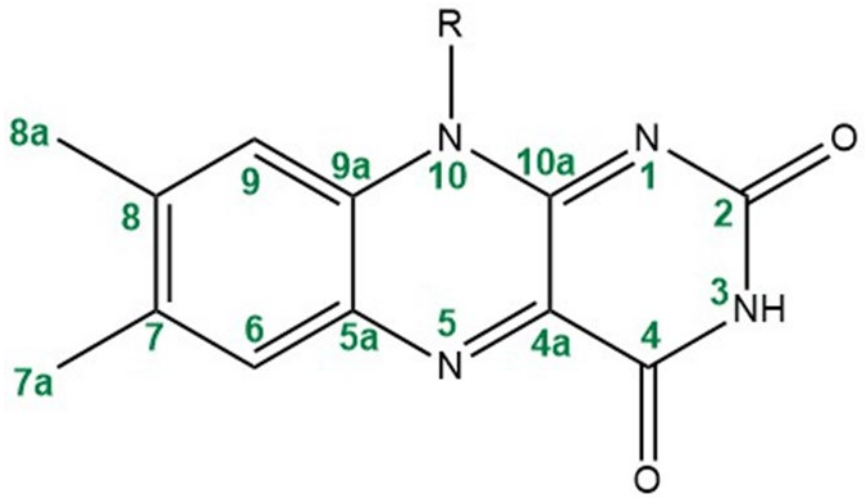

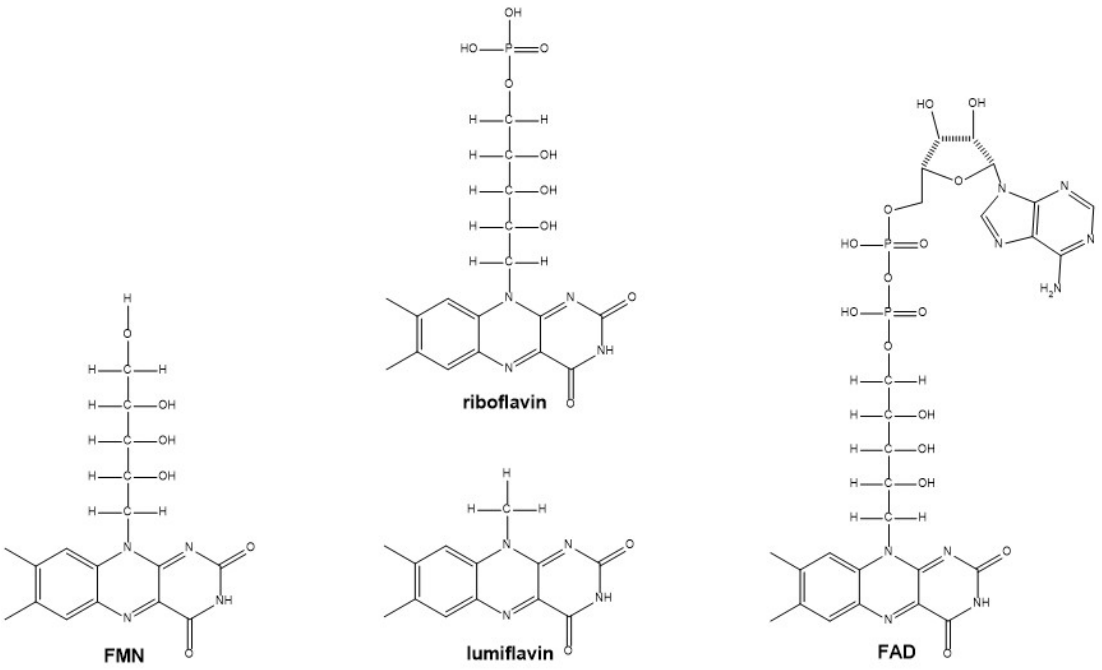

Figure 1.17. Numbering of the isoalloxazine ring and the structures of flavins found in nature.

1.3.2 Synthesis of Flavins In many bacteria and plants, the pathway for ribosome biosynthesis is unknown. Studies have shown that some of the reactions in the biosynthesis of riboflavin are nonenzymatic and do not require enzymes for synthesis.[101, 102,103] Both bacteria and plants possess the bifunctional GTP cyclohydrolase II and 3,4-dihydroxy-2-butonone 4-phosphate synthase.[98] The initial pathway of riboflavin biosynthesis begins with one molecule of GTP and two molecules of ribulose 5-phosphate (Figure 1.18).[98,104,105,106,107,108] GTP cyclohydrolase (step I) catalyzes the release of pyrophosphate generating 2,5-diamino-6-ribosylamino-2,4(3H)-pyrimidinone 5′-phosphate (2).[106, 108] In eubacteria and plants, deamination of 2,5-diamino-6-ribosylamino-2,4(3H)-pyrimidinone 5′-phosphate occurs first (step II) followed by the reduction of 5-amino-6-ribosylamino-2,4(1H,3H)-pyrimidinone 5′-phosphate (step III).[101, 109] In Archaea and fungi, the 2,5-diamino-6-ribosylamino-2,4(3*H*)-pyrimidinone 5′-phosphate (2) intermediate is reduced first (step IV)

followed by the deamination step (step V).[110] The dephosphorylation (step VI) of 5-amino-6-ribitylamino-2,4(1H,3H)-pyrimidinedione phosphate (5) occurs and produces 5-amino-6-ribitylamino-2,4(1H,3H)-pyrimidinedione (6).[111,112,113,101,110,109,114,115] Skeletal rearrangement between ribulose 5-phosphate (7) generates 2,4-dihydroxy-2-butanone 4-phosphate (8), which is catalyzed by 3,4-dihydroxy-2-butanone 4-phosphate synthase (step VII).[98] The 5-amino-6-ribitylamino-2,4(1H,3H)-pyrimidinedione (6) intermediate condenses with 2,4-dihydroxy-2-butanone 4-phosphate (8) to form 6,7-dimethyl-8-ribityllumazine (9) (step VIII).[114,116,117,118,119] Riboflavin is synthesized from the dismutation of 2 molecules of 6,7-dimethyl-8-ribityllumazine (9) by riboflavin synthase (step IX).[98,120,121,122,123,124,125] One of the molecules is utilized to form riboflavin (10) while the other 6,7-dimethyl-8-ribityllumazine forms 5-amino-6-ribitylamino-2,4(1H,3H)-pyrimidinedione (6).[120,121,122,123,124,125] Once riboflavin is synthesized, riboflavin kinase and FAD synthetase are required to produce flavin mononucleotide (FMN) (11) and flavin adenine dinucleotide (FAD) (12).[126] Organisms including animals, plants, fungi, and most prokaryotes can synthesize the flavin nucleotides FMN and FAD.[127] There are two groups of riboflavin kinases with one group represented in fungi, plants, animals, archaea, and eubacteria by monofunctional riboflavin kinase proteins and the other as bifunctional riboflavin kinase and FAD synthetase in eubacteria and plants.[128,129,130,131,132,133,134,135,136,137] The riboflavin kinase utilizes riboflavin and ATP as substrates with conversion of riboflavin to FMN irreversibly, whereas conversion of FMN to FAD is reversible.[138, 139] FAD synthesis is catalyzed by FAD synthetase or FMN adenyltransferase that catalyze the transfer of adenylyl moieties from ATP to FMN.[140] Eukaryotic organisms only possess

monofunctional FAD synthetases, whereas bacteria have FAD synthetases that act as part of bifunctional riboflavin kinase and FAD synthetase.[141, 142]

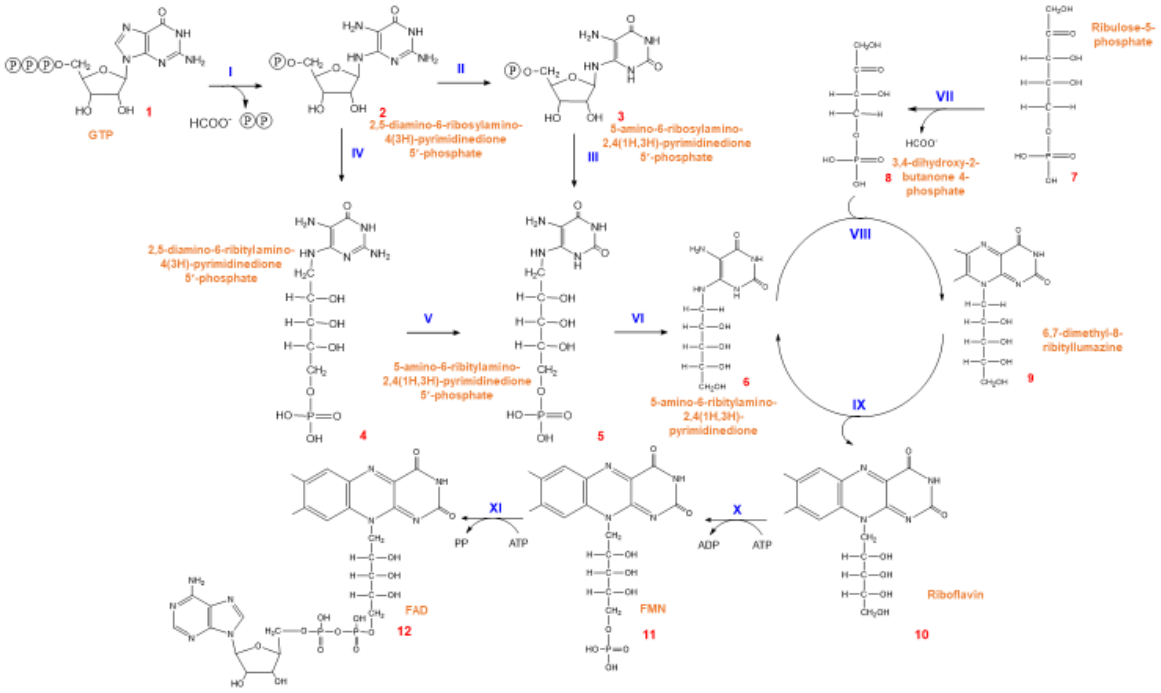

Figure 1.18. Biosynthesis of riboflavin and flavocoenzymes. The enzymes involved in flavin biosynthesis include GTP cyclohydrolase II (I), 2,5-diamino-6-ribosylamino-4(3*H*)-pyrimidinone 5′-phosphate deaminase (II), 5-amino-6-ribosylamino-2,4(1*H*,3*H*)-pyrimidinone 5′-phosphate reductase (III), 2,5-diamino-6-ribosylamino-4(3*H*)-pyrimidinone 5′-phosphate reductase (IV), 2,5-diamino-6-ribosylamino-4(3*H*)-pyrimidinone 5′-phosphate deaminase (V), Hypothetical phosphatase (VI), 3,4-dihydroxy-2-butanone 4-phosphate synthase (VII), 6,7-dimethyl-8-ribityllumazine synthase (VIII), Riboflavin synthase (IX), Riboflavin kinase (X), and FAD synthetase (XI). (Adapted from [98])

1.3.3 Spectral and Redox Properties

Spectra have been recorded of the different redox, ionic, and charge-transfer states of flavin with the different chemical properties associated with each flavin form (Figure 1.19).[143] The oxidized flavin has a bright yellow color with a signature spectrum at 450 nm.[144] However, there is a color change from yellow to red (neutral semiquinone) or to blue (anionic semiquinone) observed with a one-electron reduction.[145] The neutral and anionic forms absorb at 580 nm and 370 nm, respectively.[146] The fully reduced hydroquinone is a colorless solution with no absorbance past 400 nm.[146]

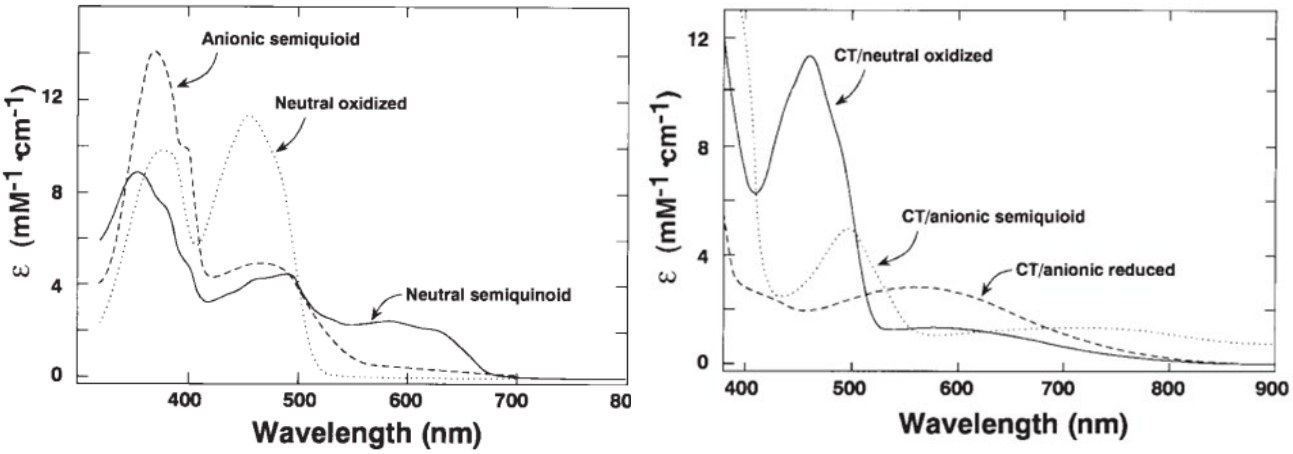

Figure 1.19. Absorption spectra of D-amino acid oxidase at different states of flavin. Top: Neutral oxidized (dotted line), anionic semiquinone (dashed line), and neutral semiquinone (solid line). Bottom: Charge transfer states that occur in different environments in enzymes with neutral oxidized (solid line), anionic semiquinone (dotted line), and anionic reduced flavin (dashed line).[143] Copyright © 2001 John Wiley & Sons, Inc. and The Japan Chemical Journal Forum

Flavin has been characterized to have three redox states.[143] These redox states are oxidized, one-electron reduced radical semiquinone, and two-electron fully reduced hydroquinone.[143,126] Each redox form of the flavin can exist in different protonated-deprotonated or ionic states.[143,126] Out of the nine forms, the neutral and anionic forms have been shown to be physiologically relevant (Figure 1.20).[143] The cationic forms can be observed at extremely low pH values. different redox/ionic states and the charge-transfer states of flavins can be identified by their distinct absorbance spectrum.[143]

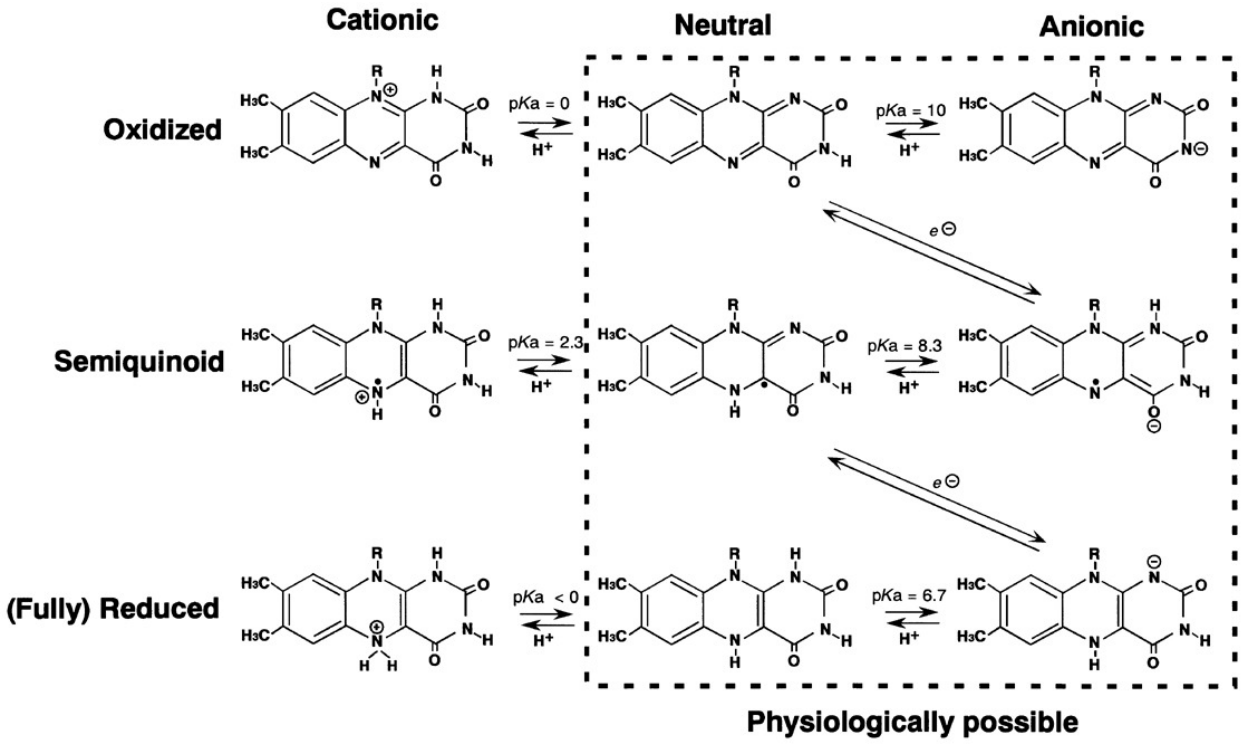

Figure 1.20. The different redox and ionic states of flavin.[143] Copyright © 2001 John Wiley & Sons, Inc. and The Japan Chemical Journal Forum

Flavoproteins can utilize flavin and participate in one-electron or two-electron redox processes.[143] Flavoproteins are divided into four subgroups: oxidases, dehydrogenases, reductases, and oxygenases. Oxidases oxidize substrates in the presence of molecular oxygen, producing

hydrogen peroxide. Flavin dehydrogenases transfer a pair of electrons and a proton from the substrate to the bound flavin cofactor to form the dehydrogenated product. Flavin oxygenases are involved insertion of an oxygen atom from molecular oxygen into an organic substrate. Flavin reductases catalyze the reduction of flavin in the presence of NAD(P)H to form reduced flavin.

1.4 Reductases

1.4.1 Structural Properties

Most flavin reductases belong to the flavodoxin-like superfamily.[147] The enzymes in this family share the α/β topology with an α-β-α sandwich (Figure 1.21).[147, 148] The typical flavodoxin fold consists of five central parallel beta-strands (β2-β1-β3-β4-β5) flanked by two α-helices (α2a and α2b) between β1 and β2 (Figure 19).[147] The α-β-α sandwich is considered to be one domain while the second domain consists of an excursion domain that extends outward forming the dimer interface.[74] The family utilizes flavin as a substrate in order to catalyze their respective reactions.

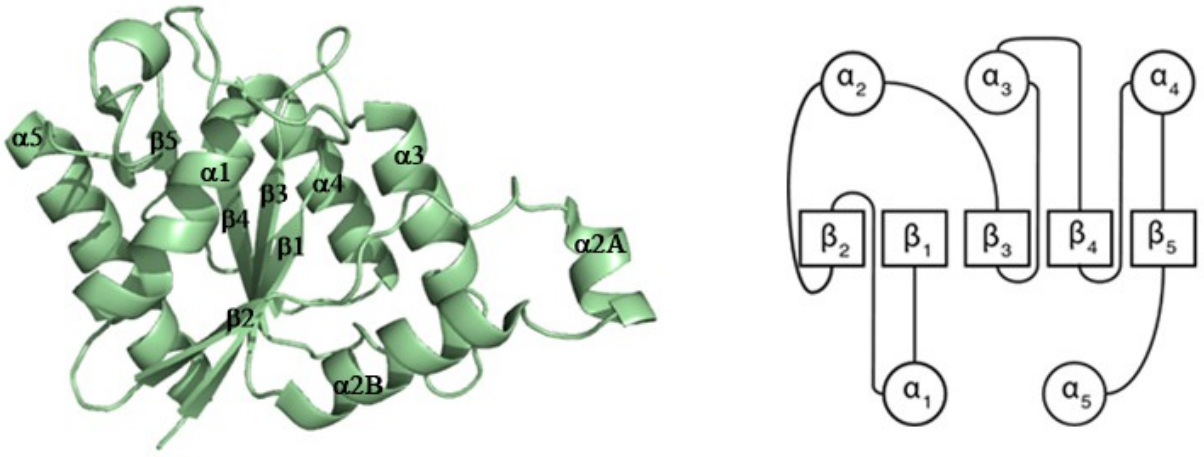

Figure 1.21. Flavodoxin fold of chromate reductase ChrR (PDB:3svl) found in the NA(D)PH:FMN Reductase Family and flavodoxin fold topography map.[148] © 2017 The Authors.

The *FEBS Journal* published by John Wiley & Sons Ltd on behalf of Federation of European Biochemical Societies.

The flavin reductase SsuE involved in sulfur metabolism from *Escherichia coli* belongs to the NAD(P)H:FMN Reductase family. SsuE can be further sub-grouped within this family due to key structural features which may provide a functional advantage.[147] Flavin reductases MsuE from *Pseudomonas aeruginosa* and SfnF from *Pseudomonas putida* also belong to the same subgroup in the NAD(P)H:FMN Reductase family. Enzymes MsuE and SfnF share a ~29% amino acid sequence identity with SsuE. As part of the flavodoxin-like superfamily, these enzymes share a common flavodoxin motif for flavin binding.[147, 149-151] The conserved classical flavodoxin sequence (T/S)XRXXSX(T/S) for SsuE is (S)PRFPSR(S) from residues 8-15, MsuE is (T)YRPSR(T) from residues 14-20, and SfnF is (S)LRAPSR(T) from residues 14-21 (Figure 1.22). This common motif amongst these enzymes enable them to bind flavin for catalysis with the aid of other active site amino acids.[149-151]

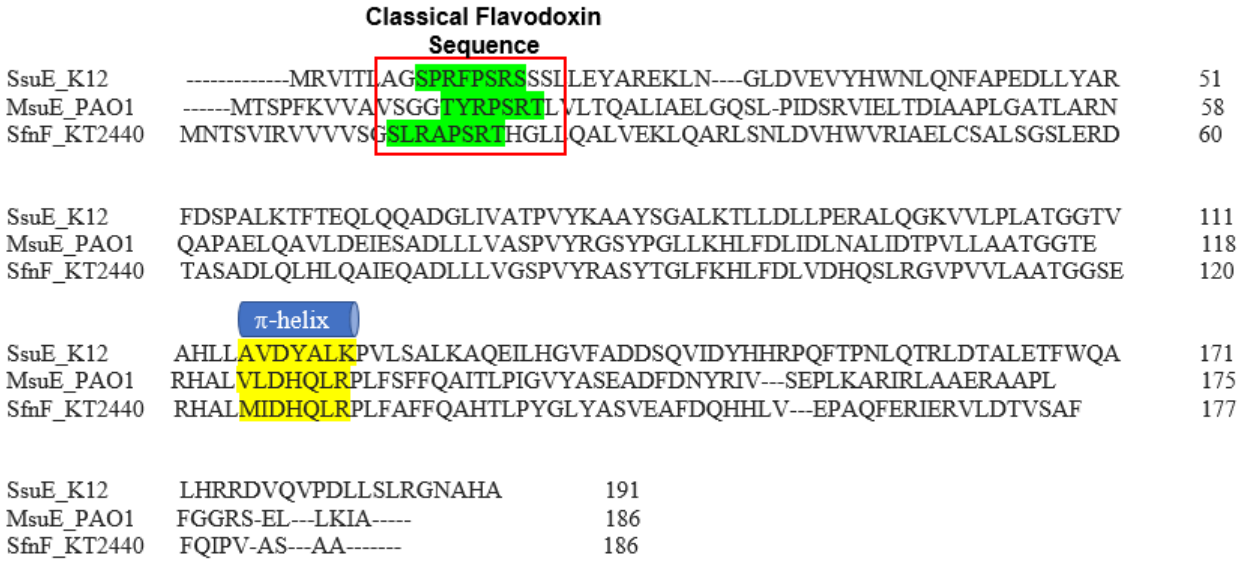

Figure 1.22. Amino acid sequence alignment of SsuE (*E. coli*), MsuE (*P. aeruginosa*), and SfnF (*P. putida*) with the helical region highlighted (yellow) and classic flavodoxin fold sequence (green).

Enzymes SsuE, MsuE, and SfnF share a similar active site and docking site for flavin that is common within the flavodoxin family.[147] Analysis of the SsuE structure identified key amino acid residues involved in interacting with the flavin substrate. Amino acid residues within the active site Ser8, Ser13, Ser15,and Arg10 coordinate the phosphate group of flavin (Figure 1.23B).[147] The ribityl portion of flavin interacts with amino acids Thr106, Asp140, Arg14, and Val75 (Figure 1.23C).[147] Hydrogen bonding with the isoalloxazine ring involve residues His112, Lys77, Ala78, Gly108, and Thr109 (Figure 1.23D). Across the dimer interface of SsuE, residues Asp89 and Lys85 aid in the stabilization of flavin binding.[147] These active site amino acid residues, MsuE and SfnF share a 61% and 89% sequence identity compared with SsuE, respectively.

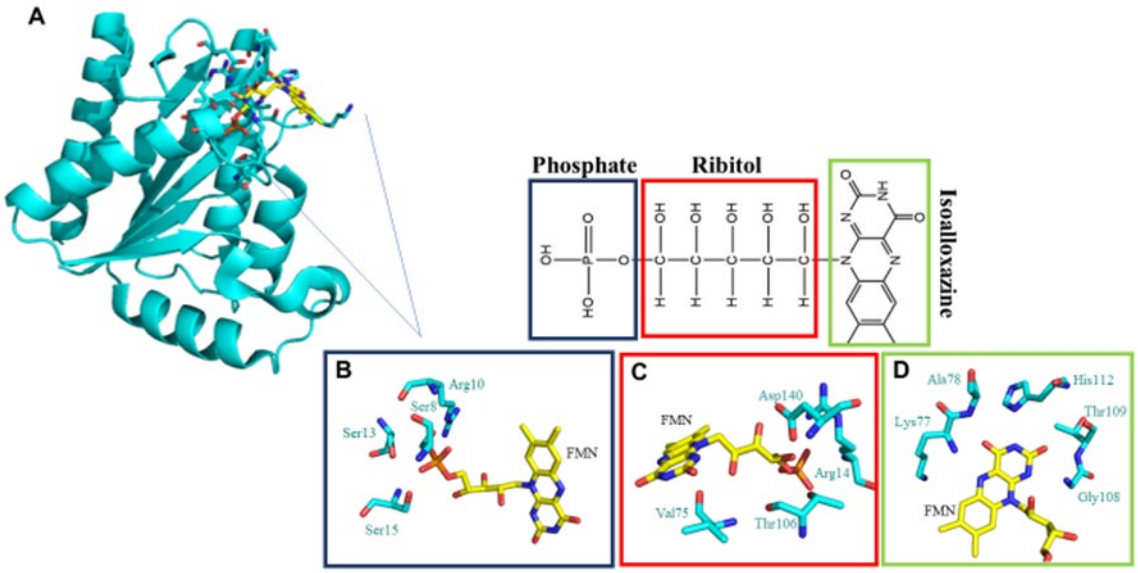

Figure 1.23. Active site amino acids identified. A)Monomer of SsuE (PDB:4PTY), B) Phosphate group interactions, C) Ribityl interactions, and D) Isoalloxazine ring interactions.[147]

1.4.2 Initial Characterization of SsuE

Flavin reductases that belong to bacterial two-component systems are essential for monooxygenase activity. The flavin reductase provides reduced flavin to the partner monooxygenase to ensure desulfonation. Flavin reduction occurs with FMN or FAD with reducing equivalents provided by nicotinamide adenine dinucleotide (NADH) or nicotinamide adenine dinucleotide phosphate (NADPH) (Figure 1.24 A and B).[74, 152] Flavin reductases differ amongst each other in their substrate preference for either FAD, FMN, or both. They may also utilize NADH, NADPH, or both.[74]

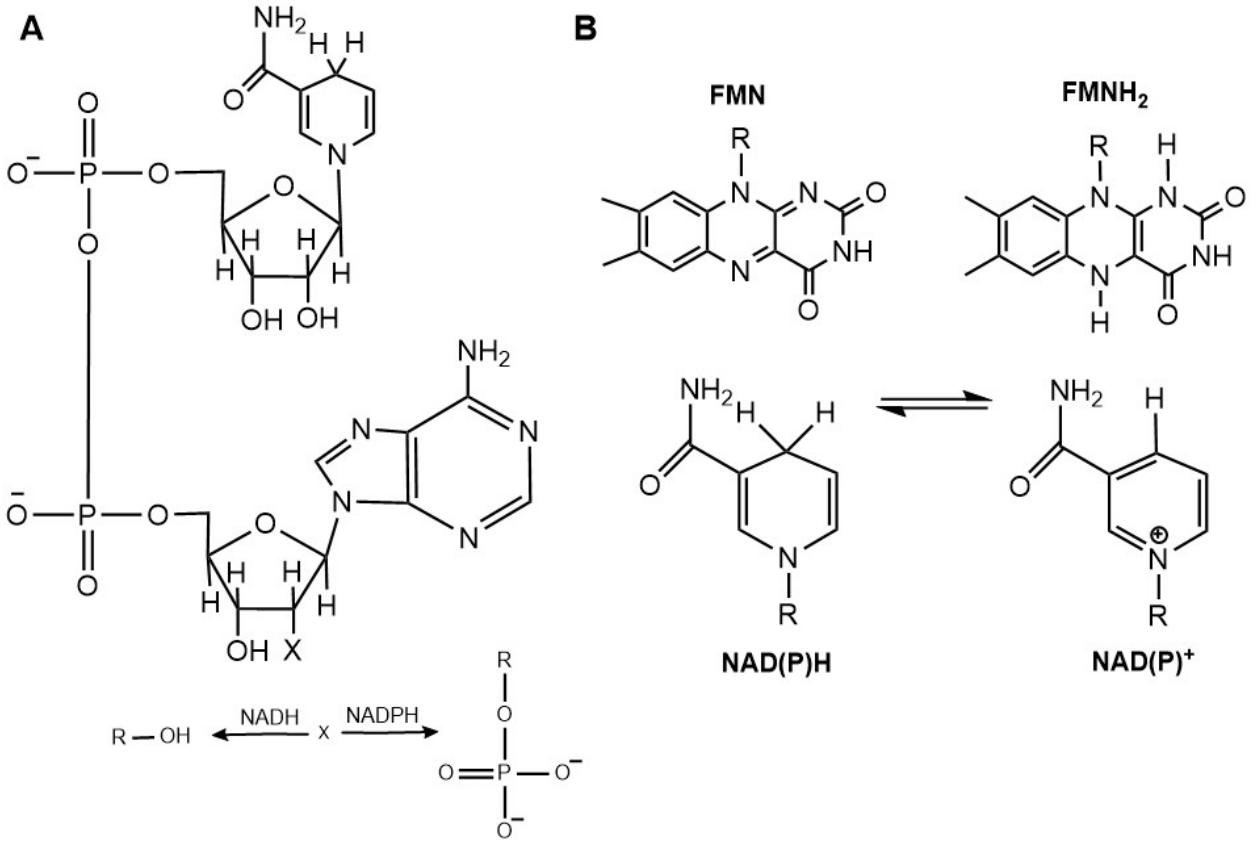

Figure 1.24. (A) Structure of pyridine nucleotides NADH or NADPH. The X represents the difference between the two molecules. (B) Reduction of FMN to $FMNH_2$ and oxidation of NAD(P)H to $NAD(P)^+$.

Flavin reductases in general utilize flavin with two different mechanisms. There are two different ping-pong mechanism involved with flavin reductases that have a tightly bound flavin. The first ping-pong mechanism involves a bound flavin cofactor that is reduced by the pyridine nucleotide. Once bound flavin cofactor is reduced, the pyridine nucleotide is released, which is followed by a second flavin substrate that binds and interacts with the reduced bound flavin. The substrate flavin is then reduced and released (Figure 1.25A).[74] The second ping-pong mechanism involves a flavin substrate that binds first and then follows the previous mechanism (Figure 1.25B). The other mechanism usually involves enzymes that are purified flavin-free that follow a sequential mechanism in which flavin is not initially bound to the enzyme but is used as substrate to reduce the pyridine nucleotide (Figure 1.25C).[74] The flavin reductase forms a ternary complex with the flavin and pyridine nucleotide.

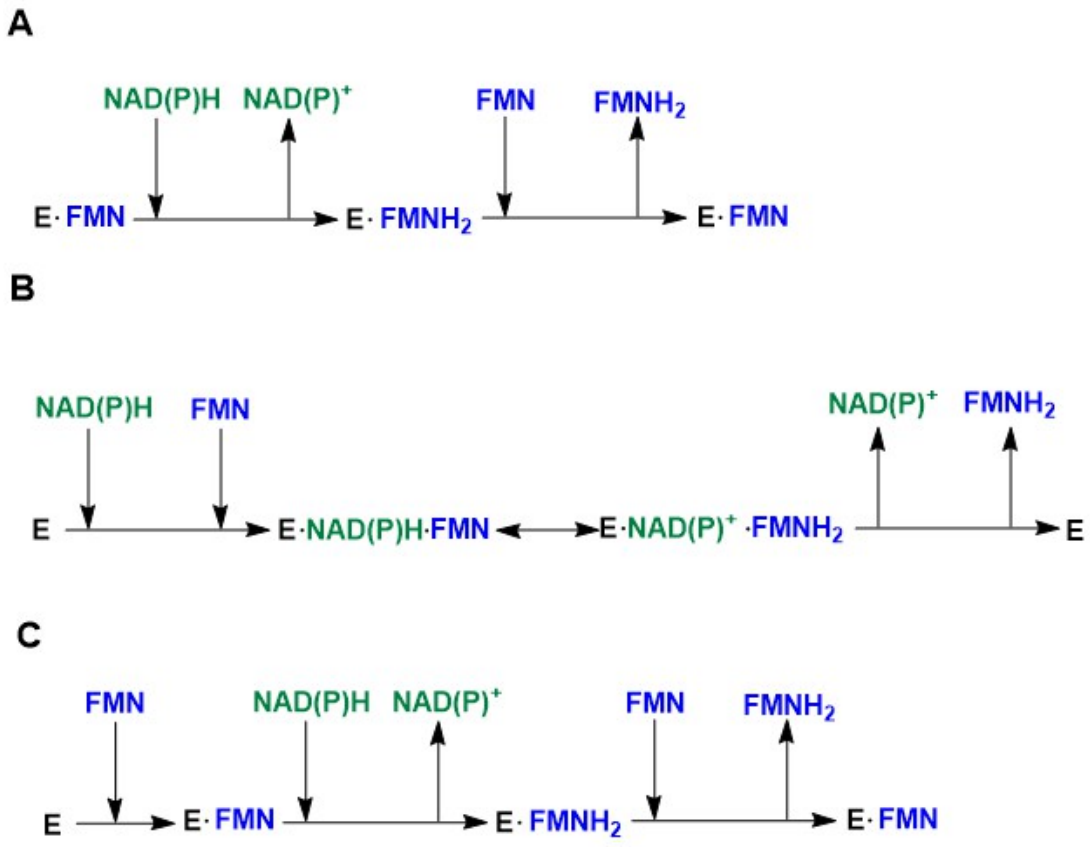

Figure 1.25. Flavin reductases will either follow one of these reaction schemes. A) Sequential mechanism which is utilized with flavin-free flavin reductases. B) Ping pong mechanism which is utilized with flavin-bound flavin reductases.(Adapted from [153])

When sulfur is limiting, SsuE from *E. coli* is expressed from the *ssu* operon.[53] The flavin reductase that is purified flavin free has a substrate preference for FMN but is able to utilize NADH or NADPH to provide reducing equivalents.[53, 154] SsuE utilizes a sequential mechanism for flavin reduction with the formation of a ternary complex with the FMN and NADPH.[75, 149] It is established that SsuE follows an ordered sequential mechanism with NADPH binding first, followed by FMN second that is followed by reduction and release of first NADPH, then reduced flavin.[75]

Rapid reaction kinetic analyses were performed to investigate the mechanism of the reductive-half reaction by SsuE that characterized a charge transfer complex.[149] In the reaction of SsuE and substrates, NADPH and FMN bind in rapid equilibrium to SsuE forming a ternary Michaelis complex (MC-1) (Scheme 1). There is a charge transfer (CT-1) that occurs between FMN and NADPH which is represented by rate constant k_1 (241 s^{-1}).[149] Once the charge transfer complex is formed, a slow phase occurs with the conversion from CT-1 to CT-2 with a rate constant (k_2) at 11 s^{-1}. The CT-2 represents the oxidation and reduction of $NAD(P)^+$ and $FMNH_2$.[149] The decay of the charge transfer complex is the final phase which forms the Michaelis complex (MC-2) with a rate constant (k_3) of 19s^{-1}.[149] Isotope studies that involved (4(R)-^{2}H] NADPH, supported hydride transfer from NADPH to FMN as the rate-limiting step.[149] In the presence of SsuD and octanesulfonate, the kinetic mechanism of SsuE was altered from the sequential-ordered to a rapid-equilibrium-ordered mechanism to ensure that the ternary complex is formed for reduced flavin transfer.[75]

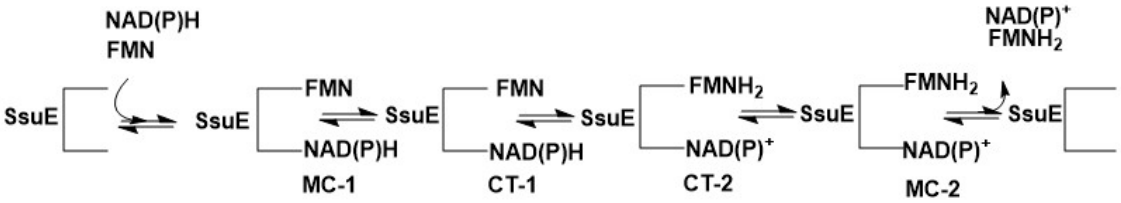

Scheme 1. Charge transfer complex with SsuE in the presence of FMN and NADPH which form a ternary complex. (Adapted from [149])

1.4.3 Oligomeric Alterations of SsuE

Previous studies with both analytical ultracentrifugation and size exclusion chromatography methods were used to analyze SsuE in solution to determine the oligomeric state. In the absence of flavin, SsuE exists as a tetramer.[147] Additionally, the three-dimensional structure of SsuE was solved and characterized as a dimer of dimers that form a tetramer (Figure 1.26).[147] SsuE is stabilized first as a dimer through monomeric interactions of subunits A/C or B/D. The SsuE dimers are further stabilized at the tetramer interface (Figure 1.26).[147] In the presence of either FMN or SsuD, SsuE shifts from a tetramer to a dimer (Figure 1.26).[147, 155] The oligomeric switch may be initiated by specific structural features that SsuE and other flavin reductases from the subgroup possess.

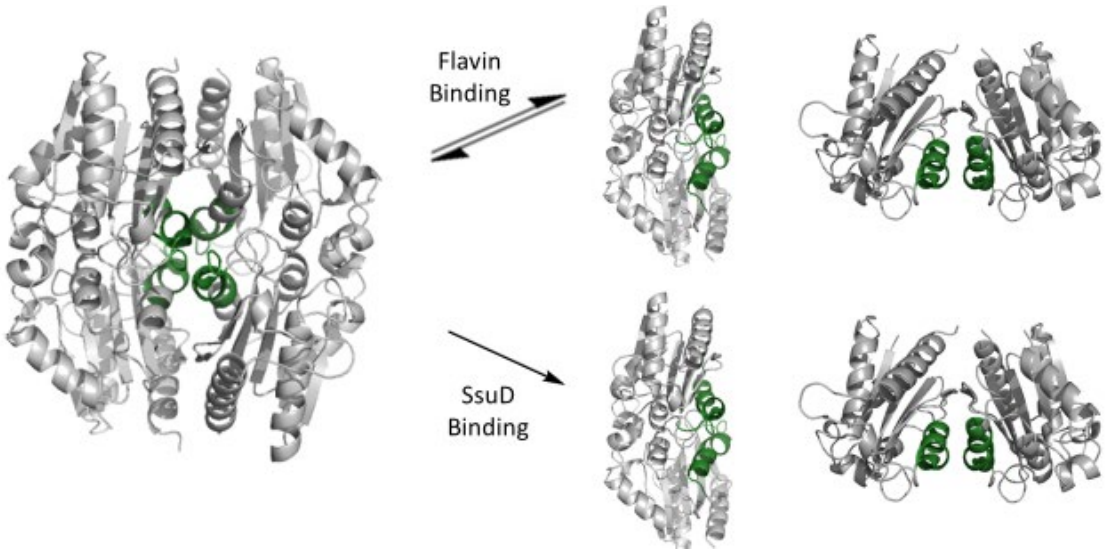

Figure 1.26. Oligomeric Structure of WT SsuE (PDB:4PTY) with the oligomeric switch from tetramer to dimer in the presence of either FMN or partner monooxygenase SsuD.(Adapted from [156])

1.4.4 π-helix

Protein secondary structures are primarily composed of helices and beta sheets .[157] Helices are characterized by number of residues per turn and number of atoms in the ring closed by intrachain $NH_{(i+n)} \rightarrow O_i$ backbone hydrogen bonds (Figure 1.27).[158] The α-helix is represented by 3.6_{13} (3.6 residues per turn with 13 atoms within the ring) and $i+4 \rightarrow i$ (NH → O hydrogen bonding 4 residues up the polypeptide backbone).[157, 158] Another helix that is derived from the α-helix is the 3_{10}-helix and the π-helix which is defined by a single amino acid insertion into an α-helix (Figure 1.27).[159] The 3_{10}-helices are proposed to be intermediates in the folding/unfolding of α-helices.[160] The hydrogen bonding occurs $i+3 \rightarrow i$ and are considered short helices.[160, 161] In comparison with the α-helix, the π-helix is represented with 4.4_{16} with an $i+5 \rightarrow i$ backbone (Figure 1.27).[162, 163]

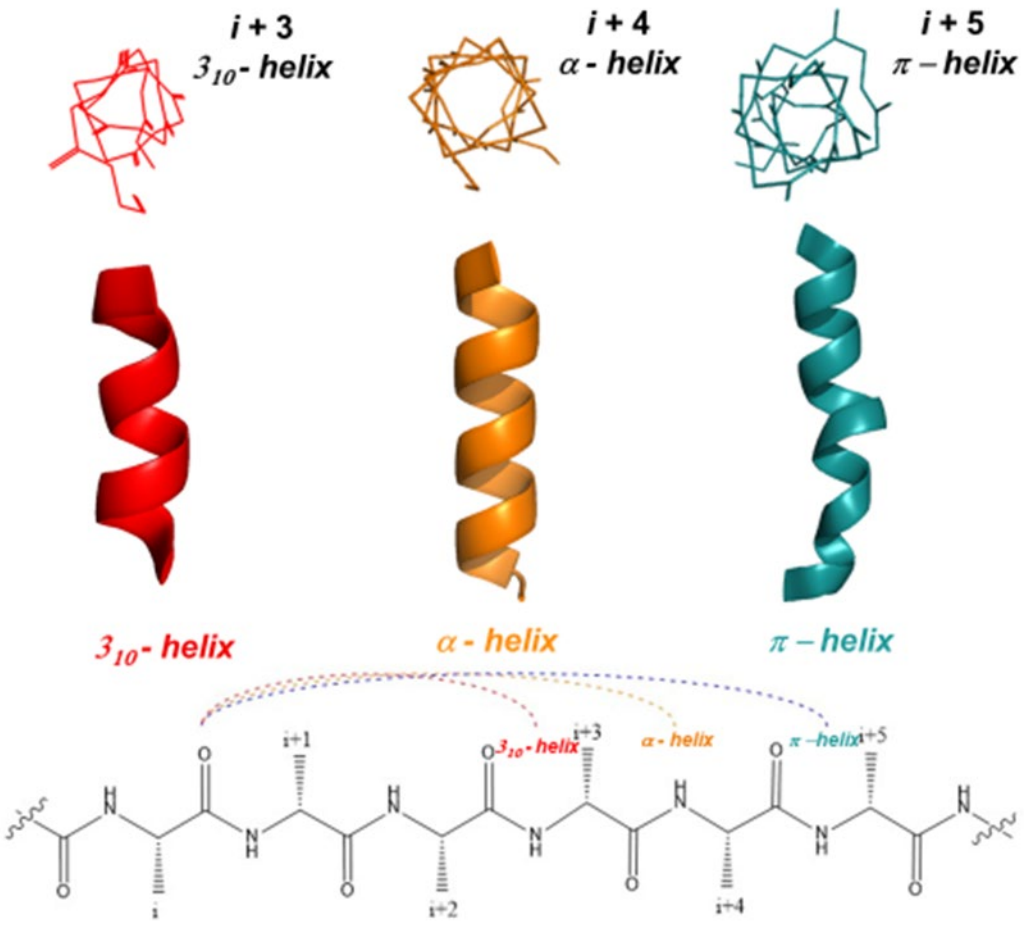

Figure 1.27. (Top) 3_{10}-helix of RNase A (*Bos taurus*) (PDB:1KF5), α-helix of ArsH (*Shigella flexineri*) (PDB:2FZV), and π-helix SsuE (*E.coli*) (PDB:4PTY) and (bottom) with backbone assigned for α-helix (orange) , 3_{10}-helix (red), and π-helix (blue). (Adapted from [164])

The π-helix was thought to be a rare occurrence due to main-chain atoms not being in van der Waals contact with a larger radius, the large entropic cost with the backbone hydrogen bonding, and unfavorable nucleation compared with the α-helix.[158, 162, 164-167] Bulky amino acids are favored within the π-helix, and provide a way to help stabilize the π-helical region.[158, 163] These large amino acids include Phe, Trp, Tyr, Ile, and Met, which are probably due to the favorable van der Waals

interactions between the side chains and shielding of the free carbonyl oxygen due to the wide turn.[163] Further stabilization of the helical region is due to the lesser rise of the π-helix compared with the α-helix, 1.2 Å and 1.5 Å respectively.[163] The π-helices were first proposed to have dihedral angles of -57.1°(ϕ),-69.7°(Ψ), but recent data support updated dihedral angles of -76°(ϕ),-41°(Ψ).[163, 168] For entropic effects, computational studies compared the volume and surface area of a π-helix with the α-helix and identified an increased stability for the π-helix due to 10% less volume and surface area compared with the α-helix.[163] However, multiple π-helices have been identified with ASSP (**A**ssignment of **S**econdary **S**tructure in **P**roteins) and Pipred, which confirms that the π-helix occurs more frequently than previously presumed.[158] Pipred is able to predict the π-helical structure with a per-residue precision of 48% and a sensitivity of 46% from a scan of 20.295 structures within the Protein Data Bank.[169]

The functional role of the π-helix has been evaluated in some enzymes. Examples of π-helices can be found with lipoxygenases that catalyze deoxygenation of polyunsaturated fatty acids (Figure 1.28).[170] Lipoxygenases have a π-helix (helix 9) that contributes side chains that coordinate the catalytic metal.[171,172,163] There is another π-helical region at helix 2 in four isoforms of soybean lipoxygenase.[170] With bacterial lipoxygenases, helix 2 is elongated with α2A and α2B inserts that form a lid over a bound phospholipid.[170] Results from spin-labeling EPR studies demonstrated that soybean lipoxygenase-1 (SBL1) had dramatic changes in the spin mobility of helix 2.[170] Whereas pH changes did not affect neighboring α-helices, the mobility of helix 2 was altered with a pH change from 7.2 to 9.[170] A higher pH is associated with lipid binding to SBL1, and all spin-labeled residues in the π-helix had increased mobility at a higher pH.[170] There was no observed opening for the fatty acid to bind in the SBL1 crystal structures.[170] However, rotations

of residues in helix 2 and 11 may provide the opening for substrate binding. While helix 2 has residues that contribute to forming the mouth of the substrate channel, lipid binding to the mobile helix would allow the substrate to enter and pass through the active site.[170] Helix 2 would have to rearrange when substrates or inhibitors are present providing an opening for substrate binding.[170]

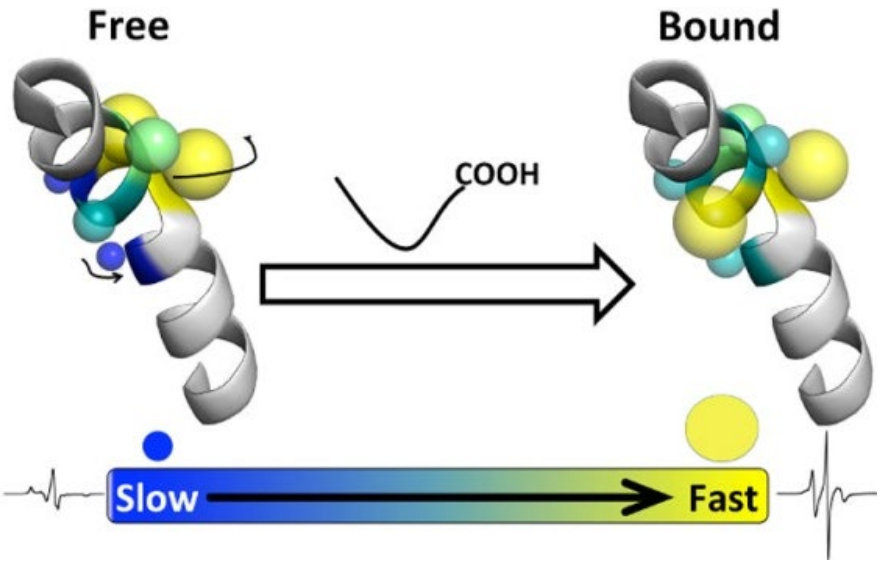

Figure 1.28. The second helix in lipoxygenases adapts access to the active site with a π-helix. Figure shows a mobile π-helix with site-directed spin-label scan. With the different pH values, unusual movement for helix 2 occurred when pH changes mimicked substrate-bound conditions. Backbone dynamics of residues in helix 2 are correlated to this dynamic change. [170] Copyright © 2014 American Chemical Society. Further permissions related to the material excerpted should be directed to the ACS.

The π-helix that defines and separates SsuE from the canonical flavoproteins in the NAD(P)H:FMN Reductase family is characterized by a Tyr118 insertion. Hydrogen bonding interactions occur between the hydroxyl group of Tyr118 and the oxygen atom backbone carbonyl of Ala78 across the tetramer interface (Figure 1.29).[155] An interesting addition to the hydrogen

bonding interactions is the π-stacking interactions that involve Tyr118 from different subunits.[155] Along with the hydrogen bonding between the interface, the π-stacking associated with the Tyr118 residues helps further stabilize the oligomeric structure. Within the tetramer interface of SsuE, π-stacking interactions occur across the tetramer interface to stabilize the overall quaternary structure (Figure 1.29).[155] The π-stacking interactions occur at a diagonal between monomers of the dimer pair with a distance of 5.3 Å (Figure 1.29).

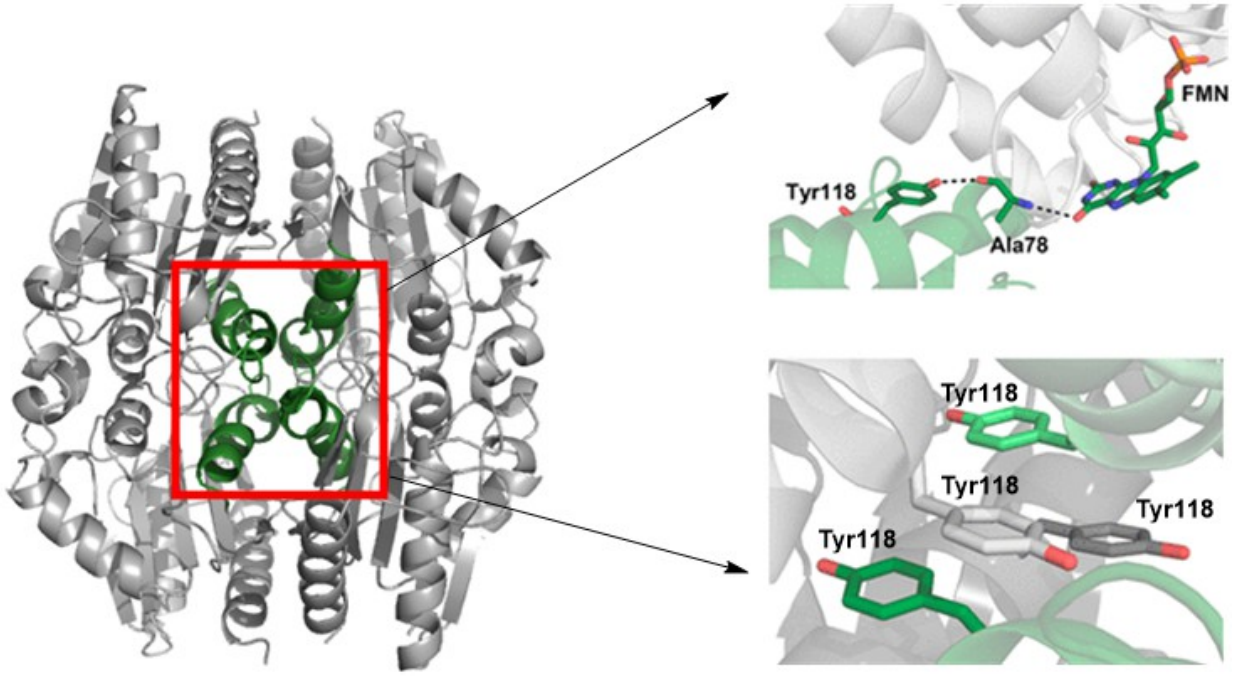

Figure 1.29. Interactions across tetramer interface of WT SsuE (PDB:4PTY).[156] Copyright © 2018, American Chemical Society

An alanine and deletion variant of Y118 in SsuE were generated to determine the functional role of the π-helix.[149] The Y118A SsuE variant was purified with flavin bound and ΔY118 SsuE was purified flavin free. The purified SsuE variants differed in their oligomeric structures. The Y118A SsuE variant with flavin bound existed as a dimer, whereas the flavin-free ΔY118 variant existed as a tetramer in solution (Table 1). The rate of oxidation of NADPH by

Y118A SsuE was slow, but the variant was able to transfer electrons to ferricyanide. There was no reductase activity observed with ΔY118 SsuE, and neither variant was able to support flavin or transfer reduced flavin to SsuD in kinetic studies.[148] These results suggested that the π-helix located at the tetramer interface of flavin reductases is necessary for the oligomeric switch to occur. The oligomeric switch enhances the protein-protein interactions that lead to efficient flavin transfer to the partner monooxygenase.[149] Both MsuE and SfnF that are in the same family subgroup as SsuE contain a histidine instead of the tyrosine insertion at position 126 and 128, respectively (Figure 1.30). The π-helical region in the two-component flavin reductases may provide the enzymes with an evolutionary advantage by allowing the substrate to be released to the partner monooxygenase. The flavin transfer activity is not needed for canonical flavin reductases within the family.

Table 1. Oligomeric states of wild-type SsuE and variants generated.[155]

	Molecular Weight (kDA)	Oligomeric Structure
wild-type SsuE	73 ± 3	Tetramer
Y118A SsuE	42 ± 1	Dimer
ΔY118	84 ± 11	Tetramer

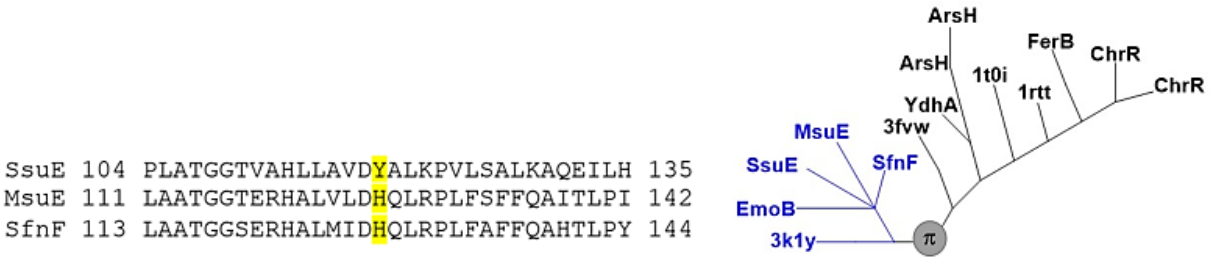

Figure 1.30. (Left) Amino acid sequence alignment with the π-helix highlighted in yellow of SsuE (*E. coli*), MsuE (*P. aeruginosa*), and SfnF (*P. putida).*(Right) Phylogenic tree of the NAD(P)H:FMN Reductase family.(Adapted from [147])

Monooxygenases

1.5.1 Monooxygenases

The flavin in flavin-dependent monooxygenases is either a tightly bound prosthetic group or functions as a substrate.[164] Flavin monooxygenases are further classified into six subclasses (A-F).[164] Subclasses A and B are involved in single-component flavin-dependent monooxygenases. These monooxygenases perform both the reductive and oxidative half reactions on a single monomer.[164] Both subclasses A and B only use FAD as prosthetic group, with subclass B utilizing only NADPH and subclass A utilizing both NADH and NADPH as the electron donor.[164] The monooxygenase subclasses C-F rely on a flavin reductase to provide reduced flavin for catalytic activity to occur.[164] The C-F subclasses are grouped based on the overall structural fold. Interestingly, all the subclasses prefer FAD except for subclass C which utilizes FMN as substrate.[164]

1.5.2 Proposed Mechanisms for Desulfonation by SsuD

Monooxygenases utilize molecular oxygen to generate a reactive flavin-oxygenating intermediate. Different flavin-oxygenating intermediates formed from the reaction of flavin with dioxygen in monooxygenases include the C4a-hydroperoxyflavin and the C4a-peroxyflavin. When reduced flavin is in the presence of oxygen, formation of oxidized flavin and hydrogen peroxide is autocatalytic due to the formation of flavin radicals and one electron reduced superoxide (O_2^-).[173] In free solution, the reaction between reduced flavin and molecular oxygen is slow due to the spin inversion associated with the singlet reduced flavin with triplet molecular oxygen (Figure 1.31).[173] In the overall reaction between reduced flavin and dioxygen, an electron is transferred from singlet reduced flavin to triplet dioxygen to generate a caged radical pair. The caged superoxide–semiquinone pair reacts by radical coupling before the intermediates can diffuse apart.[173] An oxygen–carbon bond forms between superoxide and the isoalloxazine at C4a, a site of high spin-density in the neutral semiquinone. The C4a-peroxide anion can be protonated in water to form the C4a-hydroperoxide. The reduced hydroquinone flavin intermediate is stabilized within the monooxygenase active site and can catalyze the controlled reaction of reduced flavin with dioxygen. Flavin-dependent monooxygenase enzymes catalyze diverse reactions utilizing C4a-(hydro)peroxyflavin intermediates and more recently identified N-5 oxides.[146,182,183,184,185,176]

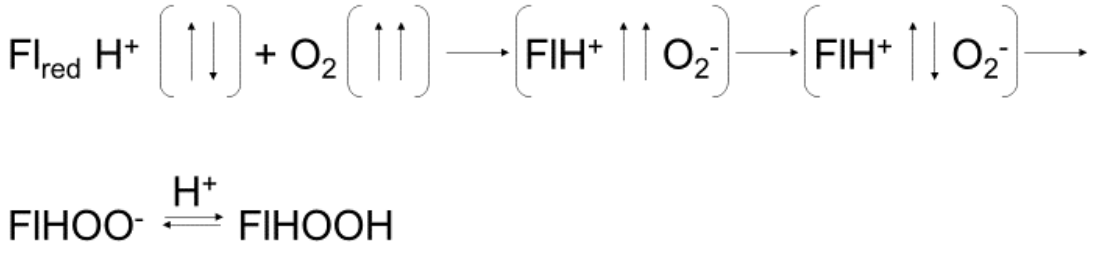

Figure 1.31. Activation of oxygen by reduced flavin. (Adapted from [173])

Although no intermediate has been identified yet with SsuD, there are two pathways to consider in the desulfonation reaction, because SsuD and bacterial luciferase share similar active sites, both the C4a-peroxyfavin or C4a-hydroperoxyflavin intermediate have been proposed to be involved during desulfonation of alkanesulfonates.[146] Formation of either intermediate is formed between dioxygen and the reduced flavin provided by SsuE. The oxygenated flavin intermediate within the monooxygenase active site is utilized to cleave the carbon-sulfur bond which produces the corresponding aldehyde and sulfite.

The proposed C4a-hydroperoxyflavin intermediate pathway begins with the formation of the intermediate (Figure 1.32 I). Once the flavin intermediate is formed, an active site base abstracts a proton from the C1 carbon of the alkanesulfonate to generate a carbanion intermediate (Figure 1.32 II and III).[146] A nucleophilic attack by the carbanion intermediate on the C4a-hydroperoxyflavin intermediate forms a 1-hydroxyalkanesulfonate (Figure 1.32 IV).[146] The unstable 1-hydroxyalkanesulfonate collapses to produce sulfite and the corresponding aldehyde.[146]

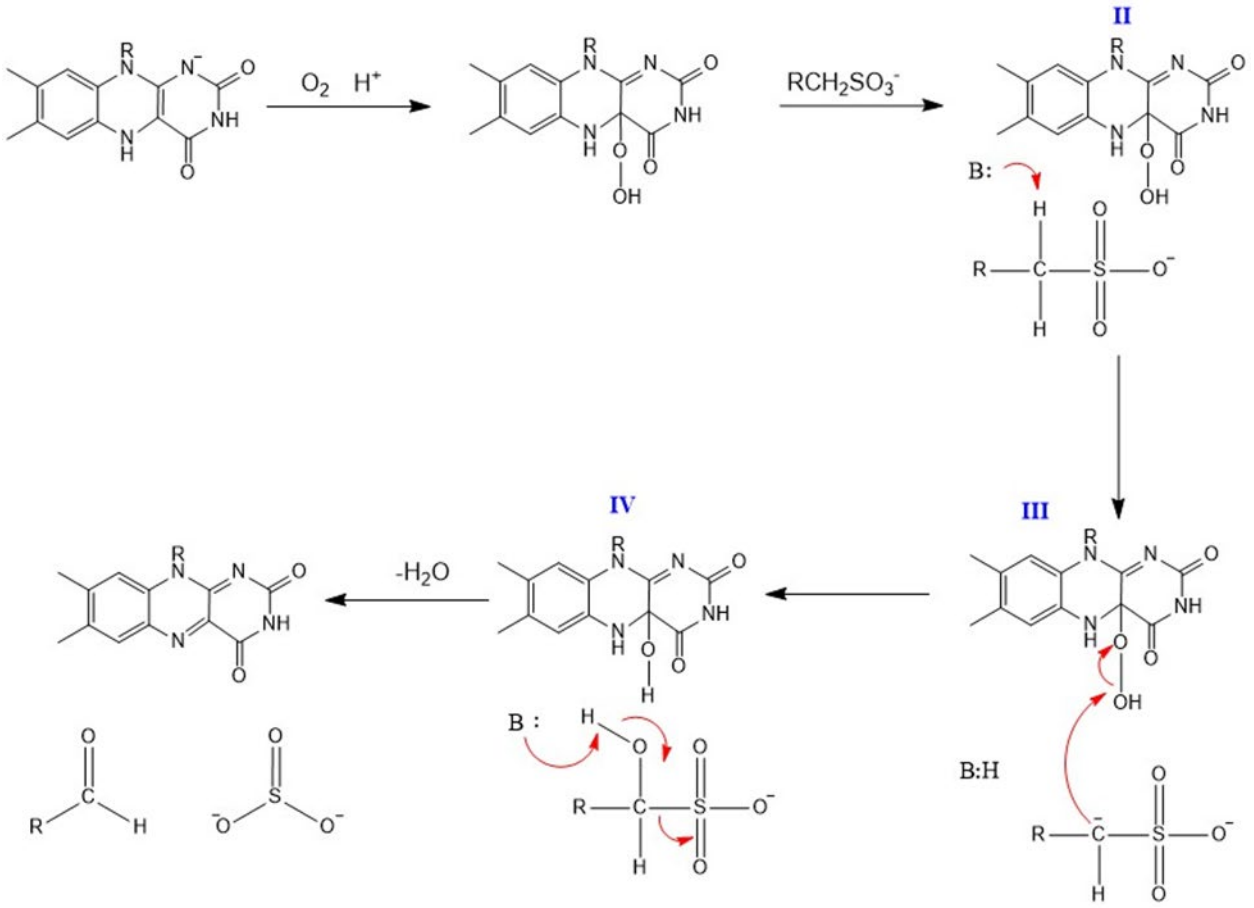

Figure 1.32. Proposed hydroperoxyflavin mechanism for SsuD. (Adapted from [153])

A peroxyflavin intermediate could make a nucleophilic attack on the sulfur atom of the alkanesulfonate substrate to form a peroxyflavin-alkanesulfonate adduct that undergoes a Baeyer-Villager rearrangement (Figure 1.33 II and III).[146] The rearrangement would produce the sulfite product and generate a peroxyalkane intermediate.[146] An active site base then abstracts hydrogen from the C1 of the alkane (Figure 1.33 IV).[146] This leads to heterolytic cleavage of the oxygen-oxygen bond of the alkane-flavin adduct to form the corresponding aldehyde and the C4a-hydroxyflavin intermediate.[146] Both mechanisms form a sulfite product, but differ in their mechanistic steps.[146]

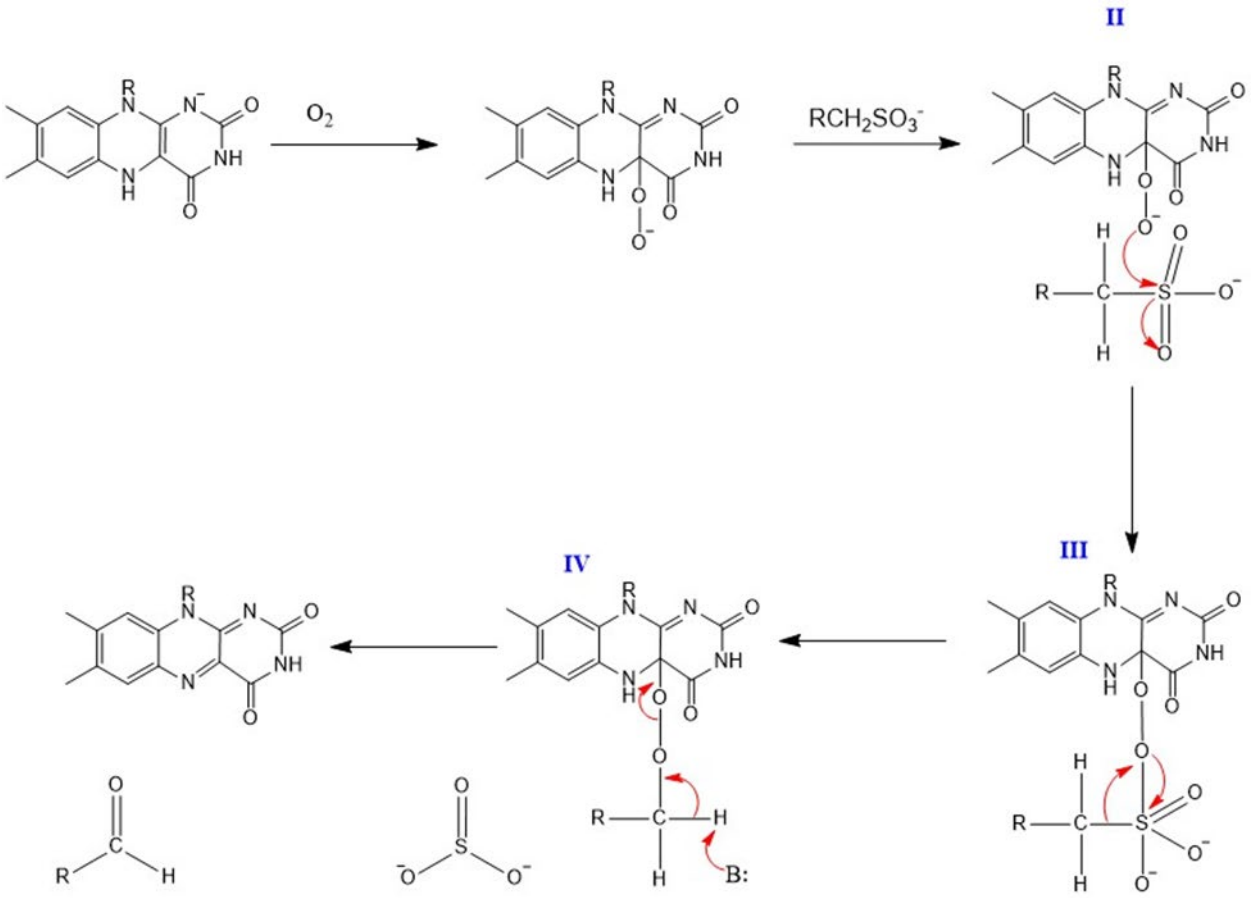

Figure 1.33. Proposed peroxyflavin intermediate pathway for SsuD. (Adapted from [153])

Recent studies have proposed a flavin-N5-oxide flavin oxygenating intermediate.[186] This has been identified with flavin-dependent monooxygenase EncM (*Streptomyces maritmus*) which catalyzes a step in the biosynthesis of the polyketide antibiotic enterocin.[186] The formation of the flavin-N5-oxide has been proposed to occur from two different pathways. The first pathway includes the production of a superoxide anion and neutral semiquinone that undergoes a radical coupling at the isoalloxazine C4a position (Figure 1.34AI).[186] The C4a-peroxide rearranges to an oxaziridine upon elimination of water (Figure 1.34AII), and undergoes a ring opening to an EncM-flavin-N5-oxide intermediate (Figure 1.4AIII).[186] The second pathway involves an initial hydrogen-transfer from the reduced flavin to molecular oxygen that yields anionic semiquinone

and protonated superoxide (Figure 1.34I).[186] Which would allow radical coupling at the N5 position of reduced flavin to yield the EncM- flavin-N5-oxide (Figure 1.34BII).[186]

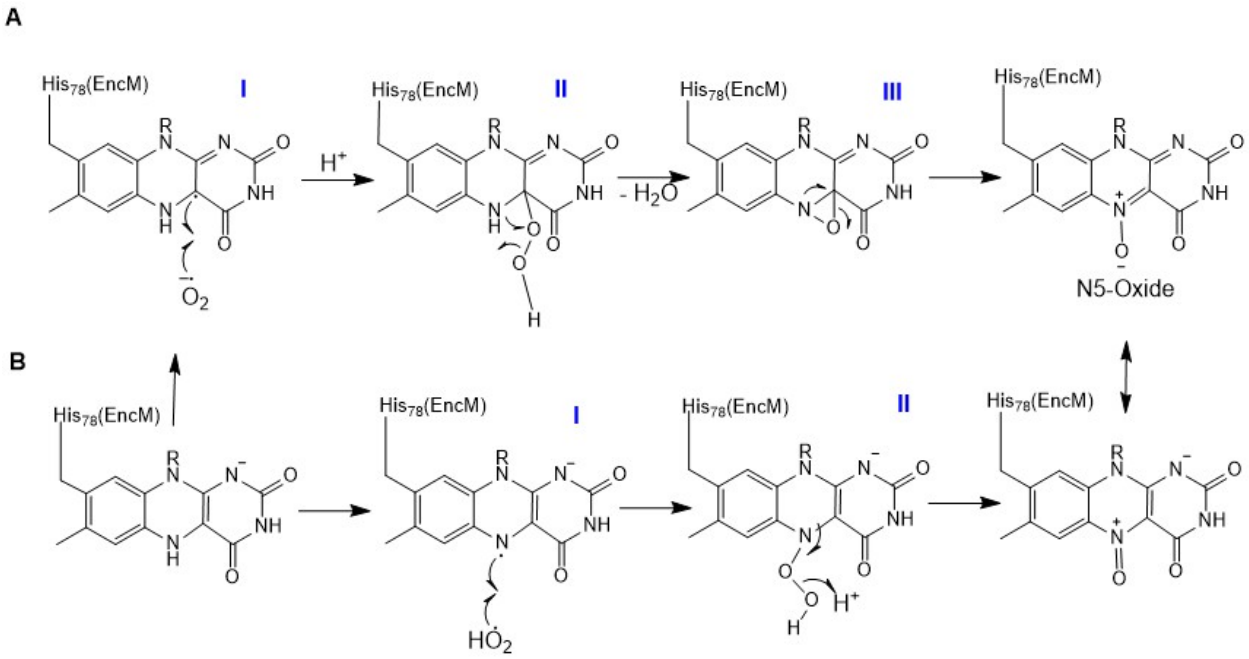

Figure 1.34. Possible formation of the flavin-N5-oxide with two different pathways that involve the flavin-dependent monooxygenase EncM. (Adapted from [174])

1.5.3 Overall Structural Properties of SsuD

Enzyme SsuD belongs to a small family of bacterial monooxygenases with a TIM-barrel fold.[165] The SsuD enzyme is characterized as a homotetramer with four monomeric subunits. The overall monomeric structure of SsuD is characterized with a triosephosphate isomerase (TIM)-barrel fold (Figure 1.35A).[165] The TIM-barrel fold consists of an eightfold repeat of (αβ) units with eight parallel β-strands on the inside with eight α-helices on the outside.[187] The active sites are located at the C-terminal end of the β-strands.[187] Numbering of the fold begins from the N-terminus as β1-β8 and α1-α8.[187] There are connecting loops between the α and β strands that are

called βα loops and αβ loops (Figure 1.35B).[187] There are minor secondary structures contained within the loop.[187]

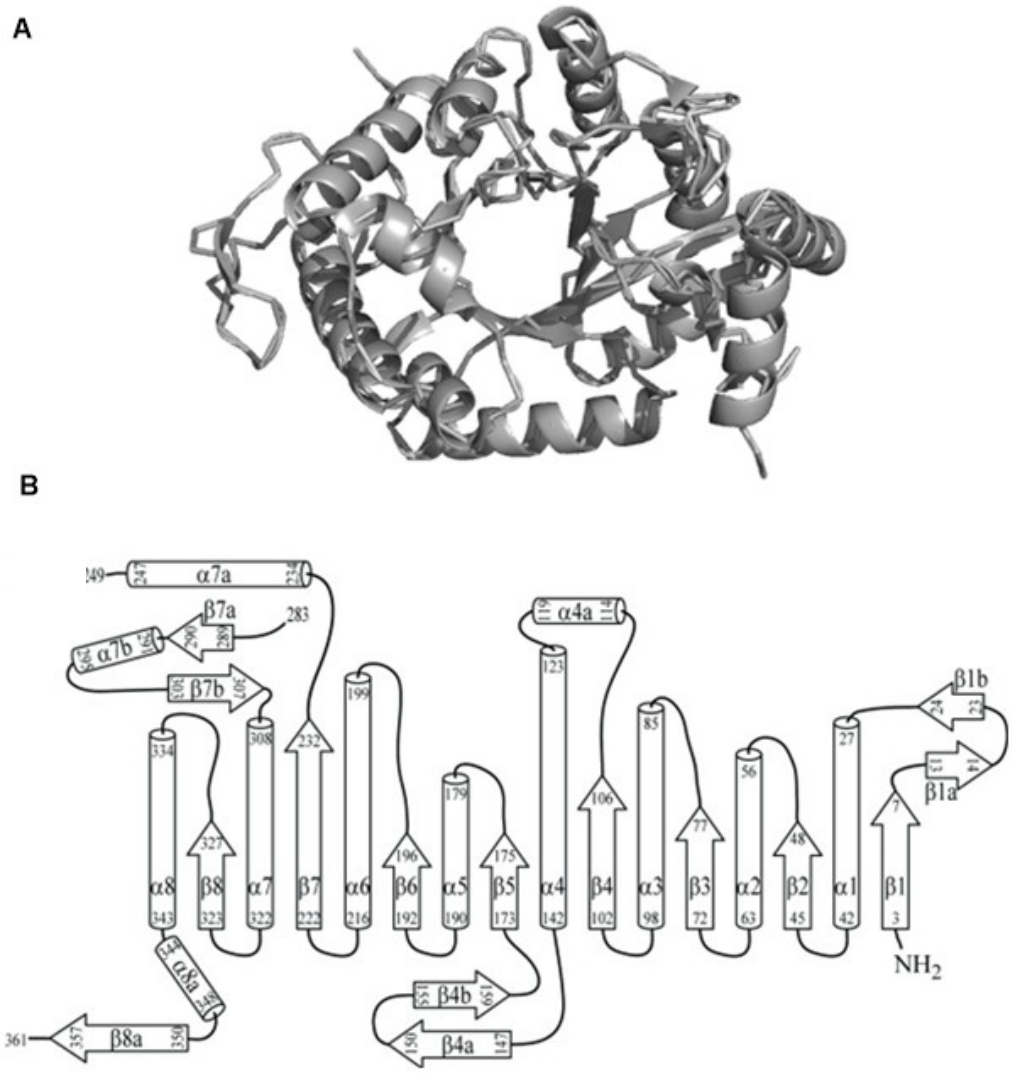

Figure 1.35. A) TIM-barrel fold of SsuD (PDB:1M41) B) Topology diagram with the highlight of secondary structure of SsuD.[175] Copyright © 2002 Elsevier Science Ltd.

As a tetramer, SsuD comprises a dimer of dimers with A/B and C/D interactions (Figure 1.36).[175] A parallel four-helix bundle forms the dimer structure between A/B and C/D, with each monomer contributing helices α2 and α3 with hydrophobic and hydrogen bond interactions

between the β-hairpin structure of one monomer (region 3) with another monomer (region 2).[175] The dimer is stabilized through hydrophobic and hydrogen bond interactions.[175] The 222 symmetry that characterizes tetramer formation occurs with interactions between the A/B dimers and C/D dimers.[175] Monomer A interacts with monomer C while monomer B interacts with monomer D.[175] Both subunits form these interactions through terminal extensions with the α1 to α1 and α8 to α8.[175]

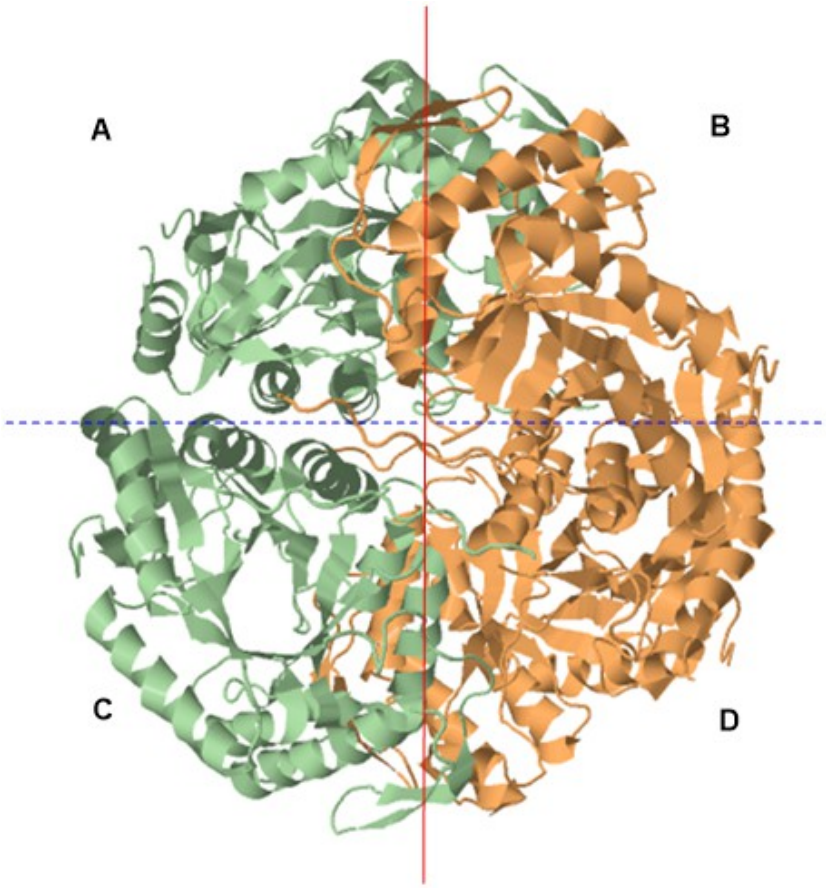

Figure 1.36. Tetramer structure of SsuD (PDB:14M1) with dimer interface interactions between A/B and C/D and the tetrameric interface interactions between A/C and B/D.

Compared with the prototypical TIM-barrel structure, SsuD has four extended insertion regions connecting the β-strands and α-helices.[175] There is also an extension at the C-terminus of

the polypeptide chain.[175] The first insertion region 1 comprises of 19 residues and is located at the N-terminus between β1 and helix α1.[175] The region is in close contact with region 4 and covers the N-terminal side of helices α1 and α8.[175] The C-terminal end of strands β1 and β8 and two small-antiparallel β-strands are interconnected by a loop.[175] Insertion region 2 located at the C-terminus of the β-barrel located between strand β 4 and α4 comprises 16 residues and contains a 3_{10}-helix (α4α).[175] Insertion region 2 covers the C-terminal end of stands β2 and β3.[175] Insertion region 3 is located between helix α4 and β5 and comprises β-strands β4α and β4β arranged as a antiparallel β-hairpin structure.[175] Insertion region 4 comprises 75 residues, and makes a large bulge over the C-terminal end of the β-barrel. Electron density was poorly defined in the crystal structure of SsuD, suggesting flexibility and movement in this region.[175] The three-dimensional structure of bacterial luciferase contained a similar disordered region that was classified as a mobile loop.[175]

1.5.4 SsuD Mobile Loop

This insertional region 4 contains a loop that protrudes over the active site at the C-terminal end of the β-barrel and plays a role in protecting reaction intermediates from bulk solvent (Figure 1.37).[175] The mobile loop was proposed to undergo a conformational change with substrate binding. Complete loop deletion for bacterial luciferase resulted in a complete loss of activity.[176] The bacterial luciferase mobile loop that is located over the active site that has two conserved residues that are adjacent to the isoalloxazine ring of the flavin substrate.[176] Alanine mutagenesis of the loop region identified two Lys residues that showed a loss in quantum yield similar to the deletion variant.[176] Substitution of the two Lys residues (Lys283 and Lys286) resulted in a decrease in quantum yield of product but still was able to form the carboxylic acid product similar to wild-

type.[176] The two Lys residues are close to the quininoid portion of the flavin, and were proposed to play a role in preventing the entry of bulk solvent into the active site.[176]

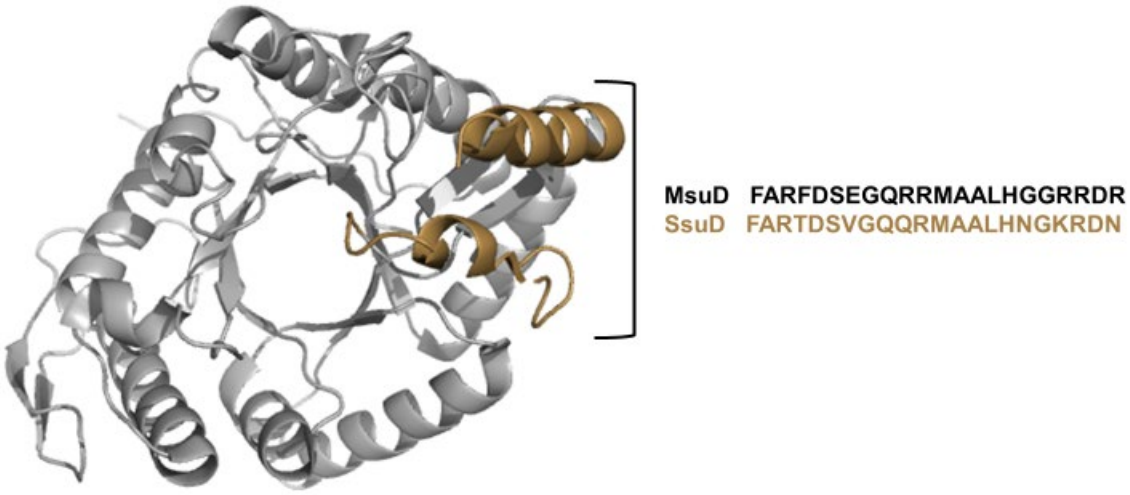

Figure 1.37. Loop Region of SsuD (PDB:14M1) from *E. coli* with the sequences of both SsuD and MsuD from *P. aeruginosa*.

The insertional region 4 of SsuD from *E. coli* contained a conserved Arg residue. (Figure 1.38).[177] An aberrant substitution of Arg to Cys when SsuD was initially characterized eliminated activity.[175] Through sequence alignments it was identified that other TIM-barrel enzymes have an arginine residue in a similar position such as nitrilotriacetate monooxygenase, pristinamycin synthase subunit A, and dibenzothiophene desulfurization enzyme.[175] An R297A SsuD variant had no detectable activity, whereas the R297K SsuD variant had a 30-fold decrease in catalytic activity compared with wild-type.[177] Both variants showed a similar affinity for reduced flavin as wild-type SsuD.[177] The susceptibility of the SsuD variants to tryptic digestion was similar to wild-type in the absence of substrates.[177] However, wild-type SsuD was protected from proteolytic digestion in the presence of reduced flavin, whereas the R297A SsuD variant was almost completely

digested over a comparable time course.[177] The results suggest the R297 on the loop is needed for loop closure once reduced flavin is introduced in order to protect the reaction intermediates from oxidation.[177] The trypsin proteolytic susceptibility of R297A and wild-type SsuD were similar in the presence of reduced flavin or both reduced flavin and octanesulfonate.[177] Two bands were identified by mass spectroscopy from the digestion of wild-type SsuD that were labeled as the insertional region.[177] These peptide fragments contained the tryptic digestion sites (Arg263 and Arg271), which indicates that the loop region is accessible for proteolytic activity.[177] Once substrates are bound to SsuD, the conformational change that occurs protects these proteolytic sites from trypsin digestion. Together, the variants were no longer able to undergo loop closure to protect the reaction intermediates, but flavin binding was not affected by the substitutions.[177]

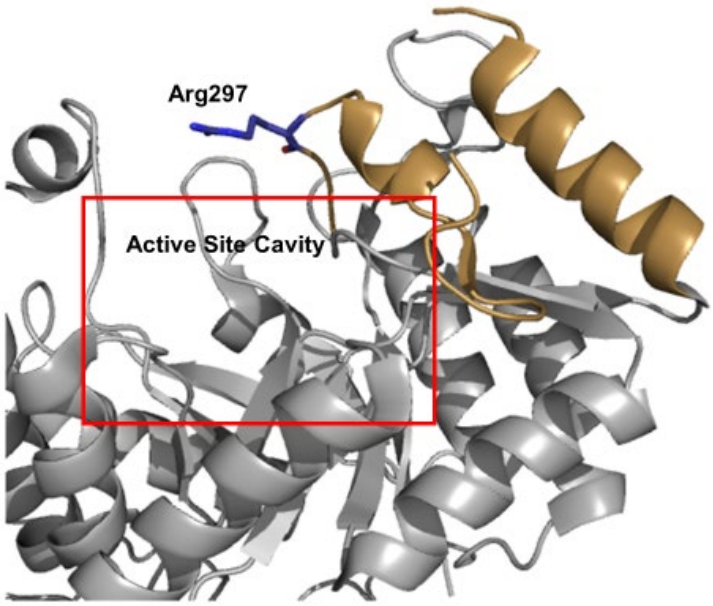

Figure 1.38. Highlight of the Arginine297 residue that is proposed to initiate conformational change of the loop to protect unstable intermediates from bulk solvent. (PDB:14M1)

Further evaluation of the loop region was performed with deletion variants. Three loop deletion variants were generated to further evaluate the functional role of this region.[178] A shorter deletion (ΔH276-N282) was engineered to evaluate the effect of charged or polar residues, a 12-amino acid deletion contained a conserved region (ΔF261-N282), and the complete deletion of 22 amino acid residues of the dynamic loop (ΔF261-N282).[178] There was no desulfonation activity observed in coupled assays with any of the variants. There was no C4a-(hydro)peroxyflavin intermediate observed with the large deletion in rapid reaction kinetic studies.[178] In single turnover studies monitored at 450 nm with both SsuE and SsuD, there is a lag phase that has been associated with flavin transfer. In the absence of SsuD, the lag phase does not exist because the flavin is released and rapidly oxidized. Results from single turnover stopped-flow kinetic studies with both SsuE and SsuD showed the absence of a lag phase and the flavin was rapidly oxidized. Results suggest that this insertional region is important for protection of reactive intermediates. The Arg297 residue may form electrostatic interactions with the phosphate group of FMN.[175]

1.5.5 Active Site of SsuD

With the similarity in fold between SsuD and LuxA, LuxA was used to identify conserved amino acid residues in the active site of SsuD.[175] The active site is located at the C-terminal end of the beta-barrel which is observed with most TIM-barrel enzymes.[179,175] The conserved active site amino acid residues of SsuD (Val107, Phe7, Leu94, Thr95, Trp196, Arg127, Glu180, and Ser179) are comparable to LuxA conserved active site amino acid residues (Val173, Phe6, Ile191, Ser193, Trp194, Arg107, Glu175, and Ser176) that are required for flavin binding.[175] There are conserved amino acid residues in LuxA that were also identified in SsuD.[175, 180] Several conserved amino acids in the active site of SsuD (Cys54, Phe7, His11, His333, Tyr331, His228, and Arg226) have been substituted in previous studies to evaluate their role in catalysis (Figure 1.39). [175] Cys54

is the only cysteine residue in the active site pocket and was hypothesized to play an important role in catalysis. Cys54 has been proposed to stabilize directly or indirectly the flavin intermediate formed during catalysis through hydrogen bonding interactions.[181] Substitution of His228 to alanine resulted in a 50-fold decrease in desulfonation activity compared with wild-type SsuD. However, substitution of His11 and His333 did not alter the kinetic parameters of SsuD. Substitution of Arg226 with Ala resulted in no observable activity. Additional kinetic isotope studies supported a role for Arg226 in proton donation to the FMNO- intermediate triggering a conformational change that releases product.[182] MsuD has a 60% amino acid identity with SsuD, and the active site amino acids are conserved between SsuD and MsuD.

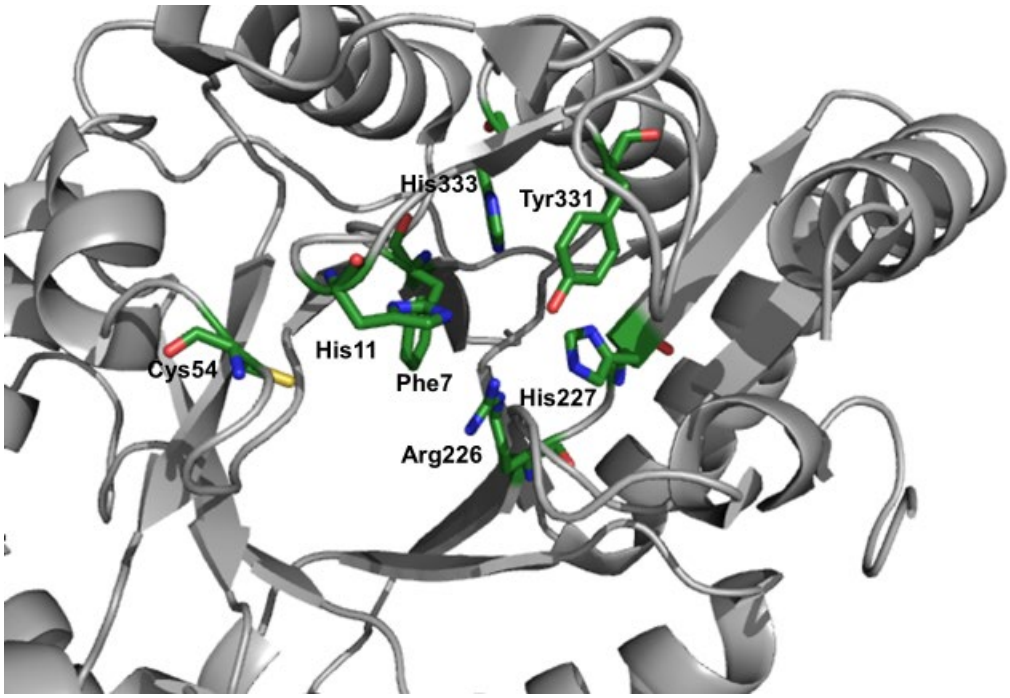

Figure 1.39. Active site amino acids of SsuD (PDB:14M1) (*E. coli*).

1.5.6 Transfer of Intermediates

Successful transfer of reactive intermediates such as reduced flavin is crucial for catalytic activity in two-component flavin-dependent systems. Reduced flavin is highly reactive with molecular oxygen producing superoxide which can be toxic to cellular function. Two-component flavin-dependent enzymes may utilize different approaches to transfer reduced flavin. The different approaches include free-diffusion, channeling that involves direct protein-protein interactions, or a combination of both diffusion and channeling (Figure 1.40).

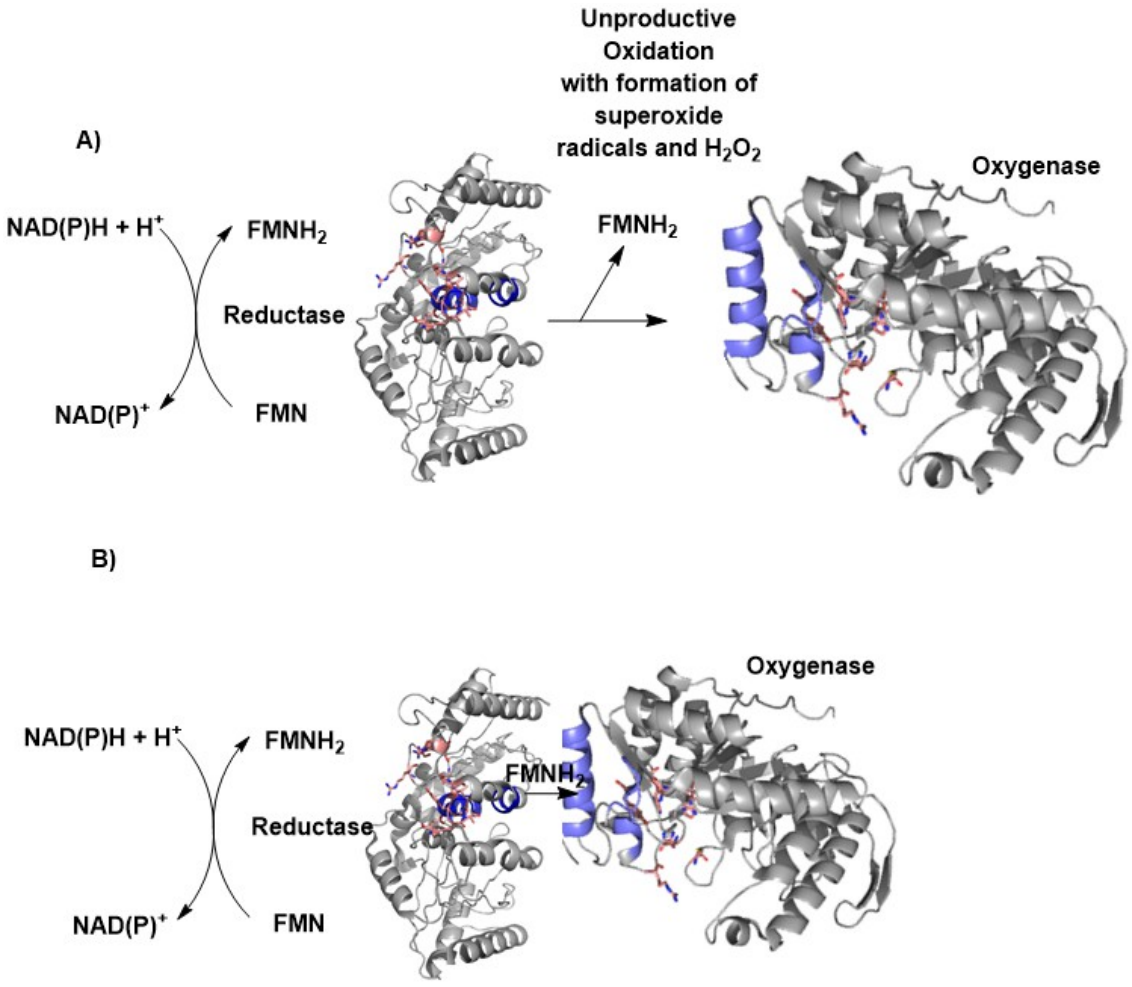

Figure 1.40. A) Free-diffusion versus B) channeling mechanism. Crystal structures pictured SsuE (PDB:4PTY) and SsuD (PDB:1M41).

Bacterial luciferase (LuxAB) has been proposed to utilize a free-diffusion mechanism for flavin transfer that involves the release of reduced flavin in bulk solvent.[183] Results from pull-down assays involving FRE (*E. coli*), FRP (*V. harveyi*) with bacterial luciferase (*V. harveyi*) supported a free diffusion mechanism for flavin transfer.[183] None of the reductase enzymes were able to form a stable complex with bacterial luciferase. Expressed on the same operon of LuxAB from *V. harveyi* was the flavin reductase LuxG, and there were no direct protein-protein interactions identified between LuxAB and LuxG.[183] Rate constants for the formation of the flavin intermediate are observed with LuxG in the presence of an oxidase component HPAH (C_2) from *A. baumanii*. [183] The rate of reduced flavin release from LuxG was the same with LuxG or C_2.[183] Based on the results, it was suggested that free-diffusion is the mechanism utilized with the transfer of reduced flavin in the presence of LuxG and LuxAB.

Both a channeling and free-diffusion mechanism was proposed with styrene monooxygenase (*P. putida*) (Figure 1.41).[184] Styrene monooxygenase is a two-component flavoenzyme that is composed of a flavin reductase (SmoB) and a styrene epoxidase (SmoA) that utilizes both NADH and FAD.[184] It is suggested that flavin dynamics play a critical role in catalysis between the two enzymes.[184] The two enzymes are able to form a transient flavin-transfer complex with the AMP portion of FAD in SmoA.[184] The isoalloxazine ring of the oxidized FAD is accessible to SmoB to provide electrons while the AMP portion is associated with SmoA.[184] Once FAD is reduced, it is released from the active site of SmoB and efficiently transferred to SmoA without interacting with molecular oxygen.[184] An alternative mechanism involves the shared binding of FAD with the isoalloxazine ring bound to SmoB and AMP bound to SmoA.[184]

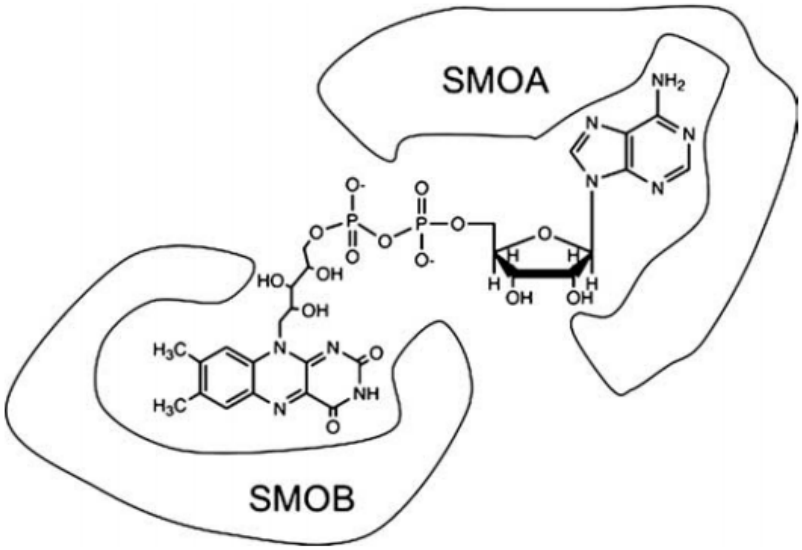

Figure 1.41. A mixture of both free diffusion and channeling that occurs between SmoA (FAD-specific styrene epoxidase) and SmoB (flavin reductase) with transfer of reduced flavin *from Pseudomonas putida*.[184] Copyright © 2005 Archives of Biochemistry and Biophysics

Channeling is another method that helps protect reduced flavin from unproductive oxidation. Protection of the reduced flavin occurs by protein-protein interactions between both SsuE and SsuD. SsuE and SsuD bind in a 1:1 stochiometric ratio with a K_d value of 2.2 ± 1.0 nM.[185] Hydrogen-deuterium exchange was used to identify residues involved in protein-protein interaction sites (Figure 1.42).[186] Protein-protein interaction regions for SsuE were identified at the π-helix (119-125) and on the α-helix (78-89).[186] Regions for SsuD were identified at two different α-helices (251-261 and 285-295).[186] The two regions identified for SsuD are located at the opening to the active site and are connected to each other by the loop. These results suggest that the active sites of both enzymes align together to transfer reduced flavin, and specific regions contribute to the protein-protein interactions.

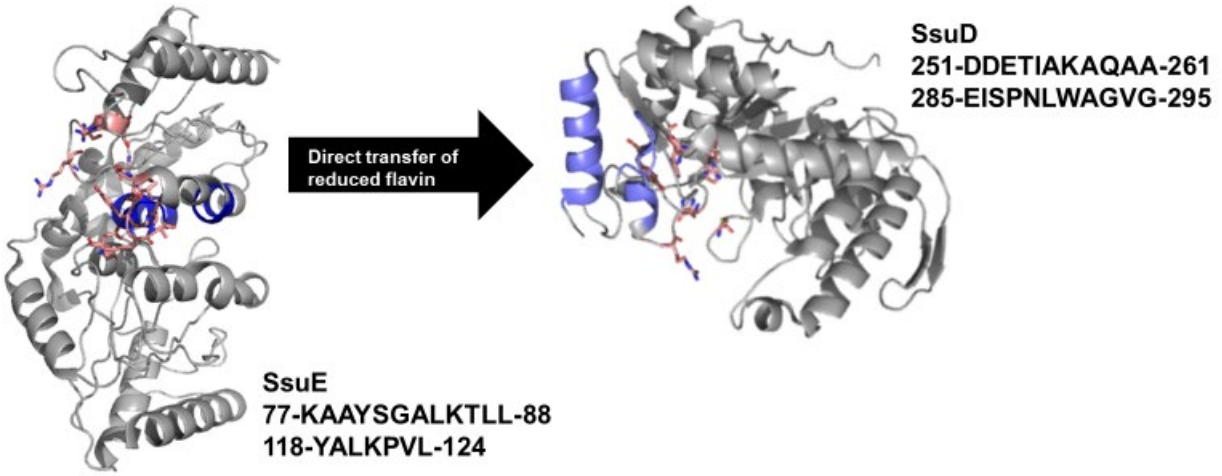

Figure 1.42. Key interaction sites identified for SsuE/SsuD (*E. coli*) through HDX. (Adapted from [186])

The protein-protein interaction regions for both SsuE and SsuD contain positive and negatively charged residues that may be involved in electrostatic interactions with each other. Electrostatic residues present in the SsuD binding region of SsuE include Lys77, Lys86, and Lys121, whereas residues for SsuD involve Asp251, Asp252, Glu253, and Lys257.[186] SsuD variants (DDE(251/252/253)AAA and ΔD251-A261) were generated to further evaluate the functional role of this region.[186] The deletion variant completely deleted the α-helical region.[186] The triple alanine variant showed a 4-fold reduction in activity compared with wild-type SsuD, but the deletion variant was no longer able to produce sulfite in coupled assays.[186] Binding of reduced flavin to the SsuD variants was not affected. The SsuD deletion variant was no longer able to interact with SsuE in fluorescent titration studies, which explains the decrease in observed activity. Without these protein-protein interaction sites for SsuD, the variants were no longer able to interact and receive reduced flavin from the flavin reductase to ensure activity.

1.6 Summary

Sulfur is common in the environment but can be inaccessible to living organisms.[1] To obtain sulfur, plants and bacteria utilize an inorganic sulfur source for the biosynthesis of the amino acid cysteine that is incorporated into various sulfur-containing cofactors that are essential in many biochemical reactions.[1,14] When inorganic sulfur is limiting in the environment, bacterial organisms express specific set of proteins to utilize alternative sulfur sources. These set of proteins are categorized as sulfate starvation-induced proteins (SSI proteins) and are involved in the transport of organosulfur compounds.[1,49,50,51] Desulfonation of organosulfur compounds is the process of cleaving the carbon-sulfur bond of organosulfonates by proteins found in FMN-dependent two-component systems.[53] These two-component systems catalyze diverse reactions consisting of a flavin reductase (FR) that transfers reduced flavin to a partner monooxygenase (MO).[53] The MO of these two-component systems will utilize the reduced flavin to activate dioxygen and insert an oxygen atom into the organosulfonates.[53] The cleavage of the carbon-sulfur bond of organosulfonates results in the production of sulfite that provides the alternative sulfur source for sulfur limited environments.[53] Diverse desulfonation pathways include SsuE (FR) and SsuD (MO) with linear alkanesulfonates (C_2-C_{10}) that produces sulfite and corresponding aldehyde, MsuE (FR) and MsuD (MO) with methanesulfonate (C_1) to produce sulfite and formaldehyde, and SfnF (FR) and SfnG (MO) that converts methanesulfinate to methanesulfonate with production of formaldehyde.[53,68,72] Multiple two-component FMN dependent systems involved in sulfur acquisition share conserved structural motifs that may be related to a common function and may contribute to catalytic function. These specific structural properties that have been identified are common for both the flavin reductase and monooxygenase that may contribute to flavin transfer and binding.[147, 175]

The flavin reductases belong in the NAD(P)H:FMN reductase family belong to the flavodoxin-like superfamily.[147] The enzymes found in this family all have a similar structural fold, but the flavin reductases from two-component systems are further subgrouped due to a π-helical region.[147] This region has been characterized with a single amino acid insertion into a conserved α-helix.[159, 162, 163] SsuE exists as a tetramer and will undergo an oligomeric switch from a tetramer to a dimer in the presence of either FMN or SsuD.[147,156] The π-helix is located within the tetramer interface of SsuE that stabilizes the overall structure with key π-stacking interactions and hydrogen bonding across the tetramer interface.[156] This conserved region of flavin reductases may play a role in initiating this oligomeric switch that exposes the active site to transfer reduced flavin to partner MO.[156] Studies evaluated the role of the single amino acid residue of SsuE (Tyr118). The Y118A SsuE variant was no longer able to provide reduced flavin to SsuD and purified flavin bound, a characteristic of other canonical FR found in the family with no π-helix.[187] These results suggest that the π-helical region is important for efficient flavin transfer to the partner monooxygenase.[187]

The FR with the conserved π-helix are characterized by residue insertion (Y118 SsuE, H126 MsuE, and H128 SfnF).[147] With the similarity of the conserved π-helix but different amino acid insertions, both SsuE and MsuE had their respective amino acid residues switched to evaluate if there is similar kinetic activity with wild-type and variants. The switched insertional residues were performed to identify if similar function could be maintained with their respective monooxygenase partners. Further analysis with the π-helix was compared with the α-helix of the structurally distant flavin reductase ChrR. There are conserved residues (proline and aspartic acid) found only in the π-helix, where the α4-helix of ChrR has two glutamine residues in a comparable location. These conserved residues may play a role in the formation of the π-helix besides the single amino acid

insertion. These conserved structural features of the flavin reductase may allow for efficient transfer of reduced flavin to the partner monooxygenase.

FMN-dependent two-component system MO SsuD has been characterized with a TIM-barrel fold.[175] Monooxygenase MsuD also belongs to a two-component system, shares high sequence identity with SsuD, but catalyzes different pathways for sulfur assimilation. Structural features of these monooxygenases may determine the organosulfonates specificity. An insertional region that separates SsuD from other TIM-barrel fold enzymes has been characterized and is proposed to close over the active site.[175] Closure over the active site provides a stable environment for the reduced flavin to form either the C4a-hydroperoxy or peroxyflavin intermediate.[74] Loop closure is essential for catalysis, with studies involving a complete loop deletion resulting in no observable activity with desulfonation.[177] The loop of SsuD has a conserved arginine residue (Arg297) that may form electrostatic interactions with the phosphate group of reduced flavin. The Arg297 on the dynamic loop may initiate conformational changes to protect reduced flavin from interacting with bulk solvent.[177] With a high amino acid identity but different sulfur specificity, other structural features may also promote sulfur specificity. Both MsuD and SsuD have a similar active site architecture, and it is proposed that both monooxygenases should have the ability to cleave the same range of organosulfur compounds.

The focus of this dissertation is to determine the structural features that promote catalysis for FMN-dependent two-component system enzymes. Studies will evaluate conserved residues found within the π-helix of all the flavin reductases. These conserved residues are not found in equivalent positions of other canonical flavin reductases from the same family. Specific amino acid substitutions will be generated, and the variants will be evaluated through kinetic, spectroscopic, and structural studies to provide insight on the functional role of the π-helix in two-component

FMN-dependent systems. The loop region for monooxygenases may play a role in substrate binding. Initial studies focused on identifying the preferred substrate of SsuD and MsuD through kinetic approaches. Additional studies will be performed to determine how the dynamic loop region contributes to substrate binding with SsuD.

Chapter Two

Not as Easy as π: An Insertional Residue does not Explain the π-helix Gain-of-Function in Two-Component FMN Reductases

2.1 Introduction

In the majority of flavoprotein monooxygenases, the flavin is tightly bound and both the reductive and oxidative half-reactions occur on the same enzyme. However, a group of flavoprotein monooxygenases have been identified that rely on a separate flavin-dependent reductase to catalyze the reductive half-reaction, with the reduced flavin transferred to a flavin-dependent monooxygenase to catalyze the oxidative half-reaction, generating an oxygenated product. While the substrates for the monooxygenases of two-component systems are quite diverse, several FMN-dependent two-component monooxygenase systems have been identified that are involved in bacterial sulfur acquisition. A common means for acquiring sulfur during sulfur limitation in diverse bacteria is the two-component alkanesulfonate monooxygenase system (Figure 2.1A). The majority of kinetic studies have focused on the alkanesulfonate monooxygenase system in *Escherichia coli*.[53,75,149,154,188,182] but these systems are widely conserved suggesting an essential role in maintaining cellular sulfur concentrations.[182] *Pseudomonas* sp. have a more complex mechanism for sulfur acquisition when sulfur in the environment is limiting.[49] Certain pseudomonads contain multiple two-component FMN-dependent systems that form a pathway to convert dimethylsulfone ($DMSO_2$) to sulfite, but also allow them to utilize long-chain aliphatic sulfonates. $DMSO_2$ is derived through the oxidation of dimethyl sulfide, a secondary metabolite in some marine algae, and is the most abundant biological sulfur compound emitted to the atmosphere.[189] $DMSO_2$ is converted to methanesulfinate by dimethylsulfone monooxygenase (SfnF/SfnG) (Figure 2.1B).[69,190,68,191,70] The

methanesulfinate produced is oxidized in some *Pseudomonas* sp. to methanesulfonate by the methanesulfinate monooxygenase system (MsuE/MsuC) (Figure 2.1C), and the methanesulfinate is further oxidized to sulfate and formaldehyde by methanesulfonate monooxygenase (MsuE/MsuD) (Figure 2.1D).[95] *Pseudomonas aeruginosa* contains a complete pathway for the conversion of $DMSO_2$ to sulfite release.

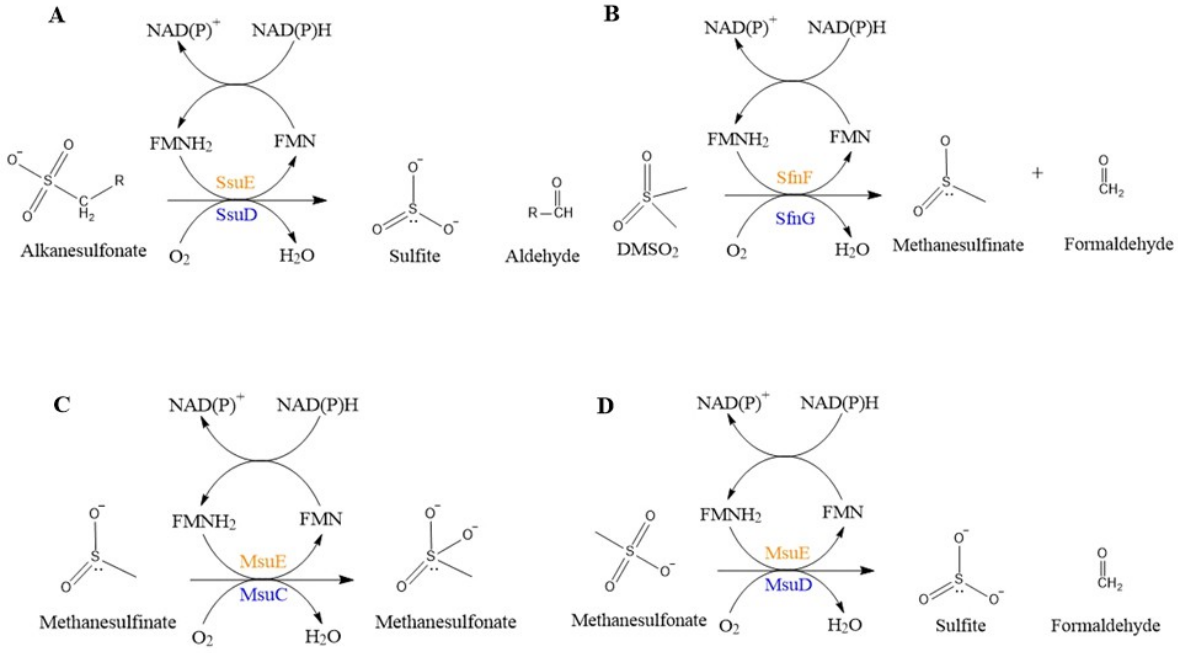

Figure 2.1. Reactions of two-component systems involved in sulfur metabolism. Two-component FMN-dependent monooxygenase reactions found in different bacterial organisms: (A) alkanesulfonate monooxygenase reaction (SsuE/SsuD); (B) dimethysulfone monooxygenase reaction (SfnF/SfnG), (C) methanesulfinate monooxgenase reaction (MsuE/MsuC); (D) methanesulfonate monooxygenase reaction (MsuE/MsuD). (Adapted from[192]). Copyright © 2018 The Protein Society

Two NAPDH:FMN reductases with high structural similarity to SsuE are YdhA from *Bacillus subtilis* and ArsH from *Shigella flexneri*.[147,193,194] The YdhA enzyme is classified as a quinone

reductase, and ArsH is a reductase involved in arsenic resistance.[193,194,195,196] Unlike the reductases of the two-component systems, YdhA and ArsH do not require a monooxygenase partner, performing the oxidation of substrate molecules themselves. All four enzymes—YdhA, ArsH, SfnF, and SsuE—are grouped into the NAD(P)H:FMN reductase family based on the flavodoxin fold. These enzymes are further divided into subgroups of the family based on helix 4. Whereas helix 4 in YdhA and ArsH is an α-helix, in the two-component FMN-dependent reductases, helix 4 is a π-helix structure. The π-helix is characterized by a wider turn due to $i + 5 \rightarrow i$ hydrogen bonding that causes a bulge in the helix. It has been proposed that π-helices arise due to an amino acid insertion in an established α-helix, which becomes the basis of a new structural element with a defined function. The π-helix has been proposed to provide a gain-of-function, thereby counterbalancing the relative structural instability compared with a continuous α-helix. Specified functional roles for π-helices have been experimentally identified in a limited number of proteins, and include active site features to promote metal or cofactor binding, or introduction of catalytic residues.[197,159]

The π-helix in SsuE has been proposed to be generated by the insertion of a Tyr residue in the conserved α4-helix.[147] In the three-dimensional structure of apo-SsuE (PDB 4PTY), π-stacking interactions are observed between the aromatic rings of Tyr118 residues across the tetramerization interface. In a flavin-bound SsuE structure, the hydroxyl group of Tyr118 hydrogen bonds to the oxygen atom backbone carbonyl of Ala78 across the tetramer interface; however, this structure was generated by soaking tetrameric crystals with excess flavin.[147] In solution, the SsuE enzyme has been shown to undergo a tetramer to dimer oligomeric change upon binding of FMN (Figure 2.2A), and this oligomeric change may promote protein–protein interactions that facilitate the release of reduced flavin to SsuE (Figure 2.2B,C). Therefore, the π-helix may provide a gain-of-

function by promoting the release of reduced flavin to the monooxygenase. Previous studies showed that conversion of Tyr118 to alanine (Y118A SsuE) generated protein that stably bound oxidized FMN and showed no NADPH oxidase activity.[187,156] A deletion variant of Tyr118 (ΔY118 SsuE) was not purified with FMN bound, but the variant also lacked reductase activity. Whereas the initial flavin reduction was observed in the SsuE variants, the $FMNH_2$ was trapped in the closed active site, preventing steady-state reductase activity.[187] Although the FMN was reduced, both Y118A and ΔY118 SsuE were also unable to support desulfonation by the SsuD monooxygenase.

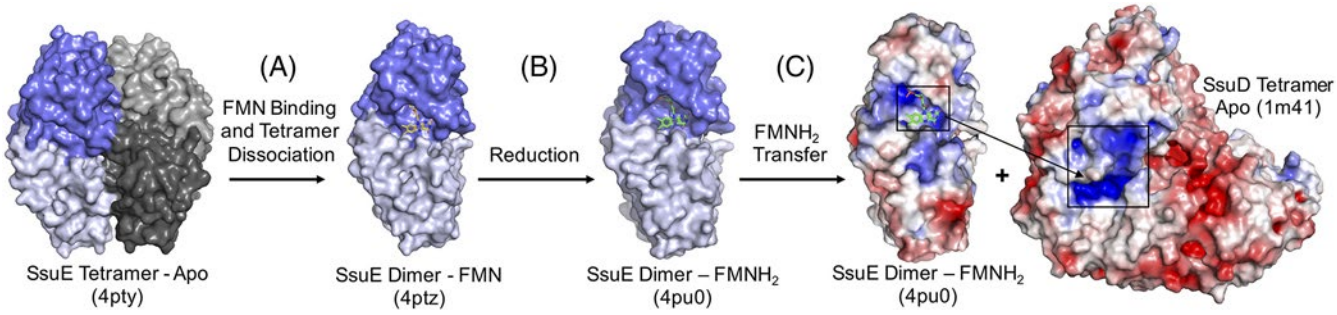

Figure 2.2. Structural scheme for the mechanism of the two-component alkanesulfonate monooxygenase system. (A) The tetramer of SsuE (monomers for dimers are shades of gray and blue) binds FMN (yellow carbons) and dissociates to a dimer. (B) FMN is reduced by NAD(P)H to $FMNH_2$ (green carbons). (C) Electrostatic surface views of SsuE and SsuD (blue, positive charge; red, negative charge). $FMNH_2$-bound SsuE associates with SsuD and transfers the reduced flavin to the SsuD monooxygenase. The predicted SsuD active site region is boxed and has a charged surface complementary to the $FMNH_2$ binding region of the SsuE dimer. The apo, FMN-bound, and $FMNH_2$ SsuE structures were rendered with PDB: 4PTY, 4PTZ, and 4PU0, respectively. The SsuD structure was rendered with PDB 1M41 (Adapted from[192]). Copyright © 2018 The Protein Society

In addition to modification of the kinetic properties, variants of Tyr118 showed altered oligomeric states compared with wild-type SsuE.[187,156] Whereas apo wild-type enzyme is tetrameric in solution and in crystals, addition of FMN promotes conversion to a dimeric state.[186] In the structure of wild-type SsuE, the Tyr118 insertional residue sits near the 222 symmetry of the tetramer, but it is not known how FMN binding alters contacts to promote the conversion from tetramer to dimer. The structure of FMN-bound wild-type SsuE was determined by soaking apo crystals in a large excess of FMN. Therefore, the oligomerization state is the result of the crystal lattice of the apo-protein and does not represent the physiological oligomeric state upon FMN binding. The Y118A variant is dimeric in solution.[187] Taken together, the above data suggest that removing the tyrosine sidechain (Y118A) prevents flavin release, and that the transition from the tetrameric to dimeric state may be important in FMNH2 transfer from SsuE to the monooxygenase SsuD. Deletion of Tyr118 (ΔY118 SsuE) also eliminates reductase activity; however, this variant was tetrameric in solution.[187] We hypothesized that in both Y118A and ΔY118 SsuE, helix 4 would be a continuous α-helix due to removal of the tyrosine insertional residue.

In *Pseudomonas putida* SfnF (PDB 4C76—we note that this protein is misannotated in the PDB as MsuE), the insertional residue is a histidine (His128), which potentially plays a similar π-stacking role as Tyr118 SsuE. Amino acid sequence analyses and structural modeling of MsuE from *P. aeruginosa* indicate that the overall structure is similar to SsuE and SfnF, with a π-helix His insertional residue. Therefore, we tested the hypothesis that interchanging the π-helix insertional residues would generate variant proteins, Y118H and H126Y MsuE, with kinetic properties consistent with those of the wild-type enzyme.

The single amino acid insertion has been proposed to be the primary cause of π-helix formation. However, there may be additional features that contribute to the π-helical structure. The chromate reductase, ChrR, from *E. coli* has 25% amino acid identity with SsuE (*E. coli*) and is structurally distant than the other homologs such as ArsH (*Shigella flexneri*). Initially the α4 helix of the enzymes characterized with the π-helix resulted in a gap insertion. However, the α4 helix of ChrR identified no insertional gap, but rather a similar tyrosine residue in the same position as the Tyr118 of SsuE. Therefore, formation of the π-helix is likely dependent on additional amino acid residues. A proline and aspartic acid are also conserved in the π-helical regions of flavin reductases SsuE (D117/P123), MsuE (D125/P130), and SfnF (D127/P132) (Figure 2.3). These residues were not identified in the α4 helix of ChrR, which had glutamine residues in similar positions (Q127/Q132) (Figure 47). Proline residue are often located at the end of a π-helix before it converts back to an α-helix, and leads to the breakage of at least two adjacent hydrogen bonds.[198,159] The disruption of the hydrogen bonding pattern has been proposed to assist in facilitating the π-turn.[199] These conserved residues may also assist in stabilizing the π-helical structure in the two-component FMN reductases. Aspartic acid and proline variants of MsuE and SsuE were also generated to evaluate the importance of these residues in helping to maintain the properties of the π-helix that influence the overall function.

Figure 2.3. Amino acid sequence alignment of the α4 helix of SsuE (*E. coli*), EmoB (*EDTA-degrading bacterium BNC1*), MsuE (*P. aeruginosa*), SfnF (*P. putida*), and ChrR (*E. coli*).

2.2 Materials and Methods

2.2.1 Materials

The *P. aeruginosa* (PAO1) cell line was purchased from ATCC type culture collection (ATCC15692). *E. coli* strains [XL-1 Blue and BL21(DE3)] were purchased from Stratagene (La Jolla, CA). Plasmid vectors and pET21a were obtained from Novagen (Madison, WI). DNA primers were synthesized by Invitrogen (Carlsbad, CA). Pfu Turbo DNA polymerase was purchased from Agilent (La Jolla, CA). Zero Blunt PCR Cloning Kit was purchased from ThermoFisher (Waltham, MA). Difco-brand Luria-Bertani (LB) media was purchased from Becton, Dickinson and company (Sparks, MD). Phenyl Sepharose™ 6 Fast Flow (high sub) was purchased from GE Healthcare Biosciences, (Uppsala, Sweden). Macro-Prep® High Q Support (Bio-Rad Laboratories, Hercules, CA). sodium dodecyl sulfate (SDS) and acrylamide were purchased from Biorad (Hercules, CA). Buffer components and chemicals for kinetic assays were purchased from Sigma (St. Louis, MO). Isopropyl-β-d-1-thiogalactoside (IPTG), sodium chloride, and glycerol were obtained from Macron Fine Chemicals (Center Valley, PA). Oligonucleotide primers were purchased from Invitrogen (Carlsbad, CA).

2.2.2 Cloning and site-directed mutagenesis of MsuE and SsuE

Cloning of the *msuE* and *msuD* gene into an expression vector was performed by PCR amplification of the gene from *P. aeruginosa*. A 100 mL culture of *P. aeruginosa* was grown overnight at 37°C. The cells were pelleted following an overnight incubation, and the chromosomal DNA from *P. aeruginosa* was extracted using the QIAprep Spin Miniprep Kit. The *msuE* gene was PCR-amplified using the primers (5′-GAT GAT CAT ATG ACC AGC CCC TTC AAA) and (5′-GAT GAT CTC GAG TCA GGC GAT CTT CAA) which included engineered *Nde* I and *Xho* I restriction sites for ligation into the pET21a expression vector. A hairpin existed between the *msuC* and *msuD* operon, which made in difficult to amplify *msuD* from the genome. Both msuC and msuD were first PCR-amplified using the primers (5′-ATGAACGTGTTCTGGTTCCTCCC) and (5′-TATGGGTAGCTCGAGTCATGAGTAG), and the resulting PCR product was cloned in to the pCR-Blunt cloning vector using the Zero Blunt PCR Cloning Kit. The DNA vectors containing representative clones were submitted for DNA sequence analysis (Eurofins/Genomics, Louisville, KY). The *ssuD* gene was PCR-amplified from the pCR-Blunt vector containing *msuC*/*msuD* using the primers (5′-GCGCATATGAACGTGTTCTGGTTC) and (5’ CCCCTCGAGTCAAGCGCC), which included engineered *Nde* I and *Xho* I restriction sites for ligation into the pET21a expression vector. The T7 RNA polymerase-dependent expression vector pET21a (Novagen, Madison, WI) and the *msuE* and *msuD* PCR products were digested with restriction enzymes *Nde* I and *Xho* I for 1 h at 37°C. A 3:1 ratio of either *msuE* or *msuD* insert to pET21a vector were ligated with T4 DNA ligase at 16°C overnight, and transformed into Top10 cells following the overnight incubation. The DNA vectors containing representative clones were submitted for DNA sequence analysis (Eurofins/Genomics, Louisville, KY).

Variants of Tyr118 in SsuE and His126 in MsuE were generated to investigate the importance of these residues in preserving the π-helix. The primers were designed as 27-base oligonucleotides for the Y118H SsuE and H126Y MsuE variants. The primers were ordered from Life Technologies by substituting the *ssuE* codon TAT representing Tyr118 with TCT and substituting the *msuE* codon TCT representing His with TAT. The substitution of the proline and aspartic acid residues to a glutamine was performed with a 27-base oligonucleotide substituting codon GAT representing D117 with CAA and codon CCA representing P123 with CAA for SsuE. Similar substitution for *msuE* were performed substituting GAC representing D125 with CAA and codon CCG representing P130 with CAA. Double variants for both were designed to evaluate the α4 helical region of ChrR for SsuE (D117Q/P123Q) and MsuE (D125Q/P130Q). The Qiagen kit plasmid purification protocol was utilized to prepare the SsuE and MsuE plasmid for site-directed mutagenesis. Following site-directed mutagenesis, the SsuE variants were confirmed through DNA sequencing analysis (Eurofins/Genomics, Louisville, KY). The FMN-dependent reductase and monooxygenase enzymes were expressed and purified in *E. coli* strain BL21(DE3) as previously described.[75] The concentrations of SsuD and SsuE proteins were determined from A_{280} measurements using a molar extinction coefficient of 47.9 and 20.3 $mM^{-1}\ cm^{-1}$, respectively.[75] Concentrations of MsuD and MsuE were determined from A_{280} measurements using a molar extinction coefficient of 49.4 and 7.5 $mM^{-1}\ cm^{-1}$, respectively.

2.2.3 Steady-state kinetic assays of SsuE and MsuE

The NAD(P)H oxidase activity for wild-type MsuE was initially evaluated to determine steady-state kinetic parameters and substrate specificity for MsuE. Kinetic parameters for FMN were determined with 0.1 μM wild-type or H126Y MsuE at varying concentrations of FMN (0.01–3 μM) with fixed concentrations of NADPH (100 μM), or varying concentrations of FMN (0.3–

13 μM) with fixed concentrations of NADH (200 μM). The kinetic parameters for NADH and NADPH were determined with 0.1 μM MsuE at varying concentrations of NADPH (2.5–150 μM) with fixed concentrations of FMN (2 μM), or varying concentrations of NADH (2.5–150 μM) with fixed concentrations of FMN (10 μM). The SsuE enzyme can utilize either NADH or NADPH in NAD(P)H oxidase assays, but has a flavin preference for FMN. Steady-state kinetic parameters for wild-type or Y118H SsuE were performed as previously described to maintain consistency with previous studies.[75] The proline and glutamate variants of SsuE and MsuE were also performed similar to their respective wild-types. All assays were performed in triplicate, and the initial rates were obtained by monitoring the decrease in absorbance at 340 nm with the oxidation of the reduced pyridine nucleotide. The steady-state kinetic parameters were determined by fitting the data to the Michaelis–Menten equation.

The steady-state coupled assay was performed as previously described.[200] The reactions were initiated with the addition of 500 μM NADPH into a reaction mixture containing wild-type, Y118H SsuE, D117Q SsuE, P123Q SsuE, or D117Q/P123Q SsuE (0.6 μM), FMN (2 μM), SsuD (0.2 μM), and varied concentrations of octanesulfonate (10–1000 μM) in 25 mM Tris–HCl (pH 7.5), and 0.1 M NaCl at 25°C. The desulfonation assays with SsuD were also performed using wild-type and H126Y MsuE (0.6 μM) in the reaction to provide reduced flavin. The reaction was quenched after 3 min with 8 M urea, and the sulfite product was quantified as previously described.[154] Conditions for the coupled reactions with wild-type MsuD and the variants were performed similar to SsuD, but the concentration of methanesulfonate was varied from 5–500 μM. All assays were performed in triplicate, and steady-state kinetic parameters were determined by fitting the data to the Michaelis–Menten equation.

2.2.4 Fluorescence Titrations

Fluorometric titrations with FMN were performed to evaluate the effects of the proline and glutamate substitutions on flavin binding. Binding of flavin to wild-type SsuE and the variants were monitored on a Cary Eclipse Agilent (Santa Clara, CA) fluorescence spectrophotometer with an excitation of 280 nm and emission measurements at 344 nm. A 1.0 mL solution of flavin-free variants or wild-type SsuE (0.1 μM) in 25 mM potassium phosphate (pH 7.5) and 0.1 M NaCl was titrated with FMN (from 0.2-1.2 μM) 1 μL increments. Due to a low intrinsic fluorescence of wild-type MsuE, binding of flavin to wild-type MsuE or the variants were monitored with an excitation of 450 nm and emission measurements at 525 nm. A 1.0 mL solution flavin (0.1 μM) in 25 mM potassium phosphate (pH 7.5) and 0.1 M NaCl was titrated with wild-type MsuE or variants (from 0.2-1.2 μM) 1 μL increments. The fluorescence spectrum was recorded following a 2 minute incubation after each addition of enzyme.

All assays were performed in triplicate, and the K_d value was determined as previously described. Bound FMN was determined with equation 1:

$$[A]_{bound} = [B]\frac{I_o - I_c}{I_o - I_f} \quad (1)$$

where $[A]_{bound}$ represents the concentration of FMN-bound SsuE or MsuE, [B] represents the initial concentration of the enzyme in cuvette, I_o represents the initial fluorescence intensity prior to addition of either FMN or MsuE, I_c represents the fluorescence intensity of the MsuE or FMN following each addition, and I_f represents the final fluorescence intensity. The concentration of FMN bound was plotted against the free substrate or MsuE concentration to obtain the dissociation constant (K_d) according to equation 2:

$$y = \frac{K_d + x + n - \sqrt{(K_d + x + n)^2 - 4xn}}{2} \quad (2)$$

where y and x represent the concentration of the bound and free substrate, respectively, following each addition, and K_d is the maximum binding at equilibrium with the maximum concentration of substrate.

2.2.5 Circular Dichroism Spectroscopy

Circular dichroism (CD) spectroscopy was performed with wild-type and variants of SsuE and MsuE to determine if substitutions of the common residues proline and aspartic acid affected folding. Spectra was obtained with 5 μM of each protein in 10 mM potassium phosphate buffer (pH 7.5). A Jasco (Easton, MD) J-810 spectropolarimeter was used to record spectra at room temperature and 0.1-cm path length cuvette. Measurements were taken in 1-nm increments from 300 to 185 nm using a scanning speed of 50 nm/min and a bandwidth of 1-nm with an average of 8 scans performed for each sample. The background correction was achieved using the default parameters of the Jasco J-270 software.

2.2.6 Crystallization of the SsuE variants

All crystals were grown in hanging drops composed of 1.5 μL of well solution and 1.5 μL of protein in 10 mM HEPES pH 8.5, 100 mM NaCl, and 10% (v/v) glycerol. The apo Y118A SsuE crystals were grown using 68 mg/mL protein and a well solution of 100 mM Tris HCl pH 8.5 and 800 mM lithium sulfate. Crystals grew within 5 days and were cryoprotected with well solution containing 2.25 M lithium sulfate prior to flash cooling. The FMN-bound Y118A SsuE crystals were grown using 12.5 mg/mL protein, supplemented with FMN to 10 mM, before combining with well solution composed of 200 mM sodium thiocyanate pH 6.9 and 20% (w/v) PEG 3350.

Crystals grew within 5 days and were cryoprotected with well solution containing 30% glycerol prior to flash cooling. The Δ118 SsuE crystals were grown using 35 mg/mL protein and a well solution composed of 100 mM CHES: NaOH pH 9.5 and 30% (w/v) PEG 3000. Crystals grew within 5 days and were cryoprotected with well solution containing 25% glycerol prior to flash cooling.

2.2.7 Data collection and structural determination of the SsuE variants

Diffraction data were collected remotely using BluIce on beamline 12–2 at the Stanford Synchrotron Radiation Lightsource (SSRL, Menlo Park, CA).[201] All data sets were collected at a wavelength of 0.97946 Å with 0.15° oscillation and 0.2 s exposure at a temperature of 100 K. For Y118A SsuE, 180° of data were collected at a detector distance of 325 mm and processed to 1.95 Å in XDS.[202] A phasing solution was determined by molecular replacement in Phaser [3] using apo SsuE (PDB: 4PTY) as a model with a resulting LLG of 1,462 and TFZ of 39.9. For FMN-bound Y118A SsuE, 360° of data were collected at a detector distance of 315 mm and processed to 1.71 Å using AutoPROC.[203] A phasing solution was determined by molecular replacement, as above, with a resulting LLG of 904 and TFZ of 31.8. For Δ118 SsuE, 240° of data were collected at a detector distance of 250 mm and processed to 1.55 Å using AutoPROC [2]. A phasing solution was determined by molecular replacement as above with a resulting LLG of 2,581 and TFZ of 47.9. For each structure, rounds of model building and refinement were completed in Coot and Phenix Refine and waters were placed by Phenix Refine, corrected manually and verified, using a $2mF_oDF_c$ electron density map contoured at 1.5 σ, following a round of refinement.[204] [205] For FMN-bound Y118A SsuE, complete density for the active site FMN was visible following molecular replacement, but was not modeled until after refining the polypeptide backbone. For the

Δ118 SsuE variant, TLS refinement was used during the last two rounds of refinement. Statistics for data collection and refinement are listed in Table 2.1.

Table 2.1. Data collection and refinement statistics

Data were collected on beamline 12-2 at the Stanford Synchrotron Radiation Lightsource. Values in parentheses are for the highest resolution shell. (Adapted from[192]).

	apo Y118A SsuE	Y118A SsuE(+FMN)	apo Δ118 SsuE
Data collection			
Spacegroup	$P2_12_12_1$	$C222_1$	$P2_12_12_1$
Unit cell: a, b, c (Å), β (°)	a=39.5, b=41.5, c=189.0 α=90, β=90, γ=90	a=80.9, b=110.8, c=41.7 α=90, β=90, γ=90	a=40.9, b=41.8, c=182.3 α=90, β=90, γ=90
Resolution range (Å)	38.0 - 1.95	33.34 - 1.71	30.8 - 1.55
Completeness (%)	97.7 (99.2)	99.6 (99.7)	99.9 (99.9)
Total reflections	174,752	272,611	397,291
Unique reflections	23,620	20,849	46,854
I / σ	17.9 (7.0)	24.9 (2.1)	19.3 (3.0)
R_{merge}[a]	7.8 (31.0)	5.7 (>100)	9.3 (91.0)
R_{pim}[b]	4.7 (18.3)	1.6 (32.7)	3.3 (33.7)
Multiplicity	7.4 (7.6)	13.1 (13.3)	8.5 (8.1)
Refinement			
Resolution range (Å)	39.5 - 1.95	33.34 - 1.71	30.8 - 1.55
No. of reflections	23,063	20,841	46,844
R_{work} / R_{free}[c]	18.5 / 23.7	18.4 / 20.7	16.0 / 17.8
No. non-hydrogen atoms	2863	1500	2927
Protein	2734	1356	2720
Ligand/ion	5	87	12
Water	124	57	195
Ramachandran allowed (%)	100	98.3	100
Ramachandran outliers (%)	0	0	0
Wilson *B*	19.8	25.9	15.3
Average *B* (Å^2)	24.7	28.4	20.8
Protein	24.7	28.3	20.4
Ligand/ion	33.1	26.0	21.9
R.m.s. deviations			
Bond lengths (Å)	0.012	0.011	0.009
Bond angles (°)	1.1	1.27	1.03

[a] $R_{merge} = \sum_{hkl} |I_{hkl} - \langle I \rangle_{hkl}| / \sum_{hkl} I_{hkl}$ where I_{hkl} is the intensity of reflection *hkl* and $\langle I \rangle$ is the mean intensity of related reflections.

[b] $R_{pim} = \sum_{hkl} \sqrt{1/n-1}\, |I_{hkl} - \langle I \rangle_{hkl}| / \sum_{hkl} I_{hkl}$ where n is the multiplicity of related reflections.

[c] $R = \sum \left| F_o - |F_c| \right| / \sum |F_o|$ where F_o = to the observed structure factors and F_c = structure factors calculated from the model. 5% of the reflections were initially reserved to create an R_{free} test set used during each subsequent round of refinement.

2.2.8 Crystallographic model analysis

The apo Y118A, FMN-bound Y118A, and Δ118 SsuE models were analyzed by MolProbity and each showed good geometry with no Ramachandran outliers.[206] Apo Y118A SsuE has two monomers in the asymmetric unit with density for residues 1–172 and 1–174. Residues H148 and R149 are in a surface loop with discontinuous backbone density in both chains. The apo Y118A SsuE model contains 124 water molecules and one sulfate ion bound in the phosphate binding site of FMN (lithium sulfate was the precipitant and cryoprotectant). The Y118A SsuE variant with FMN bound has one monomer in the asymmetric unit with continuous density for residues 1–172, as well as 59 waters and 1 glycerol. Complete density for the active site FMN is present. A second FMN with partial electron density for two conformations is stacked along the isoalloxazine ring of the active site FMN. The $mF_o–DF_c$ map shows positive density over the positions of the isoalloxazine ring oxygens in both conformers. It is possible that water molecules maintain partial occupancy in these positions. The Δ118 SsuE variant has two monomers in the asymmetric unit with continuous density for residues 1–172 and 1–173, with 193 waters and 2 glycerol molecules. The two monomers seen in the asymmetric unit of apo Y118A and Δ118 SsuE form a dimeric assembly. The FMN-bound Y118A SsuE variant also crystallized in this dimeric assembly, but it is generated using symmetry operations with the monomer in the adjacent asymmetric unit. PISA predicts interface surface areas of 1125, 1196, and 1171 $Å^2$ for the three structures, consistent with the previously reported wild-type dimer interface of 1160 $Å^2$.[147,207]

2.3 Results

2.3.1 Preparation of Y118A and Δ118 SsuE

Crystal structures of π-helix variants Y118A SsuE, with and without FMN, and ΔY118 SsuE without FMN were obtained to high resolution (all better than 2 Å) to assess how variations at the critical π-helix alter the structure and potentially contribute to changes in function. The previously published crystallization conditions for wild-type did not produce diffraction quality crystals for Y118A SsuE and produced no crystals for ΔY118 SsuE; thus, it became necessary to screen for new conditions. Indeed, each variant structure determined in these studies was from an independent crystallization condition. The original conditions for wild-type protein used PEG3350 as a precipitant and citrate as an additive. The apo Y118A SsuE structure was determined from crystals that used lithium sulfate as a precipitant. The FMN-bound Y118A SsuE crystals did use PEG3350 as a precipitant, but at more than double to concentration (20% as opposed to 7%), with thiocyanate as an additive. Finally, ΔY118 SsuE crystals required 30% PEG3000 as a precipitant. Not surprisingly, these different crystals were not isomorphous (different unit cell parameters and space groups) to each other or to the wild-type conditions.

2.3.2 Overall structure of π-helical variants

As with all structures determined to date, only the first 172–174 residues of 191 total are resolved in the maps. As expected, the monomers of the Tyr118 variants maintain a high overall structural conservation compared with the previously determined wild-type SsuE structure (PDB: 4PTY), with root mean squared deviation values from 0.59 to 0.76 for 168–172 residues.[159] Unlike wild-type SsuE, which crystallizes as a tetramer, the Tyr118 variant structures determined here all crystallized as dimers (Figure 2.4A). The π-helices do not contribute to the dimeric

assembly (Figure 2.4B), and the variants show no difference at the dimeric interface compared with wild-type.

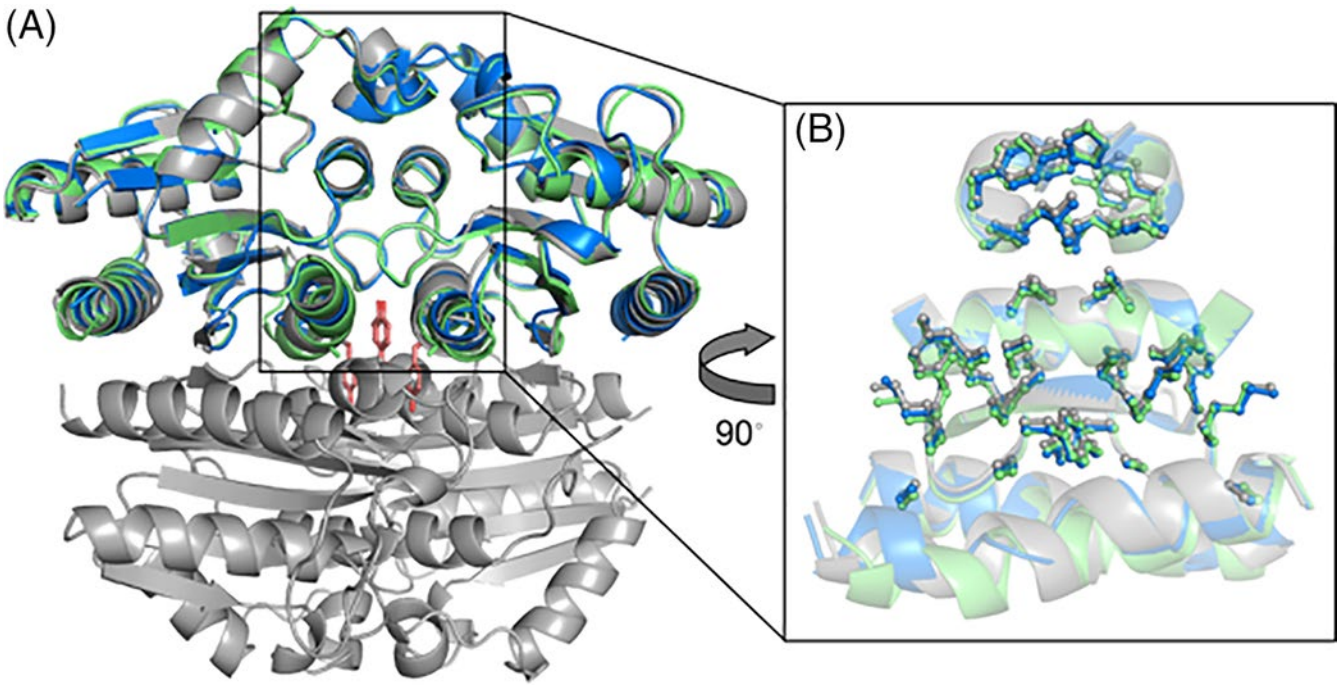

Figure 2.4. Oligomeric structures of the wild-type and Y118 SsuE variants. (A) Overlay of wild-type SsuE tetramer (gray with residue Y118 in orange) with dimers of apo Y118A SsuE (green) and Δ118 SsuE (blue) SsuE. The Y118A and Δ118 SsuE enzymes form the same homodimer as seen in the wild-type structure, but not the tetramer. (B) The position of the residues forming the 1160 $Å^2$ dimer interface remains the same in wild-type, Y118A, and Δ118 SsuE. The sidechains of the residues that make up the dimer interface are shown as ball-and-stick to emphasize their positional homology. (Adapted from[192]). Copyright © 2018 The Protein Society

The primary difference is found at the π-helix (Figure 2.5A). The Y118A SsuE variant no longer contained a π-helix, but instead helix 4 was a standard α-helix similar to that observed in ArsH and YdhA (Figure 2.5B). The original hypothesis was that the ΔY118 SsuE variant would also form a continuous α-helix for residues 110–127 through removal of the insertional tyrosine

residue. However, the electron density maps clearly demonstrate that the deletion of residue 118 prevents a helical hydrogen bonding pattern for residues 115–119, causing the helix to be broken into two smaller helices N- and C-terminal to the deletion with a random coil for the intervening 4 residues (Figure 2.5B).

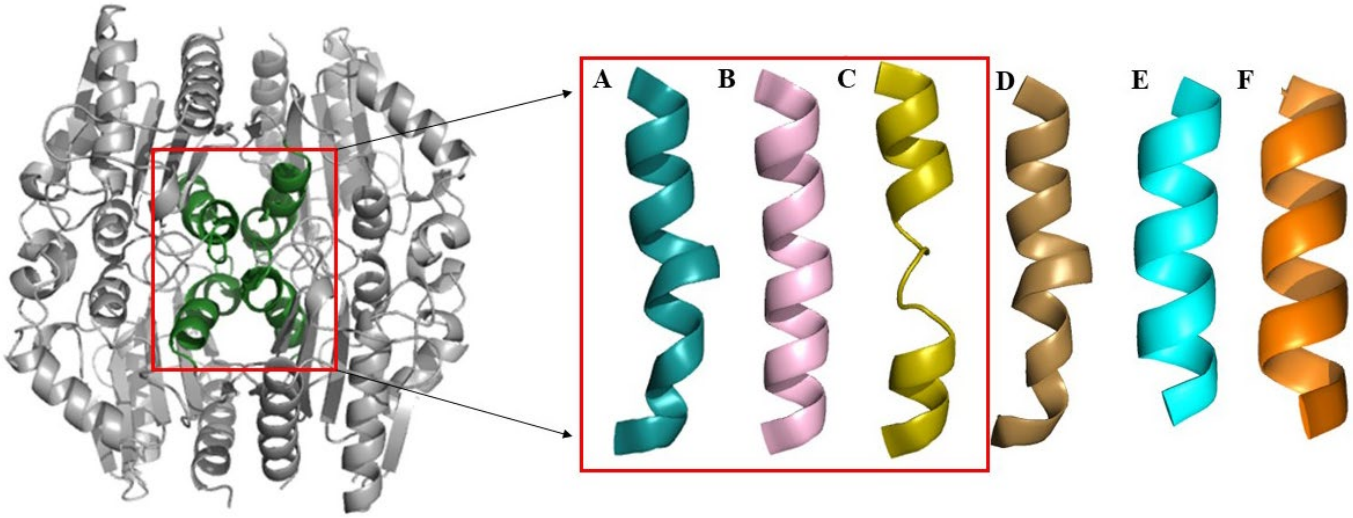

Figure 2.5. The π-helix in SsuE (A) spans residues 110–127. The Y118A (B) substitution results in the formation of a canonical α-helix, while the Y118 deletion (C) prevents hydrogen bond formation between the carbonyls and amines of the amino acid backbone for residues 115–119 breaking the helical structure. The homolog SfnF (D) with an inserted histidine forms a π-helix. In YdhA (E) and ArsH (F), the tyrosine is absent and an α-helix is formed. SsuE (PDB: 4PTY), Y118A SsuE (PDB: 6DQI), ΔY118 SsuE (PDB: 6DQP), SfnF (PDB: 4C76), YdhA (PDB: 2GSW), and ArsH (PDB: 2Q62).[147,193,194] (Adapted from[192]). Copyright © 2018 The Protein Society

2.3.3 FMN Binding to Y118A SsuE

A superposition of Y118A SsuE with and without FMN bound demonstrates the same global fold, for the active site, with minor variances seen within the loop regions. The rmsd values

between apo and FMN-bound Y118A SsuE, 0.53–1.0 Å for 173 Cα, indicate their remarkable similarity, despite their differing crystallization conditions and unit cell parameters. Complete density for the active site FMN is present. A second FMN that likely represents a crystallographic artifact is stacked along the isoalloxazine ring of the active site FMN with partial electron density for two conformations. A similar crystallographic FMN is observed in the FMN-bound wild-type structure.[147] In the wild-type structure, a hydrogen bond forms between the Tyr118 and a carbonyl oxygen of Ala78 from the opposing dimer, which in turn hydrogen-bonds to the isoalloxazine ring system of the FMN. This network was hypothesized to aid in communication between the oligomerization interface and FMN binding.[147] Whereas the Y118A SsuE variant clearly cannot hydrogen-bond to Ala78 through the deleted hydroxyl, the Ala78–FMN hydrogen bond remains intact, and the loop containing Ala78 has not shifted in conformation. The structure of the loop containing Ala78 is also maintained in the Δ118 SsuE structure.

2.3.4 Oligomeric assembly of π-helix variants

Comparison of the wild-type tetramer with the dimeric structures of FMN-bound Y118A and ΔY118 SsuE illustrates that key interactions composing the tetrameric interface are no longer possible (Fig. 2.6). The irregular helical turns in the wild-type π-helix provides a pattern of alternating hydrophobic residues that pack with the opposite homodimer (residues 110–114) (Figure 2.6B). The Y118A substitution results in helical turns of equal diameter (a continuous α-helix), but disrupts the hydrophobic packing pattern. This shift brings the N-termini of the helices in too close proximity for a stable interaction. Residues 111–114 take up new positions in the Y118A SsuE variant and reside in the three-dimensional space of the tetramerization interface of wild-type SsuE. Whereas only one π-helix is shown, the 222 symmetry of the tetramer means that this steric clash would have to be overcome twice to form a stable tetramer (Figure 2.6B). A similar

clash is predicted for the ΔY118 variant based on the structure determined here: a shift in residues 111–114 due to disruption of the helix is seen in the deletion mutant that would prevent tetramerization (Figure 2.6C). However, solution studies indicate that the primary ΔY118 SsuE oligomer is the tetramer.[156] Therefore, the less rigid broken helix must allow rearrangement of residues 115–119 to allow for packing of residues 111–114 to regenerate the tetramerization interface in solution.

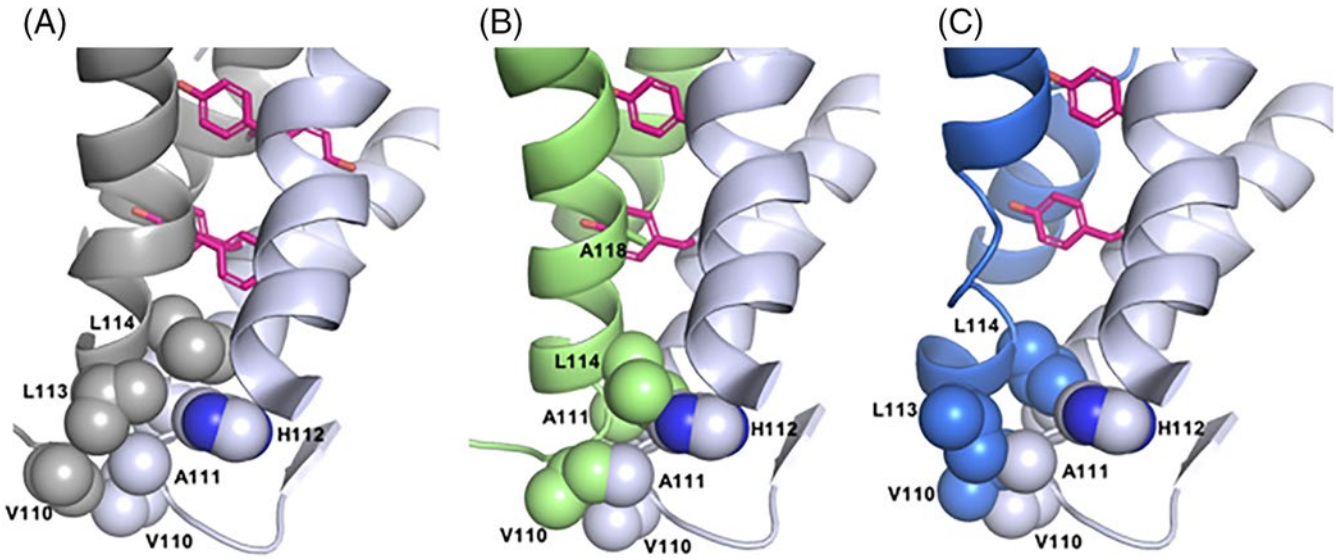

Figure 2.6. Disruption of the tetrameric interface in Y118A and Δ118 SsuE. (A) The tetramerization interface of the wild-type SsuE structure with monomers shown in grey and lavender. The Y118 residue is shown in in pink, and the residues that comprise one tetramerization interface are shown in space-filling representation. Note that for the wild-type SsuE structure, the interface forms a complementary hydrophobic surface between two monomers. (B) Y118A SsuE (green) docked with a wild-type dimer to form a tetramer (lavender). The space-filling model shows that the continuous α-helix of the variant changes the N-terminal pack compared with the π-helix, causing steric clash (atoms occupying the same three dimensional space). (C) ΔY118 SsuE variant (blue) docked with a wild-type dimer (lavender). The Y118 deletion disrupts the π-helix,

making a nonhelical center section, which displaces the N-terminus causing an even greater steric clash that prevents tetramerization. (Adapted from[192]). Copyright © 2018 The Protein Society

2.3.5 Kinetic properties of the SsuE and MsuE π-helix chimeras

The insertional residue that generates the π-helix in SsuE is Y118, whereas in MsuE this residue is H126. Aromatic π-stacking may be key in the tetramerization interaction mediated by these residues. We therefore hypothesized that interchanging these residues would result in chimeric proteins (Y118H SsuE and H126Y MsuE) that had kinetic values unchanged in comparison to the wild-type enzymes. Initial kinetic studies were performed to evaluate the reductase activity of wild-type *P. aeruginosa* MsuE, as kinetic parameters had not been determined previously. The purified MsuE did not possess a characteristic flavin spectrum similar to SsuE. The wild-type MsuE enzyme had a higher k_{cat}/K_m value $(32 \pm 10) \times 10^4\ M^{-1}\ s^{-1}$ for NADH compared with $(1.9 \pm 0.4) \times 10^4\ M^{-1}\ s^{-1}$ for NADPH (Table 2.2) (Figure 2.7). A kinetic preference for NADH was previously observed with MsuE from *P. fluorescens*.[95] Similar k_{cat}/K_m values were obtained for FMN varying NADH or NADPH at $(7 \pm 1) \times 10^6\ M^{-1}\ s^{-1}$ and $(6 \pm 2) \times 10^6\ M^{-1}\ s^{-1}$, respectively. The H126Y MsuE variant showed similar kinetic parameters as wild-type for both NADH and NADPH (Table 2.2). The comparable kinetic parameters suggest that substitution of the His insertional residue with Tyr did not disrupt the ability of the enzyme to reduce FMN. Unexpectedly, the Y118H SsuE variant behaves like the Y118A SsuE and ΔY118 SsuE variants. Y118H SsuE showed no measurable activity under any of the assay conditions tested, suggesting that Y118H SsuE protects the reduced FMN from release and reoxidation, preventing the enzyme from entering the steady state.

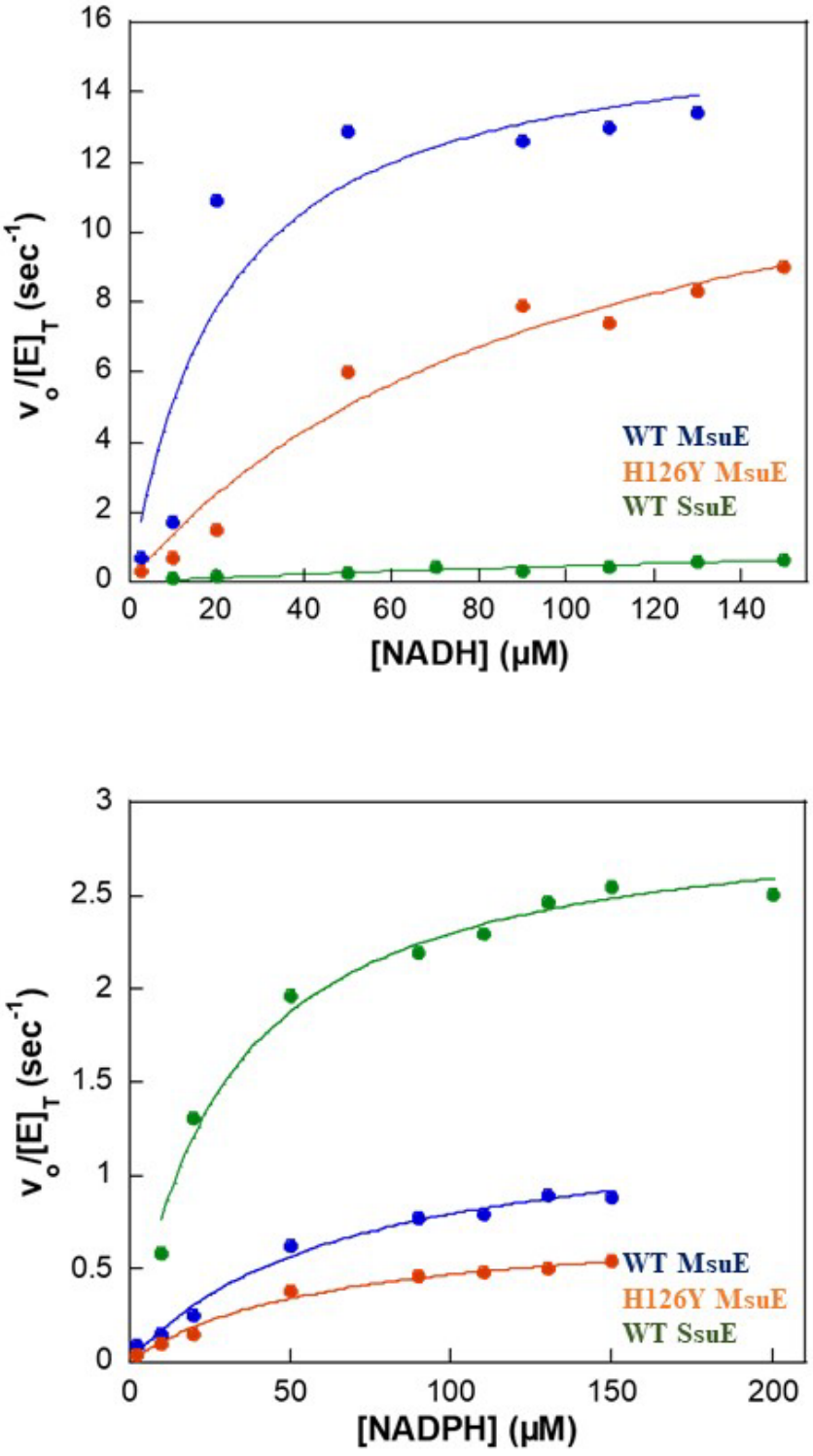

Figure 2.7. Kinetic plots from oxidase assays with wild-type SsuE (Green), wild-type MsuE (Blue), and H126Y MsuE (Orange) with either NADH (Top) or NADPH (Bottom).

Table 2.2. Steady-State Kinetic Parameters for Wild-Type and Variants of MsuE and SsuE measuring NAD(P) H-Dependent FMN Reductase Activity.

FMM Reductase Assay varying NADPH	k_{cat} (s^{-1})	K_m (M, x 10^{-6})	k_{cat}/K_m (M^{-1} s^{-1}, x 10^4)
Wild-type SsuE	3.7 ± 0.4	80 ± 20	5 ± 2
Y118H SsuE[a]	–	–	–
Wild-type MsuE	1.3 ± 0.1	70 ± 10	1.9 ± 0.4
H126Y MsuE	0.75 ± 0.05	60 ± 10	1.2 ± 0.3
FMN Reductase Assay varying NADH	k_{cat} (s^{-1})	K_m (M, x 10^{-6})	k_{cat}/K_m (M^{-1} s^{-1}, x 10^4)
Wild-type SsuE	3.0 ± 0.1	57 ± 1	5.2 ± 0.5
Y118H SsuE[a]	–	–	–
Wild-type MsuE	19 ± 3	60 ± 20	32 ± 10
H126Y MsuE	15 ± 3	100 ± 50	14 ± 7

[a] Values could not be determined within the experimental conditions.

Coupled assays that include the FMN reductase (SsuE or MsuE) and monooxygenase (SsuD or MsuD) were performed to evaluate the ability of the SsuE and MsuE variants to effectively transfer flavin to their respective monooxygenase partner. Desulfonation activity by the monooxygenase was observed with the H126Y MsuE/MsuD pair with a k_{cat}/K_m value of (4 ± 2) × 10^4 M^{-1} s^{-1}, comparable to the wild-type MsuE/MsuD value of (3 ± 1) × 10^4 M^{-1} s^{-1}(Table 2.3). Although activity was observed, the fit to the initial rates obtained in the assay were not optimal and suggested the H126Y MsuE variant was not effectively coupled with MsuD (Figure 2.8). As it is possible that the reduced flavin may be released from the Y118H SsuE when triggered by interaction with SsuD, desulfonation was also measured with this variant despite the enzyme's inability to enter the steady state for reductase activity. However, there was no measurable desulfonation activity observed in coupled assays monitoring sulfite production with the Y118H

SsuE variant and SsuD, compared to the wild-type SsuE/SsuD value of (3.1 ± 0.3) × 10^4 M^{-1} s^{-1} (Table 2.3).

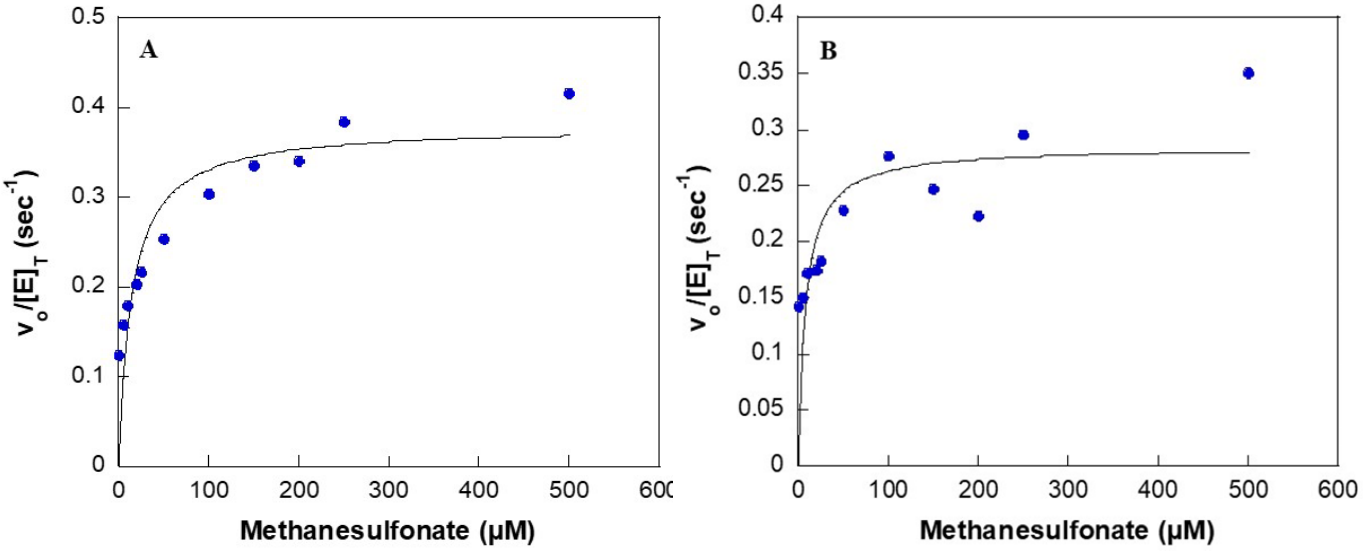

Figure 2.8. Kinetic plots of wild-type and H126Y MsuE with MsuE. A) Kinetic plot of the initial velocities MsuE and MsuD with varying methanesulfonate concentrations. B) Kinetic plot of the initial velocities of H126Y MsuE and MsuD with varying methanesulfonate concentrations. Steady-state kinetic parameters were determined by fitting the resulting plots to the Michaelis-Menten equation. An R^2 value of 0.3 was obtained from the fit of the data for the H126YMsuE and MsuD coupled reaction, compared with 0.94 for wild-type MsuE and MsuD. Sulfite production was quantified as described in Material and Methods. (Adapted from[192]).

Table 2.3. Desulfonation Activity with the Wild-Type and Variants of SsuE and MsuE.

SsuD Activity[a]	k_{cat} (s^{-1})	K_m (M, x 10^{-6})	k_{cat}/K_m (M^{-1} s^{-1}, x 10^4)
Wild-type SsuE	1.2 ± 0.1	39 ± 5	3.1 ± 0.3
Y118H SsuE[b]	–	–	–
MsuD Activity[c]	k_{cat} (s^{-1})	K_m (M, x 10^{-6})	k_{cat}/K_m (M^{-1} s^{-1}, x 10^4)
Wild-type MsuE	0.38 ± 0.03	15 ± 6	2.5 ± 1
H126Y MsuE	1.4 ± 0.1	19 ± 4	4 ± 2

[a] Assays to determine desulfonation with activity with MsuD measured oxidation of methanesulfonate as described in *Materials and Methods*.
[b] Values could not be determined within the experimental conditions.
[c] Assays to determine desulfonation activity with SsuD measured oxidation of octanesulfonate as described in *Materials and Methods*.

The release of $FMNH_2$ from the reductase enzymes may be triggered by monooxygenase binding, and the π-helix insertional residue may be important in this interaction. Therefore, the MsuE and SsuE variants were evaluated to see if they could transfer reduced flavin to the opposite monooxygenase partner. The kinetic parameters for desulfonation by SsuD were similar with wild-type MsuE as when SsuE was included in the assay with a k_{cat}/K_m value of (7 ± 2) × 10^4 M^{-1} s^{-1} (Table 2.4). Similarly, SsuE was able to effectively transfer flavin to MsuD with a k_{cat}/K_m value of (1.9 ± 0.7) × 10^4 M^{-1} s^{-1}. These kinetic parameters were analogous to the k_{cat}/K_m value of (3.1 ± 0.3) × 10^4 M^{-1} s^{-1} obtained in the SsuE /SsuD coupled reaction. Comparable desulfonation activity was observed with the H126Y MsuE variant regardless of which monooxygenase was included in the assay (Table 2.4). However, the Y118H SsuE variant was unable to support flavin transfer to either monooxygenase. The absence of desulfonation

activity with the Y118H SsuE variant suggests that the substitution of histidine for tyrosine did not maintain the same functional properties to support catalysis as observed for H126Y MsuE.

Table 2.4. Desulfonation Activity with wild-Type and Variants of SsuE and MsuE with the alternate monooxygenase partner.

SsuD Activity	k_{cat} (s^{-1})	K_m (M, x 10^{-6})	k_{cat}/K_m (M^{-1} s^{-1}, x 10^4)
wild-type MsuE	1.4 ± 0.1	19 ± 4	7 ± 2
H126Y MsuE	0.96 ± 0.03	24 ± 5	4.0 ± 0.9
MsuD Activity	k_{cat} (s^{-1})	K_m (M, x 10^{-6})	k_{cat}/K_m (M^{-1} s^{-1}, x 10^4)
wild-type SsuE	0.42 ± 0.04	22 ± 8	1.9 ± 0.7
Y118H SsuE[a]	–	–	–

[a] Values could not be determined within the experimental conditions.

2.2.6 Kinetic properties of the SsuE and MsuE Aspartate and Proline Variants

Variants were generated to evaluate the conserved proline and aspartic acid residues, that are located within the π-helix of SsuE and MsuE. The variants generated for SsuE and MsuE were all purified flavin-free compared with wild-type enzyme ChrR which purifies as ~50% flavin bound. The circular dichroism spectra of all the variants generated indicted no disruption to the secondary structure compared with the wild-types. (Figure 2.9 and 2.10) FMN-dependent reductases from two-component systems catalyze the reduction of flavin in the presence of NAD(P)H. There was no observable oxidase activity compared with the respective wild-type enzymes (Table 2.5). Flavin reduction by NAD(P)H in ChrR is not easily monitored because FMN stays

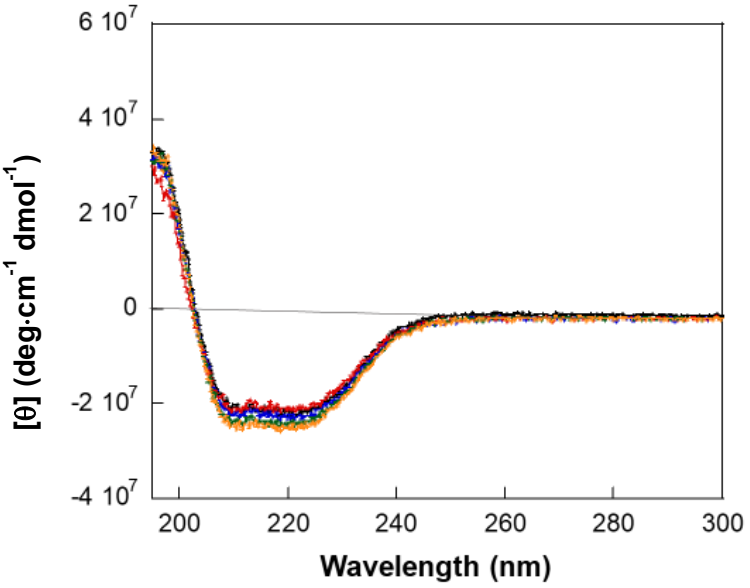

Figure 2.9. The far-UV circular dichroism spectra of wild-type MsuE (black), P130Q MsuE (blue), P130A MsuE (red), D125Q MsuE (orange), and D125Q/P125Q MsuE (green).

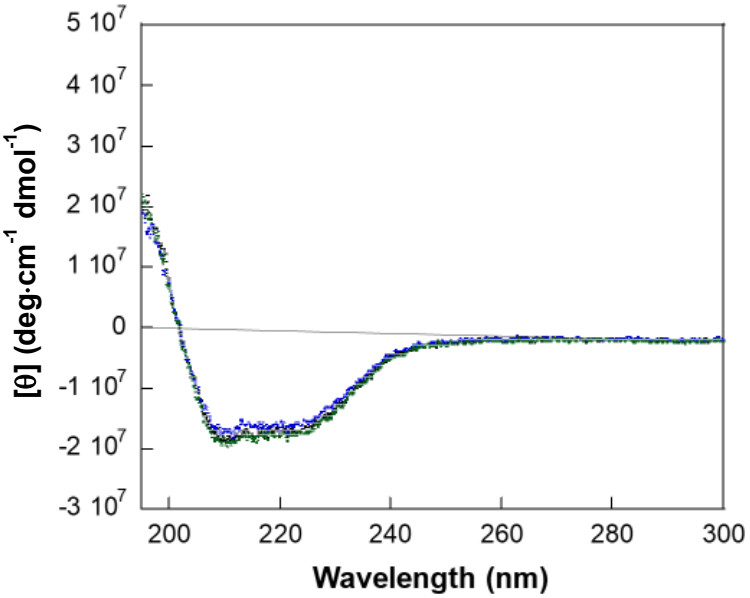

Figure 2.10. The far-UV circular dichroism spectra of wild-type SsuE (black), P123Q SsuE (blue), and D117Q SsuE (green).

Table 2.5. Steady-State Kinetic Parameters and Binding Studies with FMN for Wild-Type and Variants of MsuE and SsuE Measuring NAD(P)H-Dependent FMN Reductase Activity.

FMM Reductase Assay varying NADPH	k_{cat} (s^{-1})	K_m (M, x 10^{-6})	k_{cat}/K_m (M^{-1} s^{-1}, x 10^4)	$K_{d(FMN)}$ (μM)
Wild-type SsuE	3.7 ± 0.4	80 ± 20	5 ± 2	0.05 ± 0.01
P123A SsuE	–[a]	–	–	–
P123Q SsuE	–	–	–	–
D117Q SsuE	–	–	–	–
FMN Reductase Assay varying NADH	k_{cat} (s^{-1})	K_m (M, x 10^{-6})	k_{cat}/K_m (M^{-1} s^{-1}, x 10^4)	$K_{d(FMN)}$ (μM)
Wild-type MsuE	3.0 ± 0.1	57 ± 1	5.2 ± 0.5	0.74 ± 0.09
P130A MsuE	–	–	–	–
P130Q MsuE	–	–	–	7.4 ± 2
D125Q MsuE	–	–	–	–
D125Q/P130Q MsuE	–	–	–	–

[a] Values could not be determined within the experimental conditions.

reduced and protected from oxidation in the absence of the hexavalent chromium substrate. Therefore, the activity of canonical flavin reductases are often assayed with ferricyanide to ensure flavin electron transfer. However, even in the presence of ferricyanide there was no activity with any of the SsuE or MsuE variants. Fluorometric titrations were used to determine if the binding affinity of FMN of SsuE and MsuE variants were altered due to the substitution. The P130Q MsuE showed a 10-fold increase in FMN binding affinity, but there was no FMN binding observed with the other SsuE or MsuE variants (Table 2.5) (Figure 2.11). The flavin reductase is responsible for transferring the reduced flavin to the partner monooxygenase. Coupled assays were used to compare the desulfonation activity of the aspartic acid and proline SsuE and MsuE variants with the wild-type enzymes. There was no SsuD or MsuD desulfonation activity observed with the corresponding FMN reductase variants.(Table 2.6).

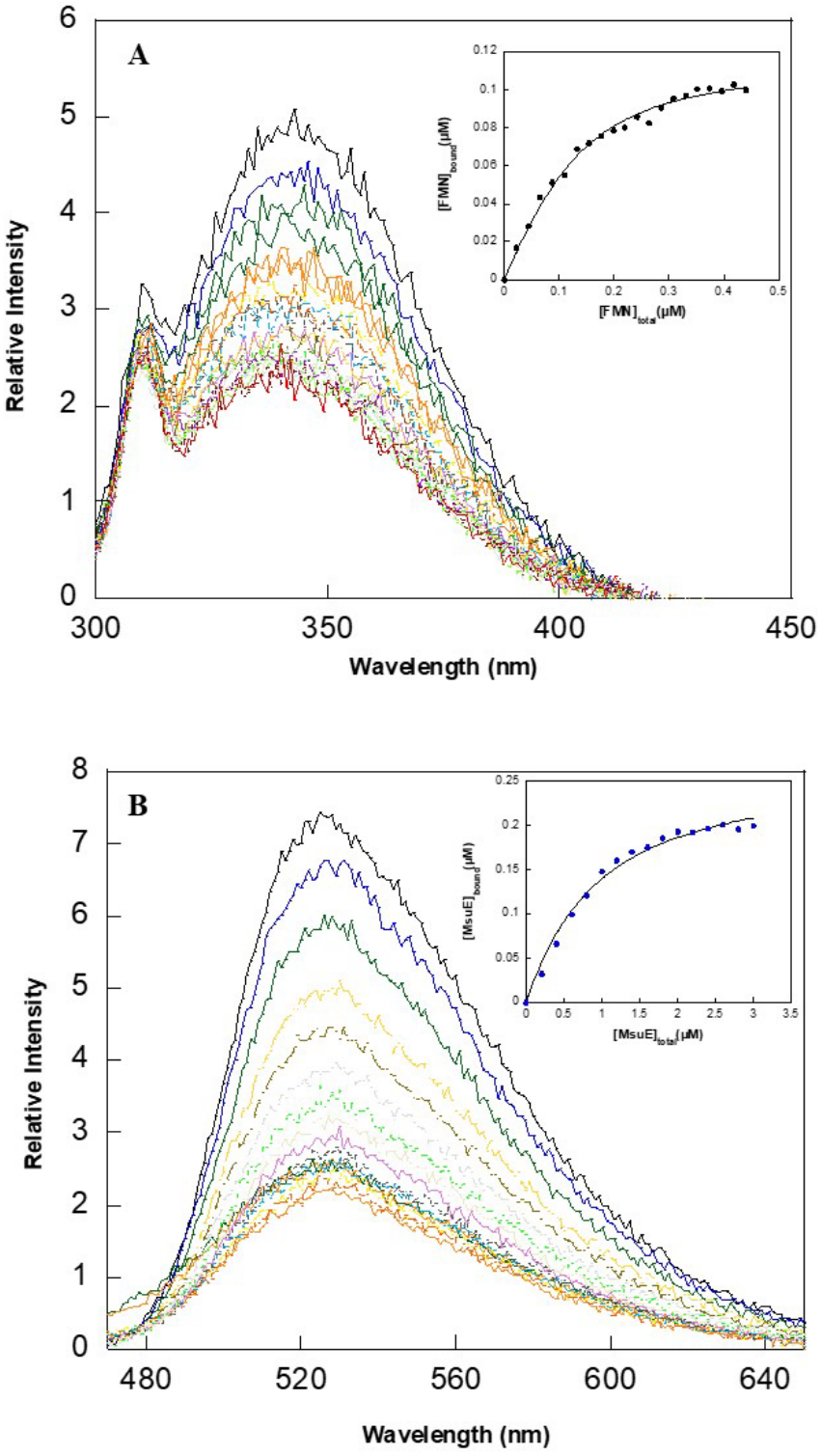

Figure 2.11. A) Fluorescence quenching of SsuE by the addition of FMN. B) Fluorescence quenching of FMN by addition of MsuE.

Table 2.6. Desulfonation Activity with the Wild-Type and Variants of SsuE and MsuE

SsuD Activity	k_{cat} (s^{-1})	K_m (M, x 10^{-6})	k_{cat}/K_m (M^{-1} s^{-1}, x 10^4)
Wild-type SsuE	3.7 ± 0.4	80 ± 20	5 ± 2
P123A SsuE	–[a]	–	–
P123Q SsuE	–	–	–
D117Q SsuE	–	–	–
MsuD Activity	k_{cat} (s^{-1})	K_m (M, x 10^{-6})	k_{cat}/K_m (M^{-1} s^{-1}, x 10^4)
Wild-type MsuE	0.35 ± 0.01	105 ± 14	0.33 ± 0.05
P130A MsuE	–	–	–
P130Q MsuE	–	–	–
D125Q MsuE	–	–	–
D125Q/P130Q MsuE	–	–	–

[a] Values could not be determined within the experimental conditions.

2.4 Conclusion

The π-helix, which was originally thought to be a rare occurrence, is now considered a more prevalent secondary structure in enzymes. It has been proposed that some π-helices are generated by the insertion of an amino acid within a conserved α-helix found in other members within a family.[197,159] The overall conformation of the conserved helix in the protein family would need to be adjusted to accommodate the insertional residue.[159] Furthermore, the instability of the π-helix would destabilize the structure of a protein relative to members of the protein family that retain an α-helix. Therefore, the generation of a π-helix would be selected against if it did not provide a gain-of-function for the enzyme.

The π-helix identified in the FMN-dependent reductase SsuE is hypothesized to be generated by the insertion of a Tyr in the conserved α4-helix.16 The conserved nature of the π-helix in the two-component NAD(P)H:FMN reductases MsuE and SfnF (albeit by insertion of a

histidine at the same site) suggests that it plays a defined mechanistic role for this subgroup of enzymes that diverges from FMN-bound reductases within this family, such as ArsH and YdhA. The π-helix in SsuE located at the tetramer interface has been proposed to trigger the oligomeric changes necessary for protein–protein interactions with SsuD. Alternatively, introduction of the π-helix may result in a more flexible protein capable of release of the reduced FMN to the monooxygenase partner.[147]

Previous studies have shown that the Y118A SsuE, which removes the side chain potentially involved in aromatic π-stacking across the tetramer interface, is incapable of release of the reduced flavin and is predominantly dimeric in solution. In agreement with these data, helix 4 of the Y118A SsuE structure is a continuous α-helix, like those of reductases that do not release their flavin. Perplexingly, the ΔY118 SsuE protein, which deletes the entire insertional residue, is incapable of releasing the reduced flavin, but is tetrameric in solution. The structure determined here shows that helix 4 of ΔY118 SsuE is broken, and the protein is dimeric in the crystal. The more flexible nature of the broken ΔY118 SsuE helix 4 may allow it to repack as a tetramer. In other words, removal of the sidechain reverts helix 4 to and α-helix as seen in the homologous single component reductases, whereas removal of the insertional residue altogether generates a unique conformation—neither α- nor π-helix.

The insertional residue in SfnF and MsuE is a histidine, and is positioned at the bulge site of the π-helix in the three-dimensional structure of SfnF. This position is homologous to Y118 in SsuE, also at the bulge of the π-helix. A histidine insertional residue would still be able to form similar interactions as Tyr118 in SsuE. Whereas MsuE is from *P. aeruginosa* and SsuE is from *E. coli*, they have a high amino acid sequence identity in the π-helical region. Therefore, interchanging the proposed insertional residues, one would expect comparable kinetics effects:

Y118H SsuE and H126Y MsuE should be kinetically equivalent. Instead, Y118H SsuE is kinetically equivalent to Y118A and ΔY118 SsuE, whereas H126Y MsuE is equivalent to wild-type MsuE. Indeed, H126Y MsuE can donate $FMNH_2$ to MsuD and SsuD with comparable success, and within error to wild-type MsuE. The results suggest that a protein–protein docking interaction for flavin transfer is not severely impacted by the generation of the variant. The less than optimal fit for the kinetic parameters could be due to a slight alteration of the protein–protein interaction region during flavin transfer. Furthermore, the Y118H SsuE is incapable of releasing $FMNH_2$ in the reductase assay and is not triggered to release the flavin by addition of SsuD or MsuD in the desulfonation assay.

A structure-based sequence alignment for the NADPH:FMN reductases and variants discussed herein shows that the "insertional residue" hypothesis is problematic (Fig. 6). First, when considering the rmsd of α-carbons, the Y118 residue of SsuE and the H126 residue of SfnF do not result in a gap (insertion) within helix 4. Furthermore, ChrR, a quinone reductase from *E. coli*, is an FMN reductase with a flavodoxin fold and an α-helical helix 4 that is more structurally distant than the other homologs discussed so far (2.8 Å rmsd for 164 Cα).[208] Nevertheless, ChrR has a tyrosine (Tyr126) at the equivalent Y118-SsuE site that aligns directly with that of the alanine in the Y118A SsuE variant. Clearly, a tyrosine at the insertion site in ChrR is not sufficient to develop a π-helix and convert a reductase into one that can deliver reduced FMN to a monooxygenase in a two-component system. Two possibilities may explain the alternative functions in the two-component FMN reductases. First, the presence of the π-helix may not fully explain the ability of two-component reductases to release flavin to a monooxygenase and other structural features may also be important. For example, the C-terminal ~20 residues have never been resolved in these reductases. A reductase–monooxygenase complex structure would be of significant import in

deciding this question. Second, if the π-helix is indeed of functional significance, generation of a π-helix through evolutionary adaptation is not as simple as insertion of a residue, and compensatory variations are likely also required for gain-of-function.

Comparison of the amino acid sequence alignment of ChrR with the two-component FMN reductases containing the π-helix identified specific differences outside of the alleged insertional residue. There are two glutamines located near Tyr128 of ChrR that are an aspartic acid and proline residue in the two-component FMN reductases. The proline and aspartic acid residues are located in the same position for both the glutamine residues for all flavin reductases characterized with the π-helical region. Multiple variants for both SsuE (P123Q, P123A, and D117Q) and MsuE (P130Q, P130A, D125Q, and D125Q/P130Q) were generated to identify if these residues play a role in formation of either the α-helix or π-helix for these enzymes. The concentration of SsuE and MsuE following purification was low, although results from circular dichroism spectroscopy suggested there were no measurable disruptions in the secondary structure. There was no measurable NAD(P)H oxidase activity with the any of the variants that were generated, and sulfite was not produced in coupled assays for any of the variants with their partner monooxygenase. ChrR would also demonstrate similar catalytic features, but the SsuE and MsuE were not able to transfer electrons to ferricyanide or bind flavin. With this inactivity for each of the variants, there may be a possible disruption that may have occurred with the π-helical region of the variants similar to that of the Δ118 SsuE.[155] The Δ118 SsuE variant was no longer a viable reduced-flavin resource for SsuD to utilize to cleave the carbon-sulfur bond of octanesulfonate.[155] The solved crystal structures revealed that a lack in activity was due to a disruption of the π-helical region. The conserved proline and aspartic acid residues may be important to the overall structure of the π-helix along with the single amino acid insertion to provide the necessary release of substrates.

Alternatively, substitution of the conserved aspartic acid and/or proline residues may disrupt the noncovalent interactions across the tetramer interface that stabilize the tetrameric structure. FMN binding is partially stabilized through a hydrogen-bonding network across the tetramer interface in the FMN-dependent reductase enzymes. Therefore, these amino acid substitutions may disrupt flavin binding, rendering the enzyme inactive.

Chapter 3

Identifying Conserved Structural Features of FMN-Dependent Monooxygenases Involved in Desulfonation

3.1 Introduction

Sulfur is an essential element found in inorganic form that is incorporated into essential metabolic sulfur compounds. Plants and bacteria assimilate sulfur through metabolic pathways that synthesize essential sulfur compounds from an inorganic sulfur source.[1] When inorganic sulfur is limiting in the environment for bacterial organisms, a set of proteins are expressed to provide bacteria with an alternative mechanism for obtaining sulfur. These enzymes belong to two-component systems that consist of a flavin reductase that transfers reduced flavin to the partner monooxygenase. FMN dependent two-component systems SsuE/SsuD (*Escherichia coli*) and MsuE/MsuD (*Pseudomonas aeruginosa*) are involved in cleaving the carbon-sulfur bond of linear alkanesulfonates. The SsuE/SsuD FMN-dependent two-component system utilizes a range of linear alkanesulfonates (C_2-C_{10}), reduced flavin, and molecular oxygen to produce the corresponding aldehyde and sulfite (Figure 3.1A).[53] The MsuE/MsuD FMN-dependent two-component system catalyzes the cleavage of the carbon-sulfur bond of methanesulfonate (C_1) in the presence of reduced flavin and molecular oxygen to produce formaldehyde and sulfite (Figure 3.1B).[72]

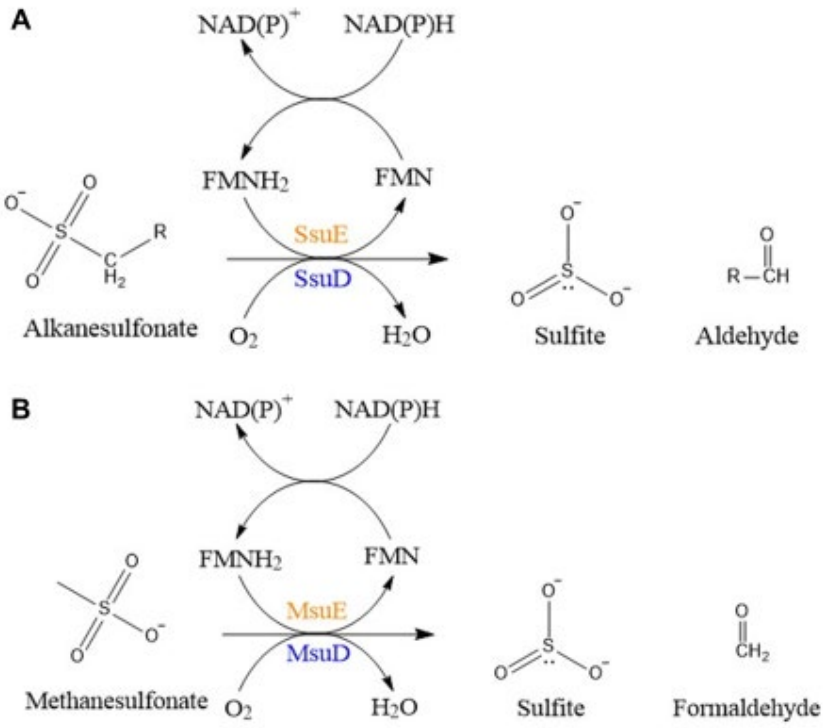

Figure 3.1. Desulfonation reaction mechanisms of A) SsuE/SsuD and B) MsuE/MsuD.

SsuD belongs to a family of bacterial monooxygenases that require reduced flavin as a substrate for activity.[175] The structure of SsuD is a classic TIM-barrel fold that is common to the bacterial luciferase TIM-barrel family.[175] Along with the similar TIM-barrel fold, SsuD shares 20% amino acid identity with the LuxA subunit of bacterial luciferase. Bacterial luciferase is a heterodimeric ($\alpha\beta$) flavin monooxygenase that catalyzes the oxidation of aliphatic aldehydes to the corresponding carboxylic acid and blue-green light.[79] Bacterial luciferase from marine luminous bacteria is able to obtain reduced flavin from flavin reductases Frp (*V. harveyi*), Frase-I (*Vibrio fischeri*), and Fre (*E. coli*), and LuxG (*V. harveyi*) .[209,210,211,212] MsuD shares 65% amino acid identity with SsuD, but the three-dimensional structure has not been determined. Based on initial studies, MsuD cleaves the carbon-sulfur bond of methanesulfonate (C_1) to produce sulfite

and formaldehyde.[72] The high amino acid sequence identity between MsuD and SsuD suggests they share similar structural properties that promote catalytic function.

Monooxygenases in the luciferase family contain a flexible loop that protrudes over the active site to protect the reaction intermediates from bulk solvents.[175,213,214,215,216,217,218,219] The bacterial luciferase flexible loop is only present in the α subunit. [180, 220] A luciferase variant containing a loop deletion was still able to bind substrates to generate the carboxylic acid, but the bioluminescence was decreased by two orders of magnitude.[221] Substitution of Lys 283 and 286 on the insertional region with alanine residue resulted in a decrease in stability of the flavin intermediates produced.[176] There is also an arginine residue (Arg291) located on the loop that may play a role in loop closure.[176] The R291A luciferase variant showed a decrease in activity and relative quantum yield compared with wild-type.[176] An arginine residue (Arg297) is located on the insertional region of SsuD at a comparable position to Arg291. The R297A SsuD variant had no kinetic activity and was not protected from proteolysis in the presence of reduced flavin.[177] Arg297 was proposed to assist in loop closure by interacting with phosphate group of FMN.

Loop closure over the active site in TIM-barrel enzymes plays a critical role in protecting intermediates from bulk solvent, the phosphodianion group of the reduced flavin may participate in loop closure. The phosphate group found on reduced flavin may form an electrostatic interaction with the arginine located on the loop. The importance of substrate phosphodianion groups have been studied and identified in other TIM-barrel enzymes. Orotidine 5-monophosphate decarboxylase (OMPDC) and TIM stabilize substrate interactions with phosphate gripper loops that close over the bound substrate.[218,219] The OMPDC gripper loop (Pro202-Val220) and the mobile loop form ionic and hydrogen-bonding interactions with the phosphate group of orotidine 5-monophosphate (OMP).[222] The interactions contribute to the conformational change required for

loop closure over the active site.[222] In the presence of a phosphite dianion, the kinetic activity of each enzyme was increased with the truncated substrate lacking the phosphate functional group to the truncated substrate alone.[223] The increased activity was associated with specific binding interactions between the enzyme and substrate that protect reaction intermediates.[223]

Given the high amino acid identity, it is unclear why SsuD and MsuD have different substrate specificities. Enzyme SsuD has a substrate range that includes C_2-C_{10} linear alkanesulfonates, ethanesulfonic acids, N-phenyltaurine, 4-phenyl-1-butanesulfonaic acid, sulfonated buffers, decanesulfonic acid, octanesulfonic acid, and 1,3-dioxo-2-isoindolineethanesulfonic acid having a high catalytic effieciency.[53] However, the FMN-dependent two-component system MsuE/MsuD has only been characterized to utilize methanesulfonic acid (C_1).[72] The active site architecture of both SsuD and MsuD are likely similar due to the high amino acid identity and similar role in the desulfonation of a alkanesulfonates (Figure 3.2). Although there is no solved crystal structure of MsuD, a structural model generated with the iTasser program showed a similar orientation of amino acids in the active sight compared with SsuD.

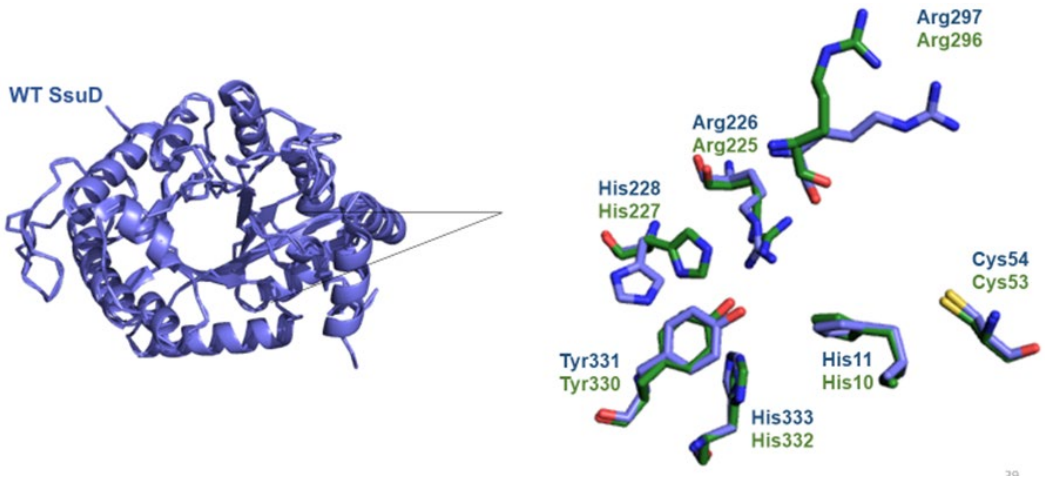

Figure 3.2. TIM-barrel fold of SsuD (PDB:1M41) with an overlay of both active sites for SsuD (blue) and MsuD (iTasser) (green).

It is hypothesized that MsuD and SsuD together broaden the range of alkanesulfonates utilized by MsuD and SsuD utilizing similar active sites and structural dynamics. Evaluation of both the mobile loop and active site features of SsuD and MsuD will be implemented to determine how these structural features contribute to substrate specificity and catalytic function. Phosphite studies with SsuD will evaluate possible key electrostatic interactions between mobile loop and phosphate group of reduced flavin. Kinetic studies with the partner flavin reductase SsuE will be performed in the presence of the truncated substrate riboflavin. The SsuE enzyme is able to effectively reduce riboflavin, which lacks the phosphate group (Figure 3.3).[53] Phosphite will be incorporated in desulfonation-coupled assays along with riboflavin to evaluate the effect of the phosphate group

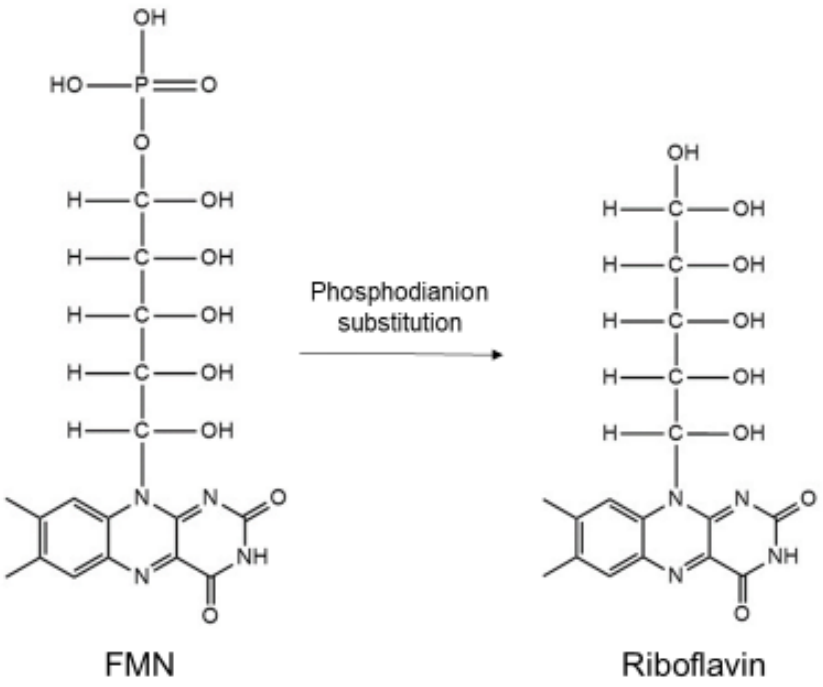

Figure 3.3. Substitution of FMN with truncated substrate riboflavin.

on catalytic function. Additional studies are described that evaluate the substrate ranges for MsuD and SsuD to evaluate whether there is overlap, or if the substrates utilized are distinct for each enzyme.

3.2 Materials and Methods

3.2.1 Materials

For steady-state coupled assays, sodium methanesulfonate and sodium 1-pentanesulfonate were purchased through Alfa Aesar (Tewksbury, MA). Ethanesulfonic acid sodium salt monohydrate, sodium 1-propanesulfonate monohydrate, sodium 1-butanesulfonate, sodium hexanesulfonate, sodium 1-decanesulfonate, sodium 1-dodecanesulfonate, and sodium 1-tetradecanesulfonate were purchased through Sigma (St. Louis, MO). Sodium 1-octanesulfonate monohydrate was purchased through Fluka (Milwaukee, WI). Buffer and additional reaction components and chemicals for kinetic assays were purchased from Sigma (St. Louis, MO). Riboflavin and sodium phosphite dibasic pentahydrate was purchased through Sigma (St. Louis, MO).

3.2.2 Steady-state kinetic assays of Riboflavin and SsuE

The NADPH oxidase activity for wild-type SsuE was initially evaluated to determine the steady-state kinetic parameters of the enzyme with riboflavin. Kinetic parameters for riboflavin were determined with a range of wild-type SsuE (0.2-1.0 μM) with a range of riboflavin concentrations (5 μM, 50 μM, or 100 μM), and fixed concentrations of NADPH (200 μM). The initial rates were obtained by monitoring the decrease in absorbance at 340 nm with the oxidation of the reduced pyridine nucleotide. The steady-state kinetic parameters were determined by fitting the data to the Michaelis–Menten equation.

3.2.3 Fluorescence Titrations

Fluorometric titrations were performed to determine the binding affinity of riboflavin to wild-type SsuE and were monitored on a Cary Eclipse Agilent (Santa Clara, CA) fluorescence spectrophotometer with an excitation of 280 nm and emission measurements at 344 nm. A 1.0 mL solution of wild-type SsuE (0.1 μM) in 25 mM potassium phosphate (pH 7.5) and 0.1 M NaCl was titrated with riboflavin (from 0.022-0.44 μM) 1 μL increments. After each recording fluorescence spectrum, increments were followed by 2-minute incubation after each addition.

All assays were performed in triplicate, and the K_d value was determined as previously described. Bound FMN was determined with equation 1

$$[A]_{bound} = [B]\frac{I_o - I_c}{I_o - I_f} \quad (1)$$

where $[A]_{bound}$ represents the concentration of riboflavin-bound SsuE, [B] represents the initial concentration of the SsuE in cuvette, I_o represents the initial fluorescence intensity prior to addition of riboflavin, I_c represents the fluorescence intensity of the SsuE following each addition, and I_f represents the final fluorescence intensity. The concentration of riboflavin bound was plotted against the free substrate concentration to obtain the dissociation constant (K_d) according to equation 2

$$y = \frac{K_d + x + n - \sqrt{(K_d + x + n)^2 - 4xn}}{2} \quad (2)$$

where y and x represent the concentration of the bound and free substrate, respectively, following each addition, and K_d is the maximum binding at equilibrium with the maximum concentration of substrate.

3.2.4 Steady-State Coupled Assays of SsuD Monitoring Phosphite Dependence on Catalysis

The steady-state coupled assays monitored sulfite production with riboflavin to determine an effective ratio for riboflavin transfer with varying concentrations of SsuE. The reaction mixture contained flavin reductase SsuE (0.6 μM, 1.2 μM, or 1.8 μM), monooxygenase SsuD (0.2 μM), riboflavin (2 μM or 10 μM), and octanesulfonate (1 μM) in 25 mM Tris-HCL (pH 7.5) and 0.1 NaCl at 25°.

The steady-state coupled assay monitoring sulfite production in the presence of riboflavin with SsuD and organosulfur compounds were performed to determine an effective concentration of riboflavin. The reaction mixture contained flavin reductase SsuE (0.6 μM), monooxygenase SsuD (0.2 μM), varying concentrations of riboflavin (0-200 μM), and octanesulfonate (1 mM) in 25 mM Tris-HCL (pH 7.5) and 0.1 NaCl at 25°.

The steady-state coupled assay monitoring sulfite production was performed to determine an effective phosphite concentration to be used with riboflavin. The reaction mixture contained flavin reductase SsuE (0.6 μM), monooxygenase SsuD (0.2 μM), riboflavin (10 μM or 4 μM), and range of octanesulfonate (0-1,000 μM) in 25 mM Tris-HCL (pH 7.5) and 0.1 NaCl at 25°.

The steady-state coupled assay was performed to evaluate the effect of increasing phosphite concentrations on the catalytic activity. The reaction mixture contained flavin reductase SsuE (0.6 μM), monooxygenase SsuD (0.2 μM), riboflavin (2 μM), octanesulfonate (1 μM), and range of phosphite concentrations (0-2,500 μM) and (0-15,000 μM) in 25 mM Tris-HCL (pH 7.5) and 0.1 NaCl at 25°.

Reactions were repeated with a 2:1 ratio of SsuE:SsuD to determine if lower concentrations of flavin reductase would increase activity. The reaction mixture contained flavin reductase SsuE

(0.4 μM), monooxygenase SsuD (0.2 μM), octanesulfonate (500 μM), phosphite (1 mM) and a range of riboflavin (0-200 μM) in 25 mM Tris-HCL (pH 7.5) and 0.1 NaCl at 25°. These reactions were initiated by the addition of NADPH (500 μM) followed by a 3-minute incubation period. Urea (2 M) was used to quench the reaction for 3 minutes. Then, 50 μL of DTNB (1 mM) is added to an aliquoted 200μL reaction solution.[154] After 2 minutes at room temperature, the colorimetric reaction was measured at 412 nm with the production of TNB anion in the presence of sulfite. The $v_o/[E_t]$ is determined using the molar extinction coefficient of the TNB anion of 14.1 mM^{-1} cm^{-1}. All steady-state kinetic parameters were determined by fitting the data to the Michaelis-Menten equation.

3.2.5 SsuD and MsuD Steady-State Coupled Assays with Varying Sulfur Substrates

Both SsuD and MsuD share a high amino acid sequence identity but have been reported to catalyze the desulfonation of different alkanesulfonate substrates. Steady-state coupled assays monitored sulfite production of various organosulfur compounds to evaluate if both SsuD and MsuD can catalyze similar desulfonation activity. The reaction mixture contained flavin reductase (0.6 μM), monooxygenase (0.2 μM), FMN (2 μM), and range of organosulfur compounds (C_1-C_{14}) in 25 mM Tris-HCL (pH 7.5) and 0.1 NaCl at 25°. The reactions were assayed as previously described. All steady-state kinetic parameters were determined by fitting the data to the Michaelis-Menten equation.

3.3 Results

3.3.1 Riboflavin and Phosphite Loop Studies

The flexible loop of SsuD is proposed to protect the reactive intermediates from bulk solvent. An arginine residue is found on the loop and may be involved in the stabilization of the

loop by forming electrostatic interactions with the phosphate group of FMN. In order to evaluate the effect of FMN phosphate on catalysis, riboflavin was used with varying phosphite concentrations. Flavin reductase activity was observable in the presence of riboflavin with SsuE. SsuE was able to bind riboflavin with a five-fold higher affinity value compared with FMN. (Figure 3.4) These results indicate that SsuE can reduce riboflavin, but not as efficiently as FMN.

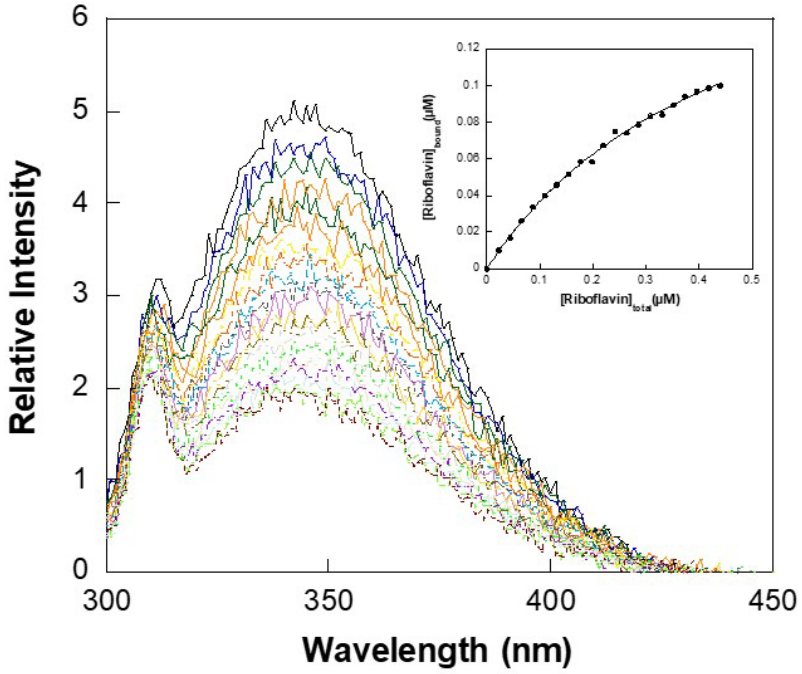

Figure 3.4. Fluorometric titration with riboflavin and wild-type SsuE.

Desulfonation activity assays were utilized in order to determine the amount of sulfite produced by SsuD with riboflavin and phosphite as substrates. Different experimental conditions were used to evaluate the optimal conditions for flavin transfer and desulfonation. Varying the ratio of SsuE and SsuD had no effect on sulfite production, even with higher concentrations of SsuE. An increase in concentration of riboflavin was used in the coupled assays due to the altered affinity of the system for riboflavin. However, increasing concentrations of riboflavin had no effect

on the catalytic activity. Although it was hypothesized that there would be no activity in the presence of riboflavin alone in coupled assays, addition of phosphite should increase the kinetic activity due to a potential interaction between the arginine guanidinium side chain and phosphite. However, there was no observable activity with phosphite addition. Regardless of the order of substrate addition, there was no observable activity with SsuD and riboflavin/phosphite.

3.3.2 Sulfur Substrate Specificity with SsuD and MsuD

Although a structure has not yet been solved for the MsuD monooxygenase enzyme from *P. aeruginosa*, the enzyme shares 65% amino acid identify with SsuD from *E. coli*. SsuD from the alkanesulfonate two-component FMN-dependent system in *E. coli* utilizes a wide range of alkanesulfonate substrates (C_2-C_{10}) .[53] Interestingly, MsuD shows a similar active site architecture and similar orientation as SsuD through predictive structural modeling with conserved amino acid residues located within the active site (Figure 1).[175] However, MsuD from the methanesulfonate two-component FMN-dependent system has been proposed to catalyze the substrate specific desulfonation of methanesulfonate (C_1).[72, 95] Which would suggest that each enzyme has a specific substrate preference, even though they have similar conserved active site residues.

Desulfonation activity was performed with the respective partners from two-component FMN-dependent systems (SsuE/SsuD and MsuE/MsuD) to evaluate the range of various substrates the enzymes may utilize. With comparison of octanesulfonate, there was an observed comparable desulfonation activity with the MsuE/MsuD pair with a k_{cat}/K_m value of $(2.6 \pm 0.5) \times 10^4$ M^{-1} s^{-1} to the value of $(1.9 \pm 0.1) \times 10^4$ M^{-1} s^{-1} of SsuE/SsuD (Table 3.1). Interestingly, there was no measurable desulfonation activity with methanesulfonate for the SsuE/SsuD pair, while a k_{cat}/K_m value of $(0.33 \pm 0.05) \times 10^4$ M^{-1} s^{-1} was observed for MsuE/MsuD (Figure 3.5). Although the two-

component system SsuE/SsuD can utilize a broad range of alkanesulfonate substrates ranging from C_2-C_{10}, octanesulfonate was the preferred substrate in the initial characterization of the enzyme.[53] However, SsuE/SsuD was able to utilize longer alkanes as effectively as octanesulfonate. These results indicate that the methanesulfonate monooxygenase system is able to utilize a broad range of comparable sulfur substrates similar to their respective counterparts (SsuE/SsuD), and may provide an evolutionary advantage for bacteria found in diverse environmental conditions.

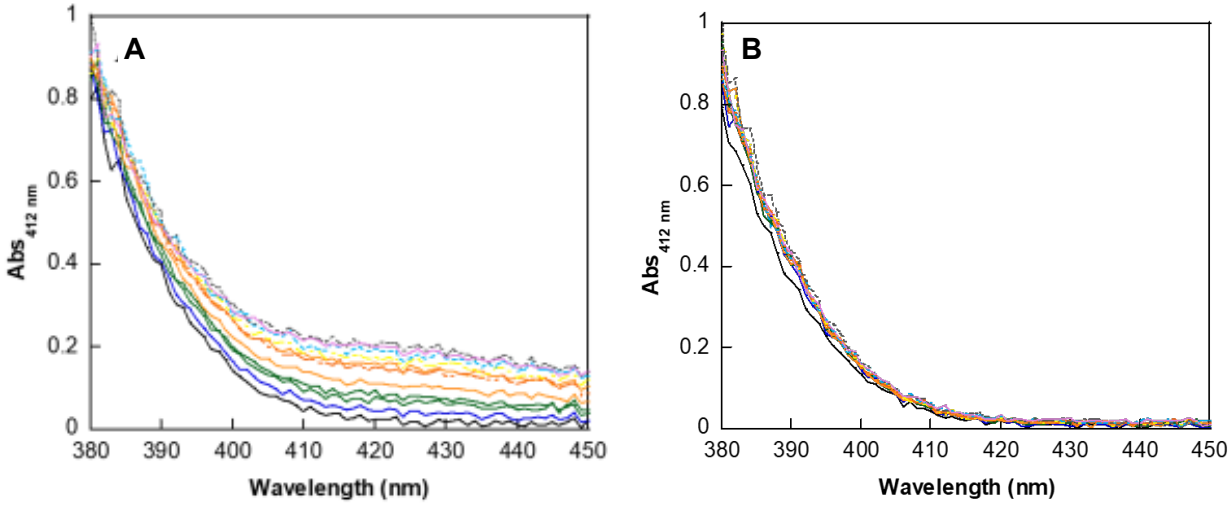

Figure 3.5. UV-spectrum data of TNB^- anion generated from desulfonation activity measured at 412 nm after 2 minutes of incubation at room temperature. (A) SsuE/SsuD in the presence of octanesulfonate. (B) SsuE/SsuD in the presence of methanesulfonate.

Table 3.1. Sulfur substrate ranges for both MsuE/D and SsuE/D.

Substrate	Enzyme	k_{cat}/K_m (M^{-1} s^{-1}, x 10^4)
Methanesulfonate	MsuED	0.33 ± 0.05
	SsuED[a]	–
Ethanesulfonate	MsuED	0.12 ± 0.02
	SsuED	0.02 ± 0.01
Propanesulfonate	MsuED	0.03 ± 0.01
	SsuED	0.04 ± 0.01
Butanesulfonate	MsuED	0.10 ± 0.03
	SsuED	0.08 ± 0.03
Pentanesulfonate	MsuED	0.06 ± 0.02
	SsuED	0.15 ± 0.04
Hexanesulfonate	MsuED	1.2 ± 0.1
	SsuED	1.0 ± 0.1
Octanesulfonate	MsuED	2.6 ± 0.5
	SsuED	1.9 ± 0.1
Decanesulfonate	MsuED	2.7 ± 0.4
	SsuED	2.9 ± 0.3
Dodecanesulfonate	MsuED	3.3 ± 0.2
	SsuED	3.7 ± 0.5
Tetradecanesulfonate	MsuED	4.3 ± 1.7
	SsuED	2.8 ± 1.9

[a] Values could not be determined within the experimental conditions.

3.4 Discussion

When sulfur is limiting, FMN-dependent two-component monooxygenase systems are expressed to provide alternative sources. There is a difference in the organosulfur compounds utilized by bacteria during sulfur starvation. *Pseudomonas sp.* utilize a more diverse range of organosulfur compounds to maintain adequate sulfur levels in the cell. The monooxygenases that catalyze carbon-sulfur bond cleavage from organosulfur compounds share between 30-80% amino acid sequence identity. The high amino acid sequence identity suggests that they have evolved similar structural properties and mechanistic strategies for desulfonation, while still maintaining defined substrate specificities.

The characterized two-component system MsuE/MsuD system has been identified to being involved in desulfonation of methanesulfonate (C_1), whereas the SsuE/SsuD two-component system is involved in desulfonation of a range of linear alkanesulfonates (C_2-C_{14}). With similar active site architecture, it was proposed that both two-component systems may be similar in their substrate specificity. *P. aeruginosa* contain multiple two-component FMN-dependent systems that form a pathway to convert dimethylsulfone ($DMSO_2$) to sulfite, but also allow them to utilize long-chain aliphatic sulfonates. Both the MsuE/MsuD and SsuE/SsuD monooxygenase systems are expressed in different *Pseudomonas sp.,* but the MsuE/MsuD enzymes are not found in *E. coli*. *Pseudomonas sp.* (*P. aeruginosa*, *P. fluorescens*, and *P. putida*) comprise a substantial makeup of the bacterial microbiome and can utilize a wide range of organosulfur compounds when sulfur is limiting. Although the genes expressed during sulfur limitation catalyze similar reactions, bioinformatic analyses have uncovered some unique differences among these organisms relating to the organization of operons expressed during sulfur limitation.

An interesting finding from these studies was the ability of MsuD to utilize alkanesulfonates other than methanesulfonate, contrary to previously published studies.[72] The amino acids present in the active site of MsuD and SsuD are identical, so the diverse substrate specificity of MsuD was not too surprising. However, the inability of SsuD to utilize methanesulfonate was unexpected. Although both the *ssu* and *msu* operon are expressed during sulfur limitation, their activity would be dictated by substrate availability. The *ssu* operon also expresses an ABC-type transporter to transport alkanesulfonates into the cell.[56] Expression of a transporter specific for alkanesulfonates provides direct access to organosulfur compounds. This MsuC/MsuD enzymes are proposed to catalyze the conversion of methanesulfinate to sulfite and formaldehyde. Methanesulfinate is formed from the breakdown of $DMSO_2$ derived from dimethylsulfide by the SfnG monooxygenase. Therefore, the activity of MsuC/MsuD is dependent on the availability of the methanesulfinate provided by a previous metabolic reaction. It is not yet known if there are other mechanisms for methanesulfinate formation in the cell. In addition, the regulation of both operons is controlled by CysB, but it is unclear if different inducers are responsible for their activation. Another possibility is there are subtle differences in the active site that have not been identified, or that additional enzyme-substrate contacts are formed when substrate binds.

The mobile loop of SsuD is proposed to initiate the conformational change that is necessary for protecting reactive intermediates from bulk solvent. Arg297 on the loop that may interact with the phosphate group of FMN to stabilize loop closure over the active site when substrates bind. With loop closure over the active site in TIM-barrel enzymes playing a critical role in protecting intermediates from bulk solvent, the phosphodianion group of the reduced flavin may enable this closure. Studies with OMPDC utilized the truncated substrate of OMP in which the phosphate group was replaced with a single hydrogen to give 1-(β-D-erythrofuranosyl)orotic acid (EO) to

evaluate the contribution of the phosphodianion in loop closure.[223] In the presence of both the EO and the phosphite dianion, kinetic activity was increased with OMPDC compared with the EO substrate analog alone.[223] The conformational changes that occur with the binding of the EO fragment and phosphite leads to additional interactions. These binding energies are used to drive the conformational changes to form a closed conformation to drive catalysis.[223] With a similar phosphodianion group on FMN, SsuD was proposed to show an increase in activity utilizing the riboflavin and the phosphite dianion. However, there was no observable increase in activity for SsuD with both riboflavin and phosphite compared with riboflavin alone. Unlike other TIM-barrel enzymes, SsuD has to form protein-protein interactions for reduced flavin transfer. Previous studies suggest the phosphate group may be essential for the transfer event, and addition of a phosphite may not be able to compensate for the FMN phosphate group.[223]

Overall, these studies were able to determine the substrate specificity for SsuD and MsuD. *Pseudomonas sp*. are able to catalyze multiple sulfur substrates with the involvement of both SsuD and MsuD.[224] With a proposed similar active site, comparable catalytic activity should occur with similar alkanesulfonates, but SsuD was unable to utilize methanesulfonate. With the absence of MsuD in *E. coli*, desulfonation of methanesulfonate by MsuD would suggest an evolutionary advantage MsuD gives the *Pseudomonas sp.* to utilize methanesulfonate as an additional source of sulfur. With the absence of the ABC-type transporters on the operon, an explanation for methanesulfonate utilization would be that MsuC may have specificity for methanesulfinate and only provides methanesulfonate as the sulfur source. Another explanation to the different substrate specificity would be the mobile loop that has been characterized for SsuD. Although it has been identified with other TIM-barrel enzymes, the phosphate portion of substrate may initiate the closure of the loop over the active site. However, the phosphate group on FMN proves to be

essential in the closure of the loop with the absence of activity in coupled assay analysis. The phosphite itself may not be able to initiate closure once reduced flavin is transfers due to protein-protein interactions of SsuE and SsuD. The lack of loop closure exposes the active site resulting no protection for reactive intermediates.

Chapter 4

Summary

When inorganic sulfur is limiting in the environment, bacterial organisms will express enzymes from FMN-dependent two-component systems.[1] These two-component systems comprise a flavin reductase that supplies reduced flavin to the partner monooxygenase.[53] Once the monooxygenase receives the reduced flavin, the enzyme catalyzes the cleavage of carbon-sulfur bonds. In the alkanesulfonate monooxygenase system, SsuE supplies SsuD with reduced flavin for the desulfonation of linear alkanesulfonates (C_2-C_{10}) producing sulfite and the corresponding aldehyde.[53] In addition to the alkanesulfonate monooxygenase system, some *Pseudomonas sp.* utilize the methanesulfinate monooxygenase system to catalyze the desulfonation of methanesulfonate (C_1).[72] The FMN-dependent enzymes in these two-component systems share similar structural properties, but catalyze specific reactions.

Flavin reductases SsuE and MsuE belong to the NAD(P)H:FMN reductase family that is part of the flavodoxin-like superfamily.[147] Within this family, flavin reductases utilize FMN and NAD(P)H as substrates.[147] However, the majority of the flavin reductases found in this family are purified flavin-bound, whereas the flavin reductases in two-component systems purify flavin-free.[147] Both SsuE and MsuE are further subgrouped in the family due to a conserved π-helix located at the tetramer interface.[147] While there have been different amino acid specifications proposed for π-helix formation, most π-helices identified contain an amino acid insertion in a conserved α-helix.[163 159 225] This amino acid insertion generates a unique wide turn that deviates from the tightly coiled α-helix.[163] The π-helix has been identified in 15% of enzymes, and often imparts a gain of function for the enzyme.[163] A predominant functional difference between the

two-component FMN reductases and canonical flavoproteins in the NAD(P)H-FMN reductase family is the flavin transfer event.[147] Therefore, based on prior and current studies, we have proposed that this conserved region of the flavin reductase initiates an oligomeric shift from tetramer to the dimer form.[156] Once in the dimer oligomeric state, the active site is exposed allowing transfer of reduced flavin to the partner monooxygenase.[156]

The amino acid insertion proposed to generate the π-helix has been characterized for SsuE (Tyr118).[147] A Y118A SsuE variant was generated to determine if the amino acid substitution disrupted flavin reduction and subsequent flavin transfer.[156] The Y118A SsuE variant was purified flavin bound, and showed decreased rate of NADPH oxidation compared with wild-type.[187] There was no observable activity in coupled assays with SsuD, indicating the flavin substrate was not effectively transferred.[187] Although we expected the Tyr118 to alanine substitution to disrupt the π-helix, the π-helix had been converted to three-dimensional structure of the variant SsuE, and Δ118 variants were solved. Conversely, the deletion of Tyr 118 disrupted the π-helical region. These results indicate that the single amino acid insertion of the π-helix is not the only feature that contributes to the generation and stabilization of the π-helix.

SsuE and MsuE have ~30 amino acid sequence identity, and the *msu* operon has been proposed to have evolved from the *ssu* operon.[72] We first wanted to evaluate whether the partner monooxygenases of SsuE and MsuE could accept reduced flavin from the other FMN reductase. MsuD and SsuD were able to accept electrons from MsuE or SsuE with comparable activity. These results indicate these enzymes share similar interaction sites that allow transfer of reduced flavin from flavin reductase to monooxygenase. Previous studies identified interaction sites through hydrogen deuterium exchange experiments.[186] The protein-protein interaction regions for both SsuE and SsuD contain positive and negatively charged residues that may be involved in

electrostatic interactions with each other.[186] Electrostatic residues present in the SsuD binding region of SsuE include Lys77, Lys86, and Lys121, whereas residues for SsuD involve Asp251, Asp252, Glu253, and Lys257.[186] Through amino acid sequence alignment, MsuE has equivalent residues (Arg85, Lys93, and Arg129) that may form electrostatic interactions with either MsuD or SsuD. Additional studies also need to be performed with residues found on the interaction site of SsuE (Lys77 and Lys86) with coupled kinetic assays and fluorescent spectroscopy. Initial studies involved the Lys77Ala SsuE variant that resulted in no observable flavin reductase activity; yet activity was observed in the presence of SsuD, which would suggest communication from SsuD that may stabilize the active site of SsuE to generate the reduced flavin. Additional studies should identify similar interaction sites with MsuE and MsuD with hydrogen-deuterium exchange mass spectrometry.

Both SsuE and MsuE have a π-helix with conserved amino acids, but the insertional residue differs between the two enzymes. The insertional residue is usually a bulky amino acid, which assists in the stabilization of the wide turn. The two insertional residues were switched to evaluate if the nature of the insertional residue was important, or if a bulky amino acid was the only criteria (Y118H SsuE and H126Y MsuE). H126Y MsuE variant was purified flavin free and activity was observed in both flavin reductase and coupled assay activity. The H126Y MsuE variant was able to transfer the reduced flavin to the MsuD and SsuD similar to wild-type. Conversely, the Y118H SsuE variant generated was purified flavin-bound comparable to the Y118A SsuE variant. The Y118H SsuE flavin bound variant was no longer able to support NAD(P)H-dependent FMN reductase activity or transfer the reduced flavin to SsuD or MsuD. The differences observed for the insertional residues in each variant suggest there are inherent differences in the structural roles of each amino acid that play a role in the overall function. The substitution of Tyr for His would

disrupt the hydrogen-bonding and observed π-stacking interactions across the tetramer interface. There are currently no three-dimensional structures of MsuD to provide insight as to why it is more amenable to substitutions. to provide insight into the interaction sites. Additional studies with the SfnF flavin reductase due to the similar histidine residue characterized as the pi helix insertional residue would involve mutagenesis and structural analysis. This information will identify the interactions of the His128 and provide insight for the His126 of MsuE.

Previous studies suggest a gap insertion when comparing the α4-helix of flavin reductases of the NAD(P)H:FMN reductase family, but these results were performed with structurally distant enzymes. When this conserved region is compared with a more structurally similar flavin reductase, ChrR, the gap insertion is not present. The chromate reductase has a Tyr126 in an equivalent position to the Tyr118 residue of SsuE. The single amino acid insertion is not enough to provide the wide turn that is common in π-helices. Further evaluation of the π-helical region identified conserved residues in the two-component flavin reductases that differed in the canonical flavoprotein. All the flavin reductases with a π-helix have a conserved proline and aspartic acid residues in similar position as the glutamines found in the α-helix ChrR. Variants were generated for both SsuE (D117Q, P123Q, and D117Q/P123Q) and MsuE (D125Q, P130Q, and D125Q/P130Q) to determine if the glutamine residues form the α-helix comparable to ChrR. Each variant generated had minimal purification success with lower than normal concentrations compared to wild-type. They were unable to bind to the flavin substrate while no longer being efficient in reducing and transferring reduced flavin to monooxygenase partner. The P130Q MsuE variant was the only variant to bind at a 10-fold high K_d value but unsuccessfully transferred electrons to ferricyanide. These results suggest a possible disruption in the π-helix that is comparable to the Δ118 SsuE variant. The Δ118 variant had no observable activity in flavin

reductase and coupled assays. The proline and aspartic acid residues may play a role in stabilizing the wide turn that allows the oligomeric switch to occur to transfer reduced flavin. The π-helix that the flavin reductases from the NAD(P)H:FMN reductase family have is a conserved feature that is proposed to facilitate flavin transfer. This ability is not seen with other flavin reductases in the family due to the tightly coiled α-helix. Additional studies will be needed with the ChrR flavin reductase to generate variants with the conserved residues located in the π-helix of flavin reductase. Variants of ChrR with proline and aspartic acid residues would mimic the π-helix of flavin reductases. With both residues located near the tetramer interface, the proline residue is known to disrupt the hydrogen-bond patten which may allow the large aromatic residue to form the characteristic bulge.[158] These substitutions may disrupt the hydrogen bonds and convert the α-helix of ChrR to a π-helix.

The SsuD and MsuD monooxygenases share a high amino acid sequence identity. Structural features that promote catalysis have been identified for SsuD.[175] SsuD belongs to the TIM-barrel family that can be further separated due to the insertional loop that it possesses.[175] Loop studies have suggested the necessity of this mobile loop to close over the active site to protect the reactive intermediates from bulk solvent.[177] There is a conserved arginine residue that is present on the loop of monooxygenases.[175] The Arg297 residue on the loop of SsuD has been proposed to be involved with electrostatic interactions with the phosphate group of reduced flavin. This interaction initiates the conformational changes needed to close over the active site. Previous substitutions of the Arg297 residue with alanine resulted in a loss of kinetic activity in coupled assays.[177] Riboflavin and phosphite were not able to support catalysis in coupled assays no matter what the alternate experimental. This may be due to the length of the loop of SsuD not being able to fully close over the active site. With proposed similar structural features for both SsuD and

MsuD there would have to be other structural features that differentiate the sulfur source that both have been characterized to utilize.

The active site of both SsuD and MsuD have a similar architecture but utilize different sulfur sources to alleviate a limited sulfur environment. In coupled assays, both SsuD and MsuD utilized similar organosulfur substrates from C_2-C_{14}, but SsuD was unable to utilize methanesulfonate (C_1) while MsuD was able to. These results suggest an evolutionary advantage the FMN-dependent two-component system MsuE and MsuD have when sulfur is limiting. While SsuE and SsuD are unable to utilize methanesulfonate, MsuE and MsuD may provide an additional pathway for sulfur assimilation for bacterial organisms. Additional studies would identify the affinity of SsuD and MsuD for each substrate through anaerobic fluorescent titration studies. Molecular dynamic simulations would also be used to determine if additional amino acids may be contributing to the specificity.

The results from this study provide a foundation for future studies of the structural features of both the flavin reductase and monooxygenase that promote catalytic activity. Based on the evidence provided, the single amino acid is not enough to form the bulge that characterizes the π-helix but requires other conserved residues to help stabilize the structure of flavin reductases to facilitate flavin transfer. Additional studies with other flavin reductases SfnF and ChrR to further characterize the role of the conserved residues. Whereas SsuD was unable to utilize methanesulfonate, MsuD may provide an additional pathway for sulfur assimilation for bacterial organisms. Additional studies with molecular dynamic simulations could be performed to view the interactions with active site and substrates.

References

1. Kertesz, M. A., Riding the Sulfur Cycle- Metabolism of Sulfonates and Sulfate Esters in Gram-negative Bacteria. *FEMS Microbiology Reviews* **1999,** *24*, 135-175.
2. Mandeville, C. W., Sulfur: A ubiquitous and useful tracer in Earth and planetary sciences. *Elements* **2010,** *6*, 75-80.
3. Fuentes-Lara, L. A.; Medrano-Macías, J.; Pérez-Labrada, F.; Rivas-Martínez, E. N.; García-Enciso, E. L.; González-Morales, S.; Juárez-Maldonado, A.; Rincón-Sánchez, F.; Benavides-Mendoza, A., From Elemental Sulfur to Hydrogen Sulfide in Agricultural Soils and Plants *Molecules* **2019,** *24*, 1-17.
4. Andreae, M. O., Ocean-atmosphere interactions in the global biogeochemical sulfur cycle. *Mar. Chem.* **1990,** *30*, 1-29.
5. Mikkelsen, R.; Norton, R., Soil and fertilizer sulfur. *Better Crop* **2013,** *97*, 7-9.
6. Rendig, V. V.; Oputa, C.; McComb, E. A., Effects of sulfur deficiency on non-protein nitrogen, soluble sugars, and N/S ratios in young corn (Zea mays L.) plants. *Plant Soil* **1976,** *44*, 423-437.
7. Stipanuk; M.H., Metabolism of sulfur-containing amino acids . *Annu. Rev. Nutr.* **1986,** *6*, 179-209.
8. Giovanelli, J., *Methods Enzymol.* **1987,** *143*, 419-426.
9. Saint-Girons, I.; Parsot, C.; Zakin, M. M.; Barzu, O.; Cohen, G. N., *CRC Crit. Rev. Biochem.* **1988,** *23*, S1-S42.
10. Marzluf, G. A., *Adv. Genet.* **1994,** *31*, 187-206.
11. Thomas, D.; Surdin-Kerjan, Y., *Microbiol. Mol. Biol. Rev.* **1997,** *61*, 503-532.
12. Ravanel, S.; Gakiere, B.; Job, D.; Douce, R., The specific features of methionine biosynthesis and metabolism

in plants. *Proc. Natl. Acad. Sci* **1998,** *95*, 7805-7812.
13. Kredich, N. M., Biosynthesis of Cysteine. *EcoSal Plus* **2008,** *3* (1), 1-30.
14. Black, K. A.; Dos Santos, P. C., Shared-intermediates in the biosynthesis of thio-cofactors: Mechanism and functions of cysteine desulfurases and sulfur acceptors. *Biochimica et Biophysica Acta* **2015,** *1853*, 1470-1480.
15. Hidese, R.; Mihara, H.; Esaki, N., Bacterial cysteine desulfurases: versatile key players

in biosynthetic pathways of sulfur-containing biofactors. *Appl Microbiol Biot.* **2011,** *91*, 47-61.
16. Hidese , R.; Inoue , T.; Imanaka, T.; Fujiwara, S., Cysteine desulphurase plays an important role in environmental adaptation of the hyperthermophilic archaeon T*hermococcus kodakarensis*. *Mol. Microbiol.* **2014**.
17. Roche , B.; Aussel , L.; Ezraty , B.; Mandin , P.; Py, B.; Barras, F., Iron/sulfur proteins biogenesis in prokaryotes: formation, regulation and diversity. *Biochim. Biophys. Acta.* **2013,** *1827*, 455-469.
18. Lill , R.; Hoffmann , B.; Molik , S.; Pierik , A. J.; Rietzschel , N.; Stehling , O.; Uzarska , M. A.; Webert , H.; Wilbrecht, C.; Muhlenhoff, U., The role of mitochondria in cellular iron–sulfur protein biogenesis and iron metabolism. *Biochim. Biophys. Acta.* **2012,** *1823*, 1491-1508.
19. C.T., L.; Kambampati, R., The iscS gene in *Escherichia coli* is required for the biosynthesis of 4-thiouridine, thiamin, and NAD. *J. Biol. Chem.* **2000,** *275*, 20096-20103.

20. Mueller , E. G.; Buck , C. J.; Palenchar , P. M.; Barnhart, L. E.; Paulson, J. L., Identification of a gene involved in the generation of 4-thiouridine in tRNA. *Nucleic Acids Res.* **1998,** *26*, 2606-2610.
21. Martinez-Gomez , N. C.; Palmer , L. D.; Vivas , E.; Roach, P. L.; Downs, D. M., The rhodanese domain of ThiI is both necessary and sufficient for synthesis of the thiazole moiety of thiamine in *Salmonella enterica*. *J. Bacteriol.* **2011,** *193*, 4582-4587.
22. You , D.; Xu , T.; Yao , F.; Zhou, X.; Deng, Z., Direct evidence that ThiI is an ATP pyrophosphatase for the adenylation of uridine in 4-thiouridine biosynthesis. *Chembiochem* **2008,** *9*, 1879-1882.
23. Dahl , J. U.; Radon , C.; Buhning , M.; Nimtz , M.; Leichert , L. I.; Denis , Y.; Jourlin-Castelli , C.; Iobbi-Nivol , C.; Mejean, V.; Leimkuhler, S., The sulfur carrier protein TusA has a pleiotropic role in *Escherichia coli* that also affects molybdenum cofactor biosynthesis. *J. Biol. Chem.* **2013,** *288*, 5426-5442.
24. Mendel, R. R.; Leimkuhler, S., The Biosynthesis of the Molybdenum Cofactors. *J. Biol. Inorg.* **2014,** *20*, 337-347.
25. Ikeuchi , Y.; Shigi , N.; Kato , J.; Nishimura, A.; Suzuki, T., Mechanistic insights into sulfur relay by multiple sulfur mediators involved in thiouridine biosynthesis at tRNA wobble positions. *Mol. Cell* **2006,** *21*, 97-108.
26. Takahashi, Y.; Nakamura, M., Functional assignment of the ORF2–iscS–iscU–iscA–hscB–hscA–fdx–ORF3 gene cluster involved in the assembly of Fe–S clusters in E*scherichia coli*. *J. Biochem.* **1999,** *126*, 917-926.
27. Raulfs , E. C.; O'Carroll , I. P.; Dos Santos , P. C.; Unciuleac, M. C.; Dean, D. R., In vivo iron–sulfur cluster formation. *Proc. Natl. Acad. Sci. U.S.A.* **2008,** *105*, 8591-8596.
28. Agar , J. N.; Krebs , C.; Frazzon , J.; Huynh , B. H.; Dean, D. R.; Johnson, M. K., IscU as a scaffold for iron–sulfur cluster biosynthesis: sequential assembly of [2Fe–2S] and [4Fe–4S] clusters in IscU. *Biochemistry* **2000,** *39*, 7856-7862.
29. Unciuleac , M. C.; Chandramouli , K.; Naik , S.; Mayer , S.; Huynh , B. H.; Johnson, M. K.; Dean, D. R., In vitro activation of apo-aconitase using a [4Fe–4S] cluster-loaded form of the IscU [Fe–S] cluster scaffolding protein. *Biochemistry* **2007,** *46*, 6812-6821.
30. Fugate, C. J.; Jarrett, J. T., Biotin synthase: insights into radical-mediated carbon–sulfur bond formation. *Biochim. Biophys. Acta.* **2012,** *1824*, 1213-1222.
31. Cicchillo , R. M.; Iwig , D. F.; Jones , A. D.; Nesbitt , N. M.; Baleanu-Gogonea , C.; Souder , M. G.; Tu, L.; Booker, S. J., Lipoyl synthase requires two equivalents of S-adenosyl-l-methionine to synthesize one equivalent of lipoic acid. *Biochemistry* **2004,** *43*, 6378-6386.
32. Urbonavicius, J.; Qian, Q.; Durand, J. M. B.; Hagervall, T. G.; Bjork, G. R., Improvement of reading frame maintenance is a common function for several tRNA modifications. *EMBO Journal* **2001,** *20*, 4863-4873.
33. Gustilo, E. M.; Vendeix, F. A. P.; Agris, P. F., tRNA's modifications bring order to gene expression. *Current Opinion in Microbiology* **2008,** *11*, 134-140.
34. Hagervall, T. G.; Ericson, J. U.; Esberg, K. B.; Li, J. N.; Bjoerk, G. R., Role of tRNA modification in translational fidelity. *Biochimica et Biophysica Acta, Gene Structure and Expression* **1990,** *1050*, 263-266.
35. Torres, A. G.; Batlle, E.; Ribas de Pouplana, L., Role of tRNA modifications in human diseases. *Trends in Molecular Medicine* **2014,** *20*, 306-314.

36. Durand, J. M. B.; Bjork, G. R.; Kuwae, A.; Yoshikawa, M.; Sasakawa, C., The modified nucleoside 2-methylthio-N6-isopentenyladenosine in tRNA of Shigella flexneri is required for expression of virulence genes. *Journal of Bacteriology* **1997,** *179*, 5777-5782.
37. Bouvier , D.; Labessan , N.; Clemancey , M.; Latour , J. M.; Ravanat , J. L.; Fontecave, M.; Atta, M., TtcA a new tRNA-thioltransferase with an Fe–S cluster. *Nucleic Acids Res.* **2014,** *42*, 7960-7970.
38. Cavuzic, M.; Liu, Y., Biosynthesis of Sulfur-Containing tRNA Modifications: A Comparison of Bacterial, Archaeal, and Eukaryotic Pathways. *Biomolecules* **2017,** *7*, 1-15.
39. Kredich; M., N., Biosynthesis of Cysteine. *EcoSal Plus* **2008,** *3*, 1-30.
40. Sekowska, A.; Kung, H. F.; Danchin, A., Sulfur metabolism in *Escherichia coli* and related bacteria: Facts and fiction,. *Journal of Molecular Microbiology and Biotechnology* **2000,** *2*, 145-177.
41. Williams, S. J.; Senarante, R. H.; Mougous, J. D.; Riley, L. W.; Bertozzi, C. R., 5'-adenosinephosphosulfate lies at a metabolic branch point in mycobacteria,. *The Journal of Biological Chemistry* **2002,** *277*, 32606-32615.
42. Jhee, K. H.; Kruger, W. D., The role of cystathionine beta-synthase in homocysteine metabolism. *Antioxid. Redox Signal* **2005,** *7*, 813-822.
43. Kraus, J. P.; Hasek, J.; Kozich, V.; Collard, R.; Venezia, S.; Janosikova, B.; Wang, J.; Stabler, S. P.; Allen, R. H.; Jakobs, C.; Finn, C. T.; Chien, Y.; Hwu, W.; Hegele, R. A.; Mudd, S. H., Cystathionine γ-lyase: clinical, metabolic, genetic, and structural studies. *Mol. Genet. Metab.* **2009,** *97*, 250-259.
44. Vermeij, P.; Kertesz, M. A., Pathways of Assimilative Sulfur Metabolism in *Pseudomonas putida*. *Journal of Bacteriology* **1999,** *181* (18), 5833-5837.
45. Watwood, M. E.; Fitzgerald, J. W.; Gosz, J. R., Sulfur processing in forest soil and litter along an elevational and vegatative gradient. *Can. J. For. Res.* **1986,** *16*, 689-695.
46. Autry, A. R.; Fitzgerald, J. W., Sulfonate S - A major form of forest soil organic sulfur. *Biol. Fertil. Soils* **1990,** *10* (50-56).
47. Vairavamurthy, A.; Mopper, K.; Taylor, B. F., Occurrence of particle-bound polysulfides and significance of their reaction with organic matters in marine sediments. *Geophys. Res. Lett.* **1992,** *19*, 2043-2046.
48. David, M. B.; Mitchell, M. J., Sulfur Constituents and Cycling in Waters, Seston, and Sediments of an Oligotrophic Lake. *Limmol. Oceanogr.* **1985,** *30*, 1196-1207.
49. Hummerjohann, J.; Kuttel, E.; Quadroni, M.; Ragaller, J.; Leisenger, T.; Kertesz, M. A., Regulation of the sulfate starvation response in *Pseudomonas aeruginosa*: role of cysteine biosynthetic intermediates,. *Microbiology* **1998,** *144*, 1375-1386.
50. Quadroni, M.; Staudenmann, W.; Kertesz, M.; James, P., Analysis of global responses by protein and peptide fingerprinting of proteins isolated by two-dimensional gel electrophoresis. Application to the sulfate-starvation response of Escherichia coli. *Eur J Biochem* **1996,** *239* (3), 773-781.
51. Kertesz, M. A.; Leisinger, T.; Cook, A. M., Proteins induced by sulfate limitation in *Escherichia coli*, *Pseudomonas putida*, or *Staphylococcus aureus*. *J. Bacteriol.* **1993,** *175*, 1187-1190.
52. Van Der Ploeg, J. R.; Weiss, M. A.; Saller, E.; Nashimoto, H.; Saito, N.; Kertiesz, M. A.; Leisinger, T., Identification of Sulfate Starvation-Regulated Genes in *Escherichia coli*: a Gene CLuster Involved in the Utilization of Taurine as a Sulfur Source. *Journal of Bacteriology* **1996,** *178* (18), 5438-5446.

53. Eichhorn, E.; van der Ploeg, J. R.; Leisinger, T., Characterization of a Two-Component Alkansesulfonate Monooxygenase from *Escherichia coli*. *Journal of Biological Chemistry* **1999,** *274* (38), 26639-26646.
54. Eichhorn, E.; van der Ploeg, J. R.; Kertesz, M. A.; Leisenger, T., Characterization of alpha-ketoglutarate dependent taurine dioxygenase from *Escherichia coli*. *J. Biol. Chem.* **1997,** *272*, 23031-23036.
55. Kahnet, A.; Vermeij, P.; James, P.; Leisinger, T.; Kertesz, M. A., The *ssu* locus plays a key role in organosulfur metabolism in *Pseudomonas putida* S-313. *J. Bacteriol* **1999,** *182* (10), 2869-2878.
56. van der Ploeg, J.; Iwanicka-Nowicka, R.; Bykowski, T.; Hryniewicz, M.; Leisenger, T., The *Escherichia coli ssu*EADCB Gene Cluster is Required for the Utilization of Sulfur from Aliphatic Sulfonates and is Regulated by the Transcriptional Activator CB1. *Biological Chemistry* **1999,** *274* (41), 29358-29365.
57. van der Ploeg, J. R.; Iwanicka-Nowicka, R.; Kertesz, M. A.; Leisenger, T.; Hryniewicz, M. M., Involvement of CysB and Cbl regulatory proteins in expression of the *tauABCD* operon and other sulfonate starvation-inducible genes in *Escherichia coli*. *J. Bacteriol* **1997,** *179*, 7671-7678.
58. Giffard; P.M.; Booth; I.R., The *rpoA341* allele of Escherichia coli specifically impairs the transcription of a group of positively-regulated operons. *Mol. Gen. Genet.* **1988,** *214*, 148-152.
59. Shi; X.; Bennett; G.N., Effects of *rpoA* and *cysB* mutations on acid induction of biodegradative arginine decarboxylase in *Escherichia coli* . *J. Bacteriol.* **1994,** *176*, 7017-7023.
60. Delic-Attree; I.; Toussaint; B.; Garin; J.; Vignais; P.M., Cloning, sequence and mutagenesis of the structural gene of *Pseudomonas aeruginosa* CysB, which can activate *algD* transcription. *Mol. Microbiol.* **1997,** *24*, 1275-1284.
61. R., T.; K.H.G., V.; E.J., D.; G.N., M.; C., A.; A.J., W., The structure of the cofactor-binding fragment of the LysR family member, CysB: a familiar fold with a surprising subunit arrangement . *Structure* **1997,** *5*, 1017-1032.
62. Oppezzo, O. J., In vivo effects of anti-inducers of the cysteine regulon in *Salmonella typhimurium* . *FEMS Microbiol. Lett.* **1998,** *163*, 143-148.
63. Ploeg, v. d.; J.R.; Iwanicka-Nowicka; R.; Bykowski; T.; Hryniewicz; M.; Leisinger; T., The Cbl-regulated *ssuEADCB* gene cluster is required for aliphatic sulfonate-sulfur utilization in *Escherichia coli* . . *J. Biol. Chem.* **1999,** *174*, 29358-29365.
64. R., I. N.; M.M., H., A new gene, *cbl*, encoding a member of the LysR family of transcriptional regulators belongs to *Escherichia coli cys* regulon . . *Gene* **1995,** *166*, 11-17.
65. Charlson, R. J.; Lovelock, J. E.; Andreae, M. O.; Warren, S. G., Oceanic phytoplankton, atmospheric sulphur, cloud albedo and climate. *Nature* **1987,** *326*, 655-661.
66. Reisch, C. R.; Stoudemayer, M. J.; Varaljay, V. A.; Amster, I. J.; Moran, M. A.; Whitman, W. B., Novel pathway for assimilation of dimethylsulphoniopropionate widespread in marine bacteria. *Nature* **2011,** *473*, 208-211.
67. Chen, Y.; Schafer, H., Towards a systematic understanding of structure-function relationship of dimethylsulfoniopropionate-catabolizing enzymes. *Molecular Microbiology* **2019,** *111*, 1399-1403.
68. T., E.; Habe, H.; Nojiri, H.; Yamane, H.; Omori, T., The Sigma 54-Dependent Transcriptional Activator SfnR Regulates the Expression of the *Pseudomonas putida*

sfnFG Operon Responsible for Dimethyl Sulphone Utilization. *Molecular Biology* **2005,** *55* (3), 897-911.

69. Endoh, T.; Habe, H.; Yoshida, T.; Nojiri, H.; Omori, T., A CysB-regulated and sigma54-dependent regulator, SfnR, is essential for dimethyl sulfone metabolism of Pseudomonas putida strain DS1. . *Microbiology* **2003,** *149*, 991-1000.
70. Endoh, T.; Kasuga, K.; Horinouchi, M.; Yoshida, T.; Habe, H.; Nojiri, H.; Omori, T., Characterization and identification of genes essential for dimethyl sulfide utilization in *Pseudomonas putida* strain DS1. . *Appl. Microbiol Biotechnol* **2003,** *62*, 83-91.
71. Lundgren, B. R.; Sarwar, Z.; Feldman, K. S.; Shoytush, J. M.; Nomura, C. T., SfnR2 Regulates Dimethyl Sulfide-Related Utilization in *Pseudomonas aeruginosa* PAO1 *Journal of Bacteriology* **2019,** *201* (4), 1-22.
72. Kertesz, M. A.; Schmidt-Larbig, K.; Wuest, T., A Novel Reduced Flavin Mononucleotide-Dependent Methanesulfonate Sulfonatase Encoded by the Sulfur-Regulated *msu* Operon of *Pseudomonas aeruginosa*. *Journal of Bacteriology* **1999,** *181* (5), 1464-1473.
73. Kelly, D. P.; Baker, S. C.; Trickett, J.; Davey, M.; Murrell, J. C., Methanesulphonate Utilization by a Novel Methylotrophic Bacterium Involves an Unusual Monooxygenase. *Microbiology* **1994,** *140*, 1419-1426.
74. Ellis, H., The FMN-Dependent Two-Component Monooxygenase Systems. *ScienceDirect* **2010,** *497*, 1-12.
75. Gao, B.; Ellis, H., Altered Mechanism of the Alkanesulfonate FMN Reductase with the Monooxygenase Enzyme. *Biochemical and Biophysical Research Communications* **2005,** *331*, 1137-1145.
76. Meighen, E. A., Molecular biology of bacterial bioluminescence. *Microbiol. Rev.* **1991,** *55*, 123-142.
77. Gibson, Q. H.; Hastings, J. W., The oxidation of reduced flavin mononucleotide by molecular oxygen. *Biochem. J.* **1962,** *83*, 368-377.
78. Hastings, J. W.; Gibson, Q. H., Intermediates in the Bioluminescent Oxidation of Reduced Flavin Mononucleotide. *J. Biol. Chem.* **1963,** *238*, 2537-2554.
79. Baldwin, T. O.; Ziegler, M. M., The Biochemistry and Molecular Biology of Bacterial Bioluminescence. *Chemistry and Biochemistry of Flavoenzymes* **1992,** *CRC Press*, 467-530.
80. Feng, L.; Wang, W.; Cheng, J.; Ren, Y.; Zhao, G.; Gao, C.; Tang, Y.; Liu, X.; Han, W.; X.; Peng; Liu, R.; Wang, L., *Proc. Natl. Acad. Sci. USA* **2007,** *104*, 5602-5607.
81. L., L.; Liu, X.; Yang, W.; Xu, F.; Wang, W.; Feng, L.; Bartlam, M.; Wang, L.; Rao, Z., Crystal Structure of Long-Chain ALkane Monooxygenase (LadA) in COmplex with Coenzym FMN: Unvieling the Long-Chain Alkane Hydroxylase. *J. Mol. Biol.* **2008,** *376*, 453-465.
82. Nissen, M. S.; Youn, B.; Knowles, B. D.; Ballinger, J. W.; Jun, S. Y.; Belchik, S. M.; Xun, L.; Kang, C., *J. Biol. Chem.* **2008,** *283*, 28710-28720.
83. Payne, J. W.; Bolton, H.; Campbell, J. A.; Xun, L., Purification and characterization of EDTA monoxygenase from the EDTA-degrading bacterium BCN1. *J. Bacterial* **1998,** *180*, 3823-3827.
84. Bohuslavek, J.; Payne, J. W.; Liu, Y.; Bolton, H. J.; Xun, L., Cloning, sequencing, and characterization of a gene cluster involved in EDTA degradation from the bacterium BNC1. *Appl. Environ. Microbiol.* **2001,** *67*, 688-695.
85. Oldfield, C.; Pogrebinsky, O.; Simmonds, J.; Olson, E. S.; Kulpa, C. F., *Microbiology* **1997,** *143*, 2961-2973.
86. Kendrew, S. G.; Harding, S. E.; Hopwood, D. A.; Marsh, E. N., Identification of a Flavin:NADH Oxidoreductase Involved in the Biosynthesis of Actinorhodin

PURIFICATION AND CHARACTERIZATION OF THE RECOMBINANT ENZYME. *J. Biol. Chem.* **1995,** *270*, 17339–17343.
87. Filisetti, L.; Fontecave, M.; Niviere, V., Mechanism and Substrate Specificity of the Flavin Reductase ActVB from *Streptomyces coelicolor*. *J. Biol. Chem.* **2003,** *278*, 296–303.
88. Valton, J.; Mathevon, C.; Fontecave, M.; Niviere, V., Mechanism and Regulation of the Two-component FMN-dependent Monooxygenase ActVA-ActVB from *Streptomyces coelicolor*. *J. Biol. Chem.* **2008,** *283*, 10287-10296.
89. Thibaut, D.; Ratet, N.; Bisch, D.; Faucher, D.; Debussche, L.; Blanche, F., Purification of the two-enzyme system catalyzing the oxidation of the D-proline residue of pristinamycin II B during the last step of pristinamycin II_A biosynthesis. *J. Bacterial* **1995,** *177*, 5199-5205.
90. Blanc, V.; Lagneaux, D.; Didier, P.; Gil, P.; Lacroix, P.; Crouzet, J., Cloning and analysis of structural genes from Streptomyces pristinaespiralis encoding enzymes involved in the conversion of pristinamycin IIB to pristinamycin IIA (PIIA): PIIA synthase and NADH:riboflavin 5'-phosphate oxidoreductase. *J. Bacteriol.* **1995,** *177*, 5206–5214.
91. Chaiyen, P.; Suadee, C.; Wilairat, P., A novel two-protein component flavoprotein hydroxylase p-Hydroxyphenylacetate hydroxylase from *Acinetobacter baumannii*. *Eur. J. Biochem.* **2001,** *268*, 5550-5561.
92. Uetz, T.; Schneider, R.; Snozzi, M.; Egli, T., Purification and characterization of a two-component monooxygenase that hydroxylates nitrilotriacetate from "*Chelatobacter*" strain 29600. *J. Bacterial* **1992,** *174*, 1179-1188.
93. Knobel, H. R.; Egli, T.; van der Meer, J. R., Cloning and characterization of the genes encoding nitrilotriacetate monooxygenase of *Chelatobacter heintzii* ATCC 29600. *J. Bacteriol.* **1996,** *178*, 6123-6132.
94. Xu, Y.; Mortimer, M. W.; Fisher, T. S.; Kahn, M. L.; Brockman, F. J.; Xun, L., Cloning, sequencing, and analysis of a gene cluster from *Chelatobacter heintzii* ATCC 29600 encoding nitrilotriacetate monooxygenase and NADH:flavin mononucleotide oxidoreductase. *J. Bacteriol.* **1997,** *179*, 1112-1116.
95. Wicht, D., The Reduced Flavin-Dependent Monooxygenase SfnG Converts Dumethylsulfone to Methanesulfinate. *Archives of Biochemistry and Biophysics* **2016,** *604*, 159-166.
96. Bentley, R.; Chasteen, T. G., Environmental VOSCs—formation and degradation of dimethyl sulfide, methanethiol and related materials. *Chemosphere* **2004,** *55*, 291-317.
97. Pinto, J. T., Riboflavin. *Adv. Nutr.* **2016,** *7*, 973-975.
98. Fischer, M.; Bacher, A., Biosynthesis of flavocoenzymes. *The Royal Society of Chemistry* **2005,** *22*, 324-350.
99. Cardoso, D. R.; Libardi, S. H.; Skibsted, L. H., Riboflavin as a photosensitizer. Effects on human health and food quality. *Food Funct.* **2012,** *3*, 487-502.
100. Kilic, M.; Ensing, B., First and Second One-Electron Reduction of Lumiflavin in Water—A First Principles Molecular Dynamics Study. *JCTC* **2013,** *9*, 3889-3899.
101. Fischer, M.; Romisch, W.; Saller, S.; Illarionov, B.; Richter, G.; Rohdich, F.; Eisenreich, W.; Bacher, A., *J. Biol. Chem.* **2004,** *279*, 36299-36308.
102. Fischer, M.; Bacher, A., Biosynthesis of vitamin B2: Structure and mechanism of riboflavin synthase,. *Archives of Biochemistry and Biophysics* **2008,** *474*, 252-265.
103. Eschenmoser, A.; Loewenthal, E., Chemistry of Potentially Prebiological Natural-Products,. *Chem. Soc. Rev.* **1992,** *21*, 1-16.
104. Plaut, G. W. E.; Florkin, M.; Stotz, E. H., *Comprehensive Biochemistry* **1971,** *21*, 11-45.

105. Bacher, A.; Mailander, B., *J. Biol. Chem.* **1973,** *248*, 6227-6231.
106. Foor, F.; Brown, G. M., *J. Biol. Chem.* **1975,** *250*, 3545-3551.
107. Le Van, Q.; Keller, P. J.; Bown, D. H.; Floss, H. G.; Bacher, A., *J. Bacterial* **1985,** *162*, 1280-1284.
108. Foor, F.; Brown, G. M., *Methods Enzymol.* **1980,** *66*, 303-307.
109. Richter, G.; Fischer, M.; Krieger, C.; Eberhardt, S.; Luttgen, H.; Gertenschalger, I.; Bacher, A., *J. Bacteriol* **1997,** *179*, 2022-2028.
110. Graupner, M.; Xu, H.; White, R. H., *J. Bacteriol* **2002,** *184*, 1952-1957.
111. Burrows, R. B.; Brown, G. M., *J. Bacterial* **1978,** *136*, 657-667.
112. Bacher, A.; Lingens, F., *J. Biol. Chem.* **1970,** *245*, 4647-4652.
113. Nielson, P.; Bacher, A., *Biochem. Biophys, Acta.* **1981,** *662*, 312-317.
114. Neuberger, G.; Bacher, A., *Biochem. Biophys. Res. Commun.* **1986,** *139*, 1111-1116.
115. Harzer, G.; Rokos, H.; Otto, M. K.; Bacher, A.; Ghilsa, S., *Biochem. Biophys. Acta.* **1978,** *540*, 48-54.
116. Kis, K.; Volk, R.; Bacher, A., *Biochemistry* **1995,** *34*, 2883-2892.
117. Volk, R.; Bacher, A., *J. Biol. Chem.* **1990,** *265*, 19479-19485.
118. Volk, R.; Bacher, A., *J. Biol. Chem.* **1991,** *266*, 20610-60618.
119. Volk, R.; Bacher, A., *J. Am. Chem. Soc.* **1988,** *110*, 3651-3653.
120. Plaut, G. W. E.; Harvey, R. A., *Methods Enzymol.* **1971,** *18*, 515-538.
121. Plaut, G. W., *J. Biol. Chem.* **1963,** *238*, 2225-2243.
122. Plaut, G. W., *J. Biol. Chem.* **1960,** *235*, PC41-PC42.
123. Plaut, G. W.; Beach, R. L.; Aogaichi, T., *Biochemistry* **1970,** *9*, 771-785.
124. Wacker, H.; Harvey, R. A.; Winestock, C. H.; Plaut, G. W., *J. Biol. Chem.* **1964,** *239*, 3493-3497.
125. Harvey, R. A.; Plaut, G. W., *J. Biol. Chem.* **1966,** *241*, 2120-2136.
126. Bacher, A.; Muller, F., CRC Press: Boca Raton, FL, 1991; Vol. 1.
127. Yatsyshyn V. Y.; Fedorovych D. V.; A., S. A., The microbial synthesis of flavin nucleotides: a review . *Appl. Biochem. Microbiol.* **2009,** *45*, 115-124.
128. A., B., *Biosynthesis of flavins ,*. CRC Press: Boca Raton, FL, 1991; Vol. 1.
129. *Bauer S*; *Kemter K*; *Bacher A*; *Huber R*; *Fischer M*; *S, S.*, Crystal structure of Schizosaccharomyces pombe riboflavin kinase reveals a novel ATP and riboflavin-binding fold. *J. Mol. Biol.* **2003,** *326*, 1463-1473.
130. Clarebout G; Villers C; R, L., Macrolide resistance gene mreA of Streptococcus agalactiae encodes a flavokinase. *Antimicrob Agents Chemother* **2001,** *45*, 2280-2286.
131. Karthikeyan S; Zhou Q; Osterman AL; H, Z., Ligand binding-induced conformational changes in riboflavin kinase: structural basis for the ordered mechanism. *Biochemistry* **2003,** *42*, 12532-12538.
132. Kashchenko VE; GM, S., Purification and properties of the riboflavin kinase of the yeast Pichia guilliermondii]. *Biokhimilia* **1976,** *41*, 376-383.
133. Mashhadi, Z.; Zhang, H.; Xu, H.; White, R. H., Identification and characterization of an archaeon-specific riboflavin kinase. *J. Bacteriol.* **2008,** *190*, 2615-2618.
134. Sandoval FJ; S, R., An FMN hydrolase is fused to a riboflavin kinase homolog in plants. *J. Biol. Chem.* **2005,** *280*, 38337-38345.
135. Santos MA; Jimenez A; JL, R., Molecular characterization of FMN1, the structural gene for the monofunctional flavokinase of Saccharomyces cerevisiae. *J. Biol. Chem.* **2000,** *275*, 28618-28624.

136. Solovieva IM; Kreneva RA; Leak DJ; DA, P., The ribR gene encodes a monofunctional riboflavin kinase which is involved in regulation of the Bacillus subtilis riboflavin operon. *Microbiology* **1999,** *145*, 67-73.
137. Yamada Y; Merrill AH Jr; DB, M., Probable reaction mechanisms of flavokinase and FAD synthetase from rat liver. *Arch. Biochem. Biophys.* **1990,** *278*, 125-130.
138. *Kearney EB*; *Goldenberg J*; *Lipsick J*; *M, P.*, Flavokinase and FAD synthetase from Bacillus subtilis specific for reduced flavins. *J. Biol. Chem.* **1979,** *254*, 9551-9557.
139. Efimov I; Kuusk V; Zhang X; WS, M., Proposed steady-state kinetic mechanism for Corynebacterium ammoniagenes FAD synthetase produced by Escherichia coli. *Biochemistry* **1998,** *37*, 9716-9723.
140. Abbas, C. A.; Sibirny, A. A., Genetic Control of Biosynthesis and Transport of Riboflavin and Flavin Nucleotides and COnstruction of RObust Biotechological Producers. *Microbiol. Mol. Biol. Rev.* **2011,** *75*, 321-360.
141. Frago S; Martínez-Júlvez M; Serrano A; M, M., Structural analysis of FAD synthetase from Corynebacterium ammoniagenes. *BMC Microbiol.* **2008,** *8*, 160.
142. Frago S; Velázquez-Campoy A; M, M., The puzzle of ligand binding to Corynebacterium ammoniagenes FAD synthetase. *J. Biol. Chem.* **2009,** *284*, 6610-6619.
143. Miura, R., Versatility and specificity in flavoenzyme: control mechanisms of flavin reactivity. *The Chemical Record* **2001,** *1*, 183-194.
144. Massey, V., The Chemical and Biological Versatility of Riboflavin. *Biochemical Society Transactions* **1999,** *28*, 283-296.
145. Massey, V.; Palmer, G., On the existence of spectrally distinct classes of flavoprotein semiquinones. A new method for the qualtitative roduction of flavoprotein semiquinones. *Biochemistry* **1966,** *5*, 3181-3189.
146. Murataliev, M. B., *Application of electron spin resonance (EPR) for detection and characterization of flavoprotein.* Humana Press Inc.: Totowa, NJ, 1999; Vol. 131.
147. Driggers, C.; Dayal, P.; Ellis, H.; Karplus, A., Crystal Structure of *Escherichia coli* SsuE; Defining a General Catalytic Cycle for FMN Reductases of Flavodoxin-like Superfamily. *Biochemistry* **2014,** *53* (21), 3509-3519.
148. Houwman, J. A.; van Mierlo, C. P. M., Folding of proteins with a flavodoxin-like architecture. *The FEBS Journal* **2017,** *284* (19), 3145-3167.
149. Gao, B.; Ellis, H., Mechanism of Flavin Reductase in the Alkanesulfonate Monooxygenase System. *ScienceDirect* **2006,** *1774* (3), 359-367.
150. Niviere, V.; Fieschi, F.; Decout, J.; Fontecave, M., The NAD(P)H:Flavin Oxidoreductase from *Escherichia coli*. *The Journal of Biological Chemistry* **1999,** *274* (26), 18252-18260.
151. Aliverti, A.; Bruns, C. M.; Pandini, V. E.; Karplus, P. A.; Vanoni, M. A.; Curti, B.; Zanetti, G., Involvement of serine 96 in the catalytic mechanism of ferredoxin-NADP+ reductase: structure--function relationship as studied by site-directed mutagenesis and X-ray crystallography. *Biochemistry* **1995,** *34*, 8371-8379.
152. Foster, J. W.; Moat, A. G., Nicotinamide adenine dinucleotide biosynthesis and pyridine nucleotide cycle metabolism in microbial systems. *Microbiol Rev.* **1980,** *44* (1), 83-105.
153. Ellis, H. R., Mechanism for Sulfur Acquisition by the Alkanesulfonate Monooxygenase System. *Bioorganic Chemistry* **2011,** (39), 178-184.

154. Zhan, X.; Carpenter, R.; Ellis, H., Catalytic Importance of the Substrate Binding Order for the $FMNH_2$-Dependent Alkanesulfonate Monooxygenase Enzyme. *Biochemistry* **2007,** *47*, 2221-2230.
155. Musila, J. M.; L. Forbes, D.; Ellis, H. R., Functional Evaluation of the π-Helix in the NAD(P)H:FMN Reductase of the Alkanesulfonate Monooxygenase System. *Biochemistry* **2018,** *57* (30), 4469-4477.
156. Musila, J. M.; Forbes, D.; Ellis, H. R., Functional Evaluation of the pi-Helix in the NAD(P)H:FMN Reductase of the Alkanesukfonate Monooxygenase System. *Biochemistry* **2018,** *57* (30), 4469-4477.
157. Pauling, L.; Corey, R. B.; Branson, H. R., The Structure of Proteins: Two Hydrogen-Bonded Helical Configurations of the Polypeptide Chain. *Chemistry* **1951,** *37*, 205-211.
158. Kumar, P.; Bansal, M., Dissecting π-Helices: Sequence, Structure, and Function *FEBS Journal* **2015,** (282), 4415-4432.
159. Cooley, R. B.; Arp, D. J.; Karplus, P. A., Evolutionary origin of asecondary structure, pi-helices as cryptic but widespread insertional variations of a alpha-helices enhancing protein functionality. *J Mol Bio* **2010,** *404* (2), 232-246.
160. Millhauser, G. L., Views of helical peptides: A proposal for the position of 3!10)-helix along the thermodynamic folding pathway. *Biochemistry* **1995,** *34*, 3873-3877.
161. Armen, R.; Alonso, D. O. V.; Daggett, V., The role of α-, 3_{10}-, and π-helix in helix coil transitions. *Protein Science* **2003,** *12*, 1145-1157.
162. Low, B. W.; Baybutt, R. B., The pi helix - A Hydrogen Bonded Configuration of the Polypeptide Chain. *J. Am. Chem. So.* **1952,** *74* (22), 5806-5807.
163. Fodje, M. N.; Al-Karadaghi, S., Occurrence, Confirmational Features and Amino Acid Propensities for the pi-helix. *Protein Engineering* **2002,** *15* (5), 353-358.
164. Chapman, R.; Kulp, J. L.; Patgiri, A.; Kallenbach, N. R.; Bracken, C.; Arora, P. S., Trapping a folding intermediate of the alpha-helix: stabilization of the pi-helix. *Biochemistry* **2008,** *47* (14), 4189-4195.
165. Rohl, C. A.; Doig, A. J., Models for the 3(10)-helix/coil, pi-helix/coil, and alpha-helix/coil transitions in isolated peptides. *5* **1996,** (8), 1687-1696.
166. Mikhonin, A. V.; Asher, S. A., Direct UV Raman Monitoring of 3 1_0 -helix and pi-buldge Premelting during alpha-helix Unfolding. *J. Am. Chem. Soc.* **2006,** *128* (42), 13789-13795.
167. Rohl, C. A.; Doig, A. J., Models for the 3(10)-helix/coil, pi-helix/coil, and alpha-helix/coil transitions in isolated peptides. *Protein Science* **1996,** *5* (8), 1687-1696.
168. Mahadevan, J.; Lee, K.; Kuczera, K., Conformational Free Energy Surfaces of Ala10 and Aib10 Peptide Helices in Solution. *J. Phys. Chem. B.* **2001,** *105*, 1863-1876.
169. Ludwiczak, J.; Winski, A.; Neto, A. M. S.; Szczepaniak, K.; Alva, V.; Dunin-Horkawicz, S., PiPred – a deep-learning method

for prediction of π-helices in protein

sequences. *Nature* **2019,** *9* (6888), 1-9.
170. Bradshaw, M. D.; Gaffney, B. J., Fluctuations of an Exposed p -helix Involved in Lipoxygenase Substrate Recognition. *Biochemistry* **2014,** *53*, 5102-5110.
171. Boyington, J. C.; Gaffney, B. J.; Amzel, L. M., The 3-dimensional structure of an arachidonic acid 15-lipoxygenase. *Science* **1993,** *260*, 1482-1486.

172. Minor, W.; Steczko, J.; Stec, B.; Otiwinowski, Z.; Bolin, J. T.; Walter, R.; Axelrod, B., Crystal structure of soybean lipoxygenase L-1 at 1.4 A resolution. *Biochemistry* **1996,** *35*, 10687-10701.
173. Massey, V., Activation of Molecular Oxygen by Flavins and Flavoproteins. *Journal of Biological Chemistry* **1994,** *269* (36), 22459-22462.
174. Teufel, R.; Stull, F.; Meehan, M. J.; Michaudel, Q.; Dorrestein, P. C.; Palfey, B.; Moore, B. S., Biochemical Establishment and Characterization of EncM's Flavin-N5-Oxide Cofactor. *Journal of American Chemical Society* **2015,** *137*.
175. Eichhorn, E.; Davey, C. A.; Sargent, D. F.; Leisinger, T.; Richmond, T. J., Crystal Structure of *Escherichia coli* Alkanesulfonate Monooxygenase SsuD. *J. Mol. Bio.* **2002,** *324*, 457-468.
176. Campbell, Z.; Baldwin, T. O., Two Lysine Residues in the Bacterial Luciferase Mobile Loop Stabilize Reaction Intermediates. *J. Biol. Chem.* **2009,** *284*, 32827-32834.
177. Carpenter, R.; Xiong, J.; Robbins, J.; Ellis, H., Functional Role of a Conserved Arginine Residue Located on a Mobile Loop of Alkanesulfonate Monooxygenase. *Biochemistry* **2011,** (50), 6469-6477.
178. Xiong, J.; Ellis, H. R., Deletional Studies to Investigate the Functional Role of a Dynamic Loop Region of Alkanesulfonate Monooxygenase. *Biochemistry* **2012,** *1824*, 898-906.
179. Wierenga, R. K., The TIM-Barrel Fold: a Versatile Framework for Efficient Enzymes. *FEBS* **2001,** *492* (3), 193-198.
180. Fisher, A. J.; Thompson, T. B.; Thoden, J. B.; Baldwin, T. O.; Rayment, I., The 1.5-Å Resolution Crystal Structure of Bacterial Luciferase in Low Salt Conditions. *Journal of Biological Chemistry* **1996,** *271* (36), 21956-21968.
181. Carpenter, R.; Zhan, X.; Ellis, H., Catalytic Role of a Conserved Cysteine Residue in the Desulfonation Reaction by the Alkanesulfonate Monooxygenase Enzyme. *Biochemistry and Biophysics* **2010,** (1804), 97-105.
182. Robbins, J. M.; Ellis, H. R., Steady-State Kinetic Isotope Effects Support a Complex Role of Arg226 in the Proposed Desulfonation Mechanism of Alkanesulfonate Monooxygenase. *Biochemistry* **2013,** *53* (1), 161-168.
183. Brodl, E.; Winkler, A.; Mecheroux, P., Molecular mechanisms of bacterial bioluminescence. *Comput Struct Biotechnol J.* **2018,** *16*, 551-564.
184. Kantz, A.; Chin, F.; Nallamothu, N.; Nguyen, T.; Gassner, G. T., Mechanism of flavin transfer and oxygen activation by the two-component flavoenzyme styrene monooxygenase. *Archives of Biochem and Biophys.* **2005,** *442*, 102-116.
185. Abdurachim, K.; Ellis, H., Detection of Protein-Protein Interactions in the Alkanesulfonate Monooxygenase System from *Escherichia coli*. *Journal of Bacteriology* **2006,** *188* (23), 8153-8159.
186. Dayal, P. V.; Singh, H.; Busenlehner, L. S.; Ellis, H. R., Exposing the Alkanesulfonate Monooxygenase Protein-Protein Interaction Sites. *Biochemistry* **2015,** (54), 7531-7538.
187. Musila, J. M.; Ellis, H. R., Transformation of a Flavin-Free FMN Reductase to a Canonical Flavoprotein through Modification of the pi-helix. . *Biochemistry* **2016,** *55* (46), 6389-6394.
188. Robbins, J. M.; Ellis, H. R., Identification of Critical Steps Governing the Two-Component Alkanesulfonate catalytic Mechanism. *Biochemistry* **2012,** *51* (32), 6378-6387.
189. Bentley, R.; Chasteen, T. G., Environmental VOSCs—formation and degradation of dimethyl sulfide, methanethiol and related materials. *Chemosphere* **2004,** *55*, 291-317.

190. Kouzuma, A.; Endoh, T.; Omori, T.; Nojiri, H.; Yamane, H.; Habe, H., Transcription factors CysB and SfnR constitute the hierarchical regulatory system for the sulfate starvation response in *Pseudomonas putida*. *J. Bacteriol* **2008,** *190*, 4521-4531.
191. Habe, H.; Kouzuma, A.; Endoh, T.; Omori, T.; Yamane, H.; Nojiri, H., Transcriptional Regulation of the Sulfate-Starvation-Induced Gene *sfnA* by a sigma 54-Dependent Activator of *Pseudomonas putida*. *Microbiology* **2007,** *153*, 3091-3098.
192. McFarlane, J. S.; Hagen, R.; Chilton, A. S.; Forbes, D.; Lamb, A.; Ellis, H. R., Not as Easy as Pi: an Insertional Residue Does Not Explain the pi-Helix Gain-of-Function in Two-Component FMN Reductases. *Protein Science* **2018**.
193. Binter, A.; Staunig, N.; Jelesarov, I.; Lohner, K.; Palfey, B. A.; Deller, S.; Gruber, K.; Macheroux, P., A single intersubunit salt bridge affects oligomerization and catalytic activity in a bacterial quinone reductase. . *FEBS J* **2009,** *276*, 5263-5274.
194. Vorontsov, I.; Minasov, G.; Brunzelle, J.; Shuvalova, L.; Kiryukhina, O.; Collart, F.; Anderson, W., Crystal Structure of an *apo* form of *Shigella flexneri* ArsH Protein with an NADPH-Dependent FMN Reductase Activity. *Protein Science* **2007,** *16*, 2483-2490.
195. Deller, S.; Sollner, S.; Trenker-El-Toukhy, R.; Jelesarov, I.; Gübitz, G.; Macheroux, P., Characterization of a thermostable NADPH:FMN oxidoreductase from the mesophilic bacterium *Bacillus subtilis*. . *Biochemistry* **2006,** *45*, 7093-7091.
196. Deller, S.; Macheroux, P.; Sollner, S., Flavindependent quinone reductases. . *Cell Mol Life Sci* **2008,** *65*, 141-160.
197. Weaver, T., The pi-helix Translate Structure into Function. *Protein Science* **1999,** *9*, 201-206.
198. Richardson, J. S.; Richardson, D. C., *Science* **1988,** *240*, 1648-1652.
199. Rajashankar, K. R.; Ramakumar, S., π-Turns in proteins and peptides: Classification, conformation, occurrence, hydration and sequence. *Protein Science* **1996,** *5* (5), 932-946.
200. Zhan, X. CATALYTIC MECHANISM OF A FLAVIN-DEPENDENT ALKANESULFONATE MONOXYGENASE FROM ESCHERICHIA COLI. 2008.
201. McPhillips, T. M.; McPhillips, S. E.; Chiu, H. J.; Cohen, A. E.; Deacon, A. M.; Ellis, P. J.; Garman, E.; Gonzalez, A.; Sauter, N. K.; Phizackerley, R. P.; Soltis, S. M.; Kuhn, P., Blu-ice and the distributed control system: software for data acquisition and instrument control at macromolecular crystallography beamlines. . *J Synchrotron Radiat* **2002,** *9*, 401-406.
202. Kabsch, W., XDS. *Acta Cryst* **2010,** *D66*, 125-132.
203. Vonrhein, C.; Flensburg, C.; Keller, P.; Sharff, A.; Smart, O.; Paciorek, W.; Womack, T.; Bricogne, G., Data processing and analysis with the autoPROC toolbox. . *Acta Cryst* **2011,** *D67*, 293-302.
204. Emsley, P.; Cowtan, K., Coot: model-building tools for molecular graphics. . *Acta Cryst* **2004,** *D60*, 2126-2132.
205. Adams, P. D.; Grosse-Kunstleve, R. W.; Hung, L. W.; Ioerger, T. R.; McCoy, A. J.; Moriarty, N. W.; Read, R. J.; Sacchettini, J. C.; Sauter, N. K.; Terwilliger, T. C., PHENIX: building new software for automated crystallographic structure determination. . *Acta Cryst* **2002,** *D58*, 1948-1954.
206. Chen, V. B.; Arendall, W. B. I.; Headd, J. J.; Keedy, D. A.; Immormino, R. M.; Kapral, G. J.; Murray, L. W.; Richardson, J. S.; Richardson, D. S., MolProbity: all-atom structure validation for macromolecular crystallography. . *Acta Cryst* **2010,** *D66*, 12-21.
207. Krissinel, E.; Henrick, K., Secondary-structure matching (SSM), a new tool for fast protein structure alignment in three dimensions. . *Acta Cryst* **2004,** *D60*, 2256-2268.

208. S., E.; Poulain, S.; Heinerwadel, R.; Bremond, N.; Sylvester, M. D.; Zhang, Y. B.; Berthomieu, C.; Van Der Lelie, D.; Matin, A., Crystal structure of ChrR—a quinone reductase with the capacity to reduce

chromate. *PloS One* **2012,** *7*, e36017.
209. Lei, B.; Liu, M.; Huang, S.; Tu, S. C., Vibrio harveyi NADPH-flavin oxidoreductase: cloning, sequencing and overexpression of the gene and purification and characterization of the cloned enzyme. *J. Bacteriol.* **1994,** *176*, 3552-3558.
210. Zenno, S.; Saigo, K.; Kanoh, H.; Inouye, S., Identification of the gene encoding the major NAD(P)H-flavin oxidoreductase of the bioluminescent bacterium *Vibrio fischeri* ATCC 7744. *J. Bactierol.* **1994,** *176*, 3536-3543.
211. Inouye, S., NAD(P)H-flavin oxidoreductase from the bioluminescent bacterium, Vibrio fischeri ATCC 7744, is a flavoprotein. *FEBS Lett.* **1994,** *347*, 163-168.
212. Spyrou, G.; Haggard-Ljungguist, E.; Krook, M.; Jornvall, H.; Nilsson, E.; Reichard, P., Characterization of the flavin reductase gene (fre) of Escherichia coli and construction of a plasmid for overproduction of the enzyme. *J. Bacterial* **1991,** *173*, 3673-3679.
213. Lolis, E.; Petsko, G. A., Crystallographic analysis of

the complex between triosephosphate isomerase and 2-phosphoglycolate at 2.5-Å resolution: implications for catalysis. *Biochemistry* **1990,** *29*, 6619-6625.
214. Davenport, R. C.; Bash, P. A.; Seaton, B. A.; Karplus, M.; Petsko, G. A.; Ringe, D., Structure of the triosephosphate isomerasephosphoglycolohydroxamate complex: an analogue of the intermediate

on the reaction pathway. *Biochemistry* **1991,** *30*, 5821-5826.
215. Noble, M. E.; Wierenga, R. K.; Lambeir, A. M.; Opperdoes, F. R.; Thunnissen, A. M.; Kalk, K. H.; Groendijk, H.; Hol, W. G., The adaptability of the active site of trypanosomal triosephosphate isomerase as observed in the crystal structures of three different

complexes. *Proteins* **1991,** *10*, 50-69.
216. Wierenga, R. K.; Borchert, T. V.; Noble, M. E., Crystallographic binding studies with triosephosphate isomerases: conformational changes induced by substrate and substrate-analogues. *FEBS Lett.* **1992,** *307*, 34-39.
217. Zhang, Z.; Sugio, S.; Komives, E. A.; Liu, K. D.; Knowles, J. R.; Petsko, G. A.; Ringe, D., Crystal structure of recombinant

chicken triosephosphate isomerase-phosphoglycolohydroxamate complex at 1.8-Å resolution. *Biochemistry* **1994,** *33*, 2830-2837.
218. Miller, B. G.; Hassell, A. M.; Wolfenden, R.; Milburn, M. V.; Short, S. A., Anatomy of a proficient enzyme: the structure of

orotidine 50

-monophosphate decarboxylase in the presence and absence

of a potential transition state analog. *Proc. Natl. Acad. Sci. U.S.A.* **2000,** *97*, 2011-2016.
219. Ou, X.; Ji, C.; Han, X.; Zhao, X.; Li, X.; Mao, Y.; Wong, L.; Bartlam, M.; Rao, Z., Crystal Structures of Human Glycerol 3-phosphate

Dehydrogenase 1 (GPD1). *Journal of Molecular Biology* **2006,** *357* (3), 858-869.

220. Fisher, A. J.; Raushel, F. M.; Baldwin, T. O.; Rayment, I., Three-dimensional structure of bacterial luciferase from *Vibrio harveyi* at 2.4 A resolution. *Biochemistry* **1995,** *34*, 6581-6586.
221. Sparks, J. M.; Baldwin, T. O., Functional implications of the unstructured loop in the (beta/alpha)(8) barrel structure of

the bacterial luciferase alpha subunit. *Biochemistry* **2001,** *40*, 15436-15443.
222. Goldman, L. M.; Amyes, T. L.; Goryanova, B.; Gerlt, J. A.; Richard, J. P., Enzyme Architecture: Deconstruction of the Enzyme-Activating Phosphodianion Interactions of Orotidine 5′-Monophosphate Decarboxylase. *JACS* **2014,** *136*, 10156−10165.
223. Amyes, T. L.; Richard, J. P.; Tait, J. J., Activation of Orotidine 5-Monophosphate Decarboxylase by Phosphite Dianion: The Whole Substrate is the Sum of Two Parts. *JACS* **2005,** *127*, 15708-15709.
224. Tralau, T.; Vuilleumier, S.; Thibault, C.; Campbell, B. J.; Hart, C. A.; Kertesz, M. A., Transcriptomic Analysis of the Sulfate Starvation Response of P*seudomonas aeruginosa. J. Bacteriol* **2007,** *189*, 6743-6750.
225. Riek, R. P.; Graham, R. M., The elusive pi-helix. *Journal of Structural Biology* **2011,** *173*, 153-160.